DR 0606-9

LA-11509-OBES

12/13/99 M.L.K. (1)

Hydrothermal Systems in Two Areas of the Jemez Volcanic Field: Sulphur Springs and the Cochiti Mining District

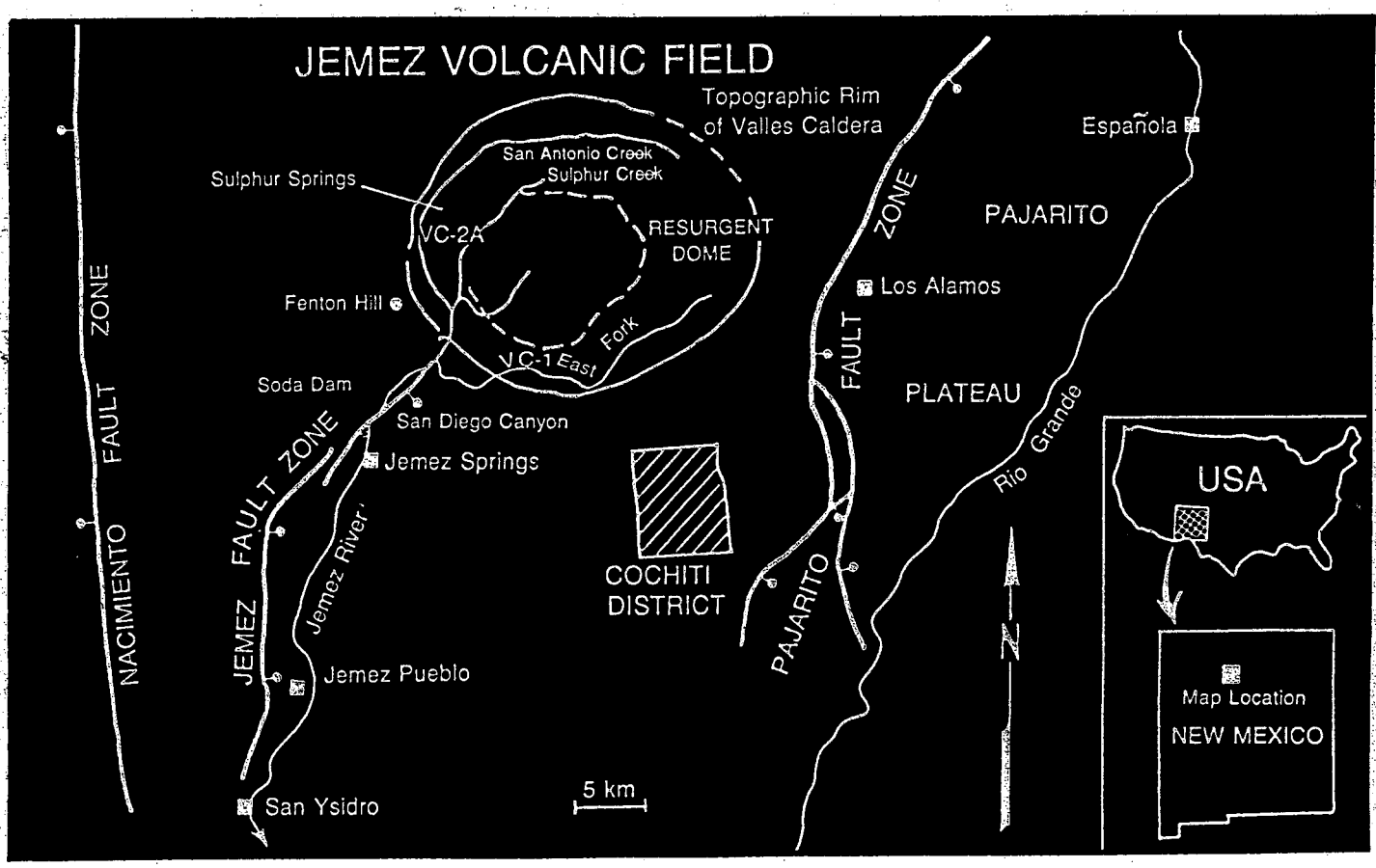

Los Alamos

Los Alamos National Laboratory is operated by the University of California for the United States Department of Energy under contract W-7405-ENG-36.

DISCLAIMER

This report was prepared as an account of work sponsored by an agency of the United States Government. Neither the United States Government nor any agency Thereof, nor any of their employees, makes any warranty, express or implied, or assumes any legal liability or responsibility for the accuracy, completeness, or usefulness of any information, apparatus, product, or process disclosed, or represents that its use would not infringe privately owned rights. Reference herein to any specific commercial product, process, or service by trade name, trademark, manufacturer, or otherwise does not necessarily constitute or imply its endorsement, recommendation, or favoring by the United States Government or any agency thereof. The views and opinions of authors expressed herein do not necessarily state or reflect those of the United States Government or any agency thereof.

DISCLAIMER

Portions of this document may be illegible in electronic image products. Images are produced from the best available original document.

Cover Map: *Tectonic framework of the Jemez volcanic field showing the Valles caldera and rift-oriented fault zones along the western margin of the Rio Grande rift.*

This work was supported by the U.S. Department of Energy, Office of Basic Energy Sciences, and by a Director-funded postdoctoral fellowship from Los Alamos National Laboratory.

An Affirmative Action/Equal Opportunity Employer

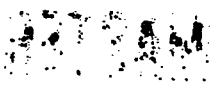

This report was prepared as an account of work sponsored by an agency of the United States Government. Neither the United States Government nor any agency thereof, nor any of their employees, makes any warranty, express or implied, or assumes any legal liability or responsibility for the accuracy, completeness, or usefulness of any information, apparatus, product, or process disclosed, or represents that its use would not infringe privately owned rights. Reference herein to any specific commercial product, process, or service by trade name, trademark, manufacturer, or otherwise, does not necessarily constitute or imply its endorsement, recommendation, or favoring by the United States Government or any agency thereof. The views and opinions of authors expressed herein do not necessarily state or reflect those of the United States Government or any agency thereof.

LA-11509-OBES

UC-403
Issued: March 1989

LA--11509-OBES

DE89 007556

Hydrothermal Systems in Two Areas of the Jemez Volcanic Field: Sulphur Springs and the Cochiti Mining District

Giday WoldeGabriel

DISCLAIMER

This report was prepared as an account of work sponsored by an agency of the United States Government. Neither the United States Government nor any agency thereof, nor any of their employees, makes any warranty, express or implied, or assumes any legal liability or responsibility for the accuracy, completeness, or usefulness of any information, apparatus, product, or process disclosed, or represents that its use would not infringe privately owned rights. Reference herein to any specific commercial product, process, or service by trade name, trademark, manufacturer, or otherwise does not necessarily constitute or imply its endorsement, recommendation, or favoring by the United States Government or any agency thereof. The views and opinions of authors expressed herein do not necessarily state or reflect those of the United States Government or any agency thereof.

MASTER

Los Alamos National Laboratory
Los Alamos, New Mexico 87545

DISTRIBUTION OF THIS DOCUMENT IS UNLIMITED

HYDROTHERMAL SYSTEMS IN TWO AREAS OF THE JEMEZ VOLCANIC FIELD: SULPHUR SPRINGS AND THE COCHITI MINING DISTRICT

by

Giday WoldeGabriel

ABSTRACT

K/Ar dates and oxygen isotope data were obtained on 13 clay separates (<2 μm) of thermally altered mafic and silicic rocks from the Cochiti mining district (SE Jemez Mountains) and Continental Scientific Drilling Project (CSDP) core hole VC-2A (Sulphur Springs, Valles caldera). Illite with K_2O contents of 6.68%-10.04% is the dominant clay in the silicic rocks, whereas interstratified illite/smectites containing 1.4%-5.74% K_2O constitute the altered andesites.

Two hydrothermal alteration events are recognized at the Cochiti area (8.07 m.y., n = 1, and 6.5-5.6 m.y., n = 6). The older event correlates with the waning stages of Paliza Canyon Formation andesite volcanism (≥13 to ≤8.5 m.y.), whereas the younger event correlates with intrusions and gold- and silver-bearing quartz veins associated with the Bearhead Rhyolite (7.54-5.8 m.y.). The majority of K/Ar dates in the hydrothermally altered, caldera-fill rocks of core hole VC-2A (0.83-0.66 m.y., n = 4) indicate that hydrothermal alteration developed contemporaneously with resurgence and ring fracture Valles Rhyolite domes (0.89-0.54 m.y.). One date of 0 ± 0.10 m.y. in acid-altered landslide debris of postcaldera tuffs from the upper 13 m of the core hole probably correlates with Holocene hydrothermal activity possibly associated with the final phases of the Valles Rhyolite (0.13 m.y.).

Oxygen isotope data from illites (SMOW) in the Cochiti district are zonally distributed (-2.15 to +2.98°/oo) around a 15-m-wide mineralized vein, while those farther out (~2-3 km) have +5 to +7.97°/oo suggesting a radial decrease in hydrothermal activity. The samples from VC-2A get lighter with depth (-0.20 to +1.62°/oo) indicating a thermal gradient in an extensive meteorically derived hydrothermal fluid-rock interaction. The $\delta^{18}O$ values of meteoric water at Valles are about -12°/oo, whereas hydrothermal fluids (220°-300°C) average about -9°/oo. The K/Ar and oxygen isotope data provide strong evidence that the epithermal quartz-vein-hosted gold-silver mineralization at Cochiti and the sub-ore-grade molybdenite at VC-2A were deposited in the late Miocene (5.90 m.y.) and mid-Quaternary (0.66 m.y.), respectively, by hydrothermal fluids composed primarily of meteoric water.

I. INTRODUCTION

The active hydrothermal systems of the Jemez volcanic field (Fig. 1) have been thoroughly explored and documented for geothermal resources and basic research on magma/hydrothermal systems resulting from geothermal research and development and, recently, research associated with the Continental Scientific Drilling Program (CSDP) (Goff et al. 1986; Hulen and Nielson 1986; Vuataz and Goff 1986). The present study is mostly concerned with the temporal and spatial relationships of fossil hydrothermal systems and associated mineralization as recognized in the Cochiti mining district (Wronkiewicz et al. 1984; southeastern Jemez volcanic field) and VC-2A (Sulphur Springs), the second CSDP core hole in the Valles caldera (Hulen et al. 1988).

Pervasive hydrothermal alteration is evident in the Cochiti mining district and surrounding areas. The Keres Group (Paliza Canyon Formation, Canovas Canyon Formation, and Bearhead Rhyolite), composed primarily of Miocene andesite, dacite, and rhyolite, represents the bulk of the outcrops (Fig. 1, inset stratigraphic column) and is characterized by widespread propylitic and locally advanced argillic zones around several epithermal mineralized quartz veins (Stein 1983; Wronkiewicz et al. 1984). The Tewa Group, which represents the latest major episode of volcanism in the Jemez volcanic field, is rarely thermally affected except in areas of hydrothermal activity such as Sulphur Springs (Goff and Gardner 1980; Goff et al. 1985). Here surface and subsurface samples exhibit phyllic and propylitic to argillic and advanced argillic alteration (Charles et al. 1986; Hulen et al. 1987).

An essential feature of hydrothermal alteration is the conversion of the initial (primary) mineral assemblage to a new set of minerals stable in the hydrothermal environment. Illite, illite/smectite, chlorite, kaolinite-family clays, epidote, calcite, pyrite, and abundant secondary silica are the dominant secondary mineral assemblages in hydrothermally altered rocks. Illitic material is a very good K/Ar clock, and the K/Ar technique can be used to date hydrothermal alteration-mineralization sequences and diagenetic phases in different geological environments (Aronson and Lee 1986; Glasmann 1985; Sillitoe 1988). In this report, K/Ar data are used to determine the temporal and spatial relationships between the tectonomagmatic history and the superimposed hydrothermal alteration in two areas of the Jemez volcanic field.

A total of 16 surface and 26 subsurface core hole samples from the Cochiti mining district and Sulphur Springs (CSDP core hole VC-2A),

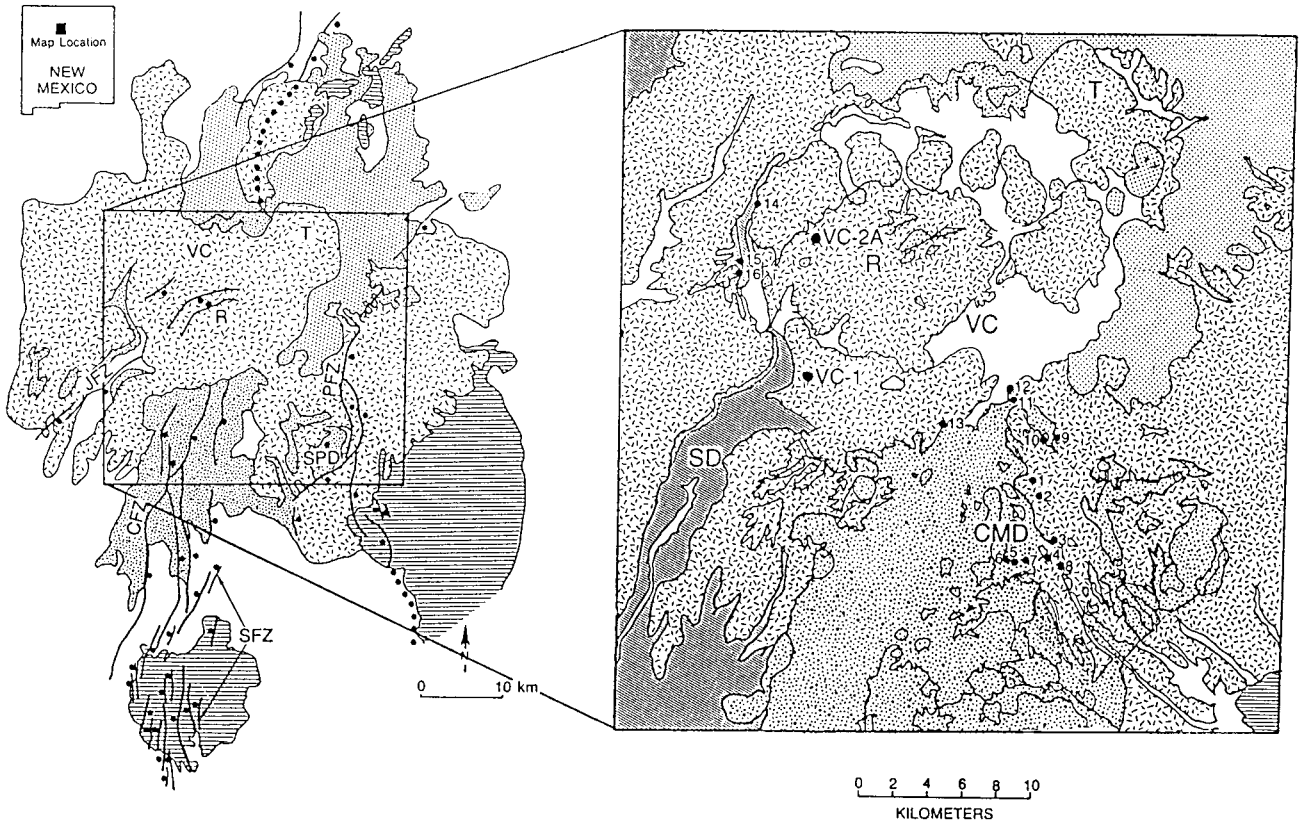

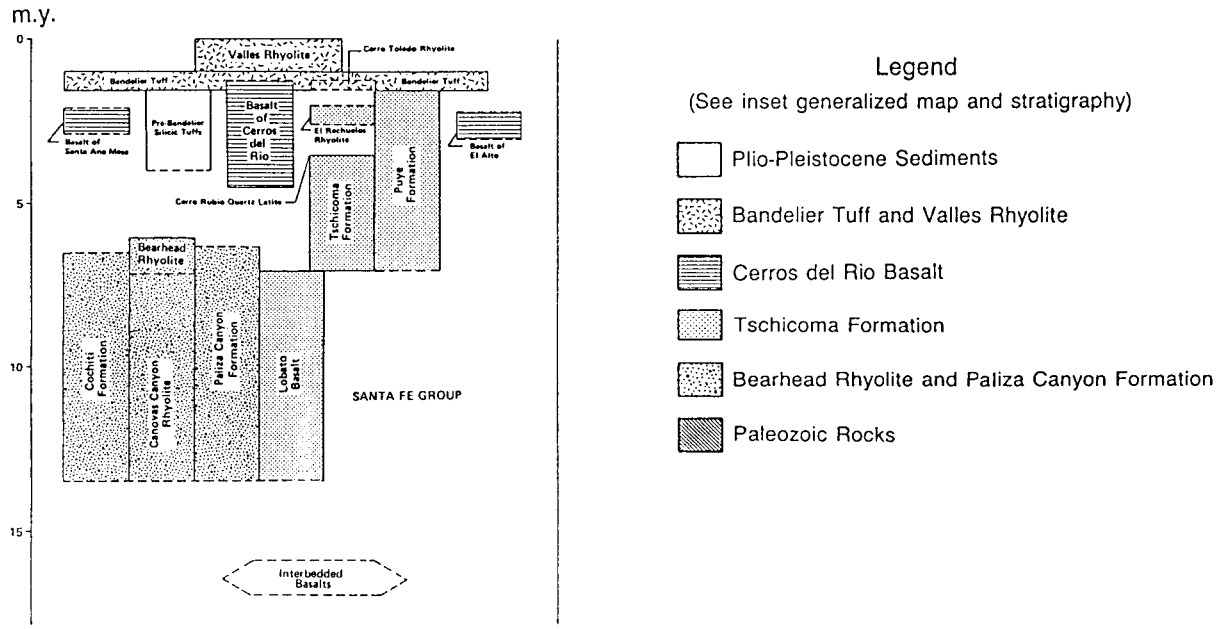

Fig. 1. Simplified geological map of the central Jemez volcanic field (after Smith et al. 1970). The inset is a generalized map that shows the stratigraphy of the Jemez volcanic field (after Gardner et al. 1986). Sample numbers as tabulated in Table I. CFZ = Canada de Cochiti Fault Zone, CMD = Cochiti Mining District, JFZ = Jemez Fault Zone, PFZ = Pajarito Fault Zone, R = Redondo Dome, SD = Soda Dam, SFZ = Santa Ana Fault Zone, SPD = St. Peters Dome, T = Toledo Embayment, and VC = Valles Caldera.

respectively, were investigated (Fig. 1). In addition to petrographic study, scanning electron microscopy (SEM) imaging and x-ray diffraction (XRD) analyses were performed on all of the above-mentioned samples, and K/Ar dating and oxygen isotope work was carried out on selected clay separates (hydrothermal alteration products) from the two localities.

Most of the clays (<2 μm) separated from the felsic rocks are dominated by illite with minor chlorite, whereas the basaltic and andesitic rocks contain smectite and subordinate amounts of chlorite, illite, and kaolinite. In silicic rocks, the alteration products in thin section are dominantly represented by birefringent and ribbon-like sericites occurring in the matrix around mineral grains and as replacements of feldspars, whereas in the basalts and andesites smectite with minor amount of chlorite represent the authigenic clay assemblage.

II. ANALYTICAL METHODS

Samples for this study were selected on the basis of lithologic variation, degree of alteration, and signs of mineralization. Slabs for thin section and clay separation were cut and thoroughly cleaned with deionized water to eliminate surface contaminants such as drilling mud and weathering rinds. Petrographic study of each individual sample was carried out to determine the degree of weathering and to estimate the amount of lithics associated with the pyroclastic units (Appendix A).

Cleaned slabs for clay separation were powdered using a Spex 8500 Shatterbox for 3 to 4 min. Rock powder splits weighing 50 to 100 g were mixed with 500-700 ml of deionized water and sonified for about 12 min. The homogenized solution was placed on a vibrationally stable surface for 45 min to 1 h. The supernatant suspension was decanted into large labeled tubes (250 ml) to separate various clay fractions using a DuPont Sorvall superspeed angle-rotor centrifuge. The fine clay fraction used in this study (<2 μm) was separated at a centrifugation speed of 8000 rpm for a spin time of 1 h. Ultrafine clay fractions (<0.1 μm) were generally insignificant in amount. Most of the fine clay fractions from the VC-2A core hole samples were air dried, and random mounts were prepared for XRD analysis. Oriented mounts were prepared for those samples that were dated by the K/Ar method.

The surface samples from the Cochiti district were treated similarly and also treated with chemicals to eliminate contaminants such as calcite, organic

matter, and iron oxides using the procedures outlined in Jackson (1978). Carbonates were removed by treating samples with a dilute mixture of acetic acid and sodium acetate until the solution reached a constant pH of 4. Organic matter was decomposed by H_2O_2 treatment, and iron oxides were removed by adding Na-citrate and bicarbonate solutions mixed with sodium dithionite and by stirring samples in a water bath of about 50°C. The rock powder-chemical solution slurries were centrifuged several times at about 2000-3000 rpm by adding and mixing with deionized water. This chemical treatment was followed by a thorough dialysis of each sample for 4 to 5 days in deionized water that was regularly changed every 4 h except during the night. The effect of chemical treatment was monitored by x-raying the samples before and after chemical treatment. Oriented mounts were made by pipetting clay suspension onto glass or quartz slides and by glycolating the mounts overnight in a container at 60°C. The XRD analysis was performed with a Siemens D-500 automated diffraction system using a Cu tube and 0.02° 2θ steps with 1 s per step for all mounts (2-36° 2θ). Identical diffractograms (Appendix B) were obtained on the pre- and postchemically treated clays. The altered rocks were also examined using SEM equipped with an energy dispersive x-ray (EDX) system for determining elemental composition, the intensity of alteration, and distribution and morphology of secondary mineral assemblages.

K/Ar age determinations were made on 13 samples (Table I) selected from the various clay separates at the Case Western Reserve University K/Ar Laboratory. Clay samples of 100 to 200 mg were used for Ar extraction in a multiload system (Aronson and Lee 1986). The system was baked 12-14 h at approximately 195°C with cooling water running in a coil around the slightly inclined sample holder. Argon was analyzed with an MS-10 mass spectrometer equipped with an on-line extraction system and a bulk-pipetted ^{38}Ar tracer calibrated by the LP-6 interlaboratory standard at 19.3×10^{-10} mol of radiogenic Ar ($^{40}Ar^*$) per gram. Except for a single sample, the clay analyses resulted in 8%-61% of the extracted Ar being radiogenic, enabling a reliable measurement of the $^{40}Ar^*$ content of the young alteration products. The K_2O analyses were made on duplicate samples with a flame photometer on acid solution of sample beads fused in lithium metaborate. Potassium decay constants used in the age calculations are those proposed by Steiger and Jager (1977). The relative age uncertainty between samples from the same location is less than 2%; however, the error associated with the Quaternary clays (VC-2A

TABLE I

K/AR AGE AND OXYGEN-ISOTOPE DATA OF CLAY FRACTIONS (<2 μm) FROM CORE HOLE VC-2A AND COCHITI MINING DISTRICT HYDROTHERMALLY ALTERED SAMPLES

CWRU Tracer[a]	Sample Number	Sample Weight,g	K_2O (%)	$^{40}Ar^*$ (10^{-10} mol/g)	$^{40}Ar^*$ (%)	Age[b] (m.y.)	$\delta^{18}O$[c] (SMOW)
Core Hole VC-2A, Sulphur Springs							
867	VC2A9-5 (9.9-13 m)	0.1269	8.3457	0	0	0 ±0.10	+0.42
866	" 34-1 (38.4-40.4 m)	0.1166	9.9812	0.9445	7.1	0.66±0.21	+1.56
	" 34-35	-----	-----	-----	-----	----------	+2.95[d]
865	" 55-2A (64.8-67.1 m)	0.1739	8.7527	0.9606	8.3	0.76±0.14	+1.62
864	" 119-9 (159-161.3 m)	0.1715	9.2462	1.4554	8.1	1.09±0.14[e]	+1.51
863	" 336E (480.2-482.9 m)	0.1595	9.8257	1.0495	8.0	0.74±0.14	+0.82
862	" 366D (524.7-527.4 m)	0.1992	10.0429	1.2033	8.2	0.83±0.11	-0.20
Cochiti Mining District, Southeast Jemez Mountains							
868	VG87 1	0.1773	7.3355	6.3303	11.5	5.99±0.36	+5.00
869	VG87 2	0.1491	5.2009	4.1968	38.9	5.60±0.29	+7.11
870	VG87 5	0.1792	9.5532	11.1180	54.6	8.07±0.22	+0.49
871	VG87 6[f]	0.1511	8.4516	7.1840	51.1	5.90±0.19	-2.15
861	VG87 7[f]	2.0028	6.6844	5.8810	61.1	6.10±0.11	+2.98
872	VG87 10	0.1290	5.7495	5.3510	24.9	6.45±0.31	+7.97
873	VG87 12	0.1469	1.4092	1.3232	22.9	6.51±0.96	----

* Radiogenic.
[a] CWRU Tracer = Case Western Reserve University K/Ar Laboratory identification number.
[b] Determined from decay constants and isotopic abundance of ^{40}K according to Steiger and Jager 1977.1
[c] SMOW = standard mean ocean water.
[d] Quartz vein material.
[e] Filament of mass spectrometer (MS-10) failed.
[f] Whole rock dated.

samples) is much higher compared with the older late Miocene ones from the Cochiti district because measuring a minimum amount of radiogenic argon in younger rocks, especially clay, is a problem.

Oxygen isotopes on clays and associated quartz veins were analyzed at the Case Western Reserve University Stable Isotope Laboratory using the technique of Clayton and Mayeda (1963) and fractionation factors of Eslinger and Savin (1973a and 1973b) and Taylor (1976). Data are presented using the standard delta notation relative to standard mean ocean water (SMOW).

III. GEOLOGIC OVERVIEW

The Jemez volcanic field is located at the intersection of the western margin of the Rio Grande rift and the NE-SW-trending Jemez Lineament (Aldrich, 1986). The Jemez volcanic field is bounded on the west by Precambrian basement rocks and Paleozoic sedimentary units of the Colorado Plateau. Tertiary basin-fill continental sediments of the rift floor are exposed on the east side of the field underlying the various units of the volcanic field. In the Jemez, compositionally diverse volcanic rocks ranging in age from mid-Miocene (>13 m.y.) to the late Pleistocene are documented (Bailey et al. 1969; Smith et al. 1970; Gardner et al. 1986). The samples for this study, as mentioned earlier, were obtained within and near the Cochiti mining district in the south-central Jemez Mountains and from the Sulphur Springs area, located inside the western structural margin of the Valles caldera (Fig. 1).

The oldest rocks in the Cochiti area belong to the Keres Group (Paliza Canyon Formation) and consist of gabbro, basalt, andesite, dacite, and volcanic breccia that are intruded by consanguineous quartz monzonite and monzodiorite stocks (11.2 ± 0.3 m.y. old) (Stein 1983). These rocks constitute the early stratovolcano-building stage of the Jemez volcanic field (Smith et al. 1970) and were derived primarily from magmas of two distinct sources: upper mantle differentiates (two-pyroxene andesites) and lower crustal melts (high-silica rhyolite), respectively (Gardner and Goff 1984). These in turn are intruded along the northwest boundary by younger dacites and andesites of the Keres Group (≥8.5 m.y.) and along the southern and western margins by Bearhead Rhyolite (7.54-5.8 m.y.) (Stein 1983; Gardner et al. 1986).

A north-trending fault zone (0.75 km wide and 3.6 km long), characterized by intensely faulted and fractured rocks permeated by major epithermal quartz veins, traverses the Cochiti mining district (Stein 1983; Wronkiewicz et al. 1984). This structural zone (Canada de Cochiti fault system) was contemporaneously formed during the eruption of the Keres Group, some lavas and domes of which were emplaced along these faults (Gardner and Goff 1984). On the basis of the distribution of quartz veins in the Keres Group rocks, Stein (1983) speculated the existence of two hydrothermal events in the Cochiti district related to quartz monzodiorite and Bearhead Rhyolite. On the other hand the propylitic and advanced argillic alteration in the Cochiti district has been attributed by Wronkiewicz et al.(1984) to the felsic intrusions of Bearhead Rhyolite that acted as a heat source, establishing a closed-cell

meteoric water convection system circulating along active tensional faults related to the Rio Grande rift. Structural relationships suggested to the later authors that the Au-bearing mineralization occurred between 6.5 and 1.4 m.y. ago. However, as will be substantiated later, the age of the clays from the altered andesites and rhyolites (8.07-5.6 m.y.) is concordant with the Keres Group volcanic extrusions (13-6 m.y., Fig. 1), implying a contemporaneous alteration associated with the waning phases of each tectonomagmatic episode.

Unlike the Cochiti district, Sulphur Springs is located between the ring fracture and the western resurgent dome of the Valles caldera (Fig. 1). Volcanic activity related to the Jemez Mountains calderas began 3.6 m.y. ago in the form of limited ash flows from calderas obliterated by the Quaternary Toledo-Valles caldera-forming eruptions (Nielson and Hulen 1984; Self et al. 1986). Following this episode, catastrophic eruptions from the Toledo and Valles calderas at 1.45 and 1.12 m.y. ago, respectively, resulted in the emplacement of large-volume felsic ignimbrites of the Otowi and Tshirege Members of the Bandelier Tuff (Doell et al. 1968; Smith 1979; Izett et al. 1980; Gardner and Goff 1984; Self et al. 1986). The Valles caldera collapse was soon followed by central resurgent activity and a series of rhyolite domes that developed along the caldera ring fracture between 1.15 and 0.13 m.y. ago (Smith and Bailey 1968; Marvin and Dobson 1979; Gardner et al. 1986).

The most active hydrothermal system (hot spring and fumarolic activity) in the Valles caldera is presently located at Sulphur Springs, the site of CSDP core hole VC-2A (Goff et al. 1987). Surface hydrothermal alteration is represented by bleached caldera-fill tuffs, breccias, and volcaniclastic sediments up to advanced argillic grade (Goff and Gardner 1980; Goff et al. 1985; Charles et al. 1986). The 527.6-m-deep VC-2A core hole penetrated four major units. The upper three units are separated by thin volcaniclastic marker horizons (Fig. 2). The four major units are (1) a near-surface intracaldera sequence of landslide debris and volcaniclastic sediments (0-21.6 m), (2) densely welded felsic ash-flow tuff comprising the Upper Tuffs (21.6-64.8 m, <1.12 m.y.), (3) the Bandelier Tuffs (Tshirege Member, 79.9-354 m; Otowi Member, 361.7-477 m; 1.12-1.45 m.y.), and (4) the pre-Bandelier Lower Tuffs (477-527.6 m, 1.45-3.6 m.y.) (Hulen et al. 1987). A detailed discussion of the alteration products, K/Ar ages, and oxygen isotope data of selected samples from both areas is presented in Table I.

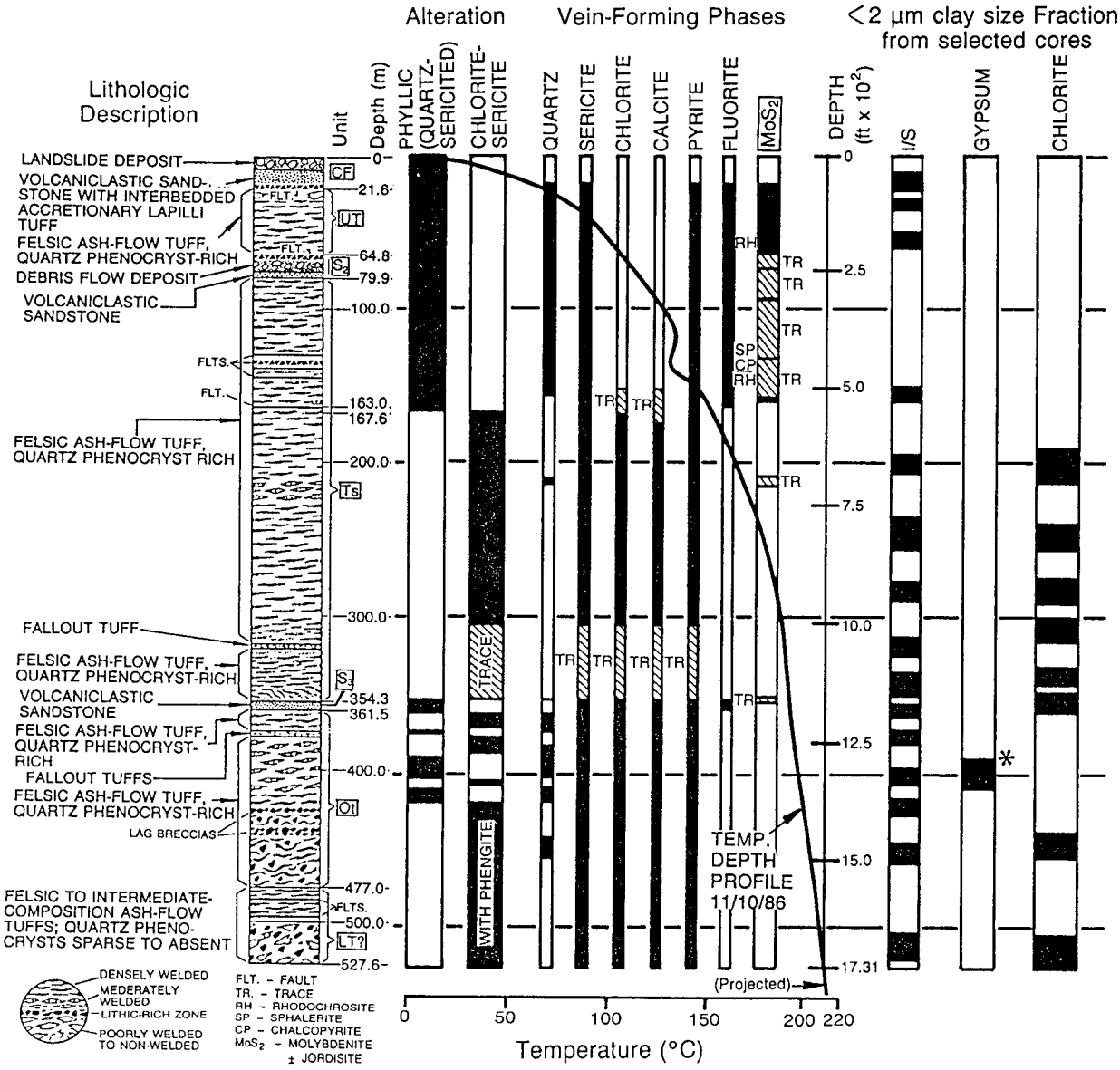

Fig. 2. Generalized lithologic alteration, vein mineralization, and less than 2-µm clay size fraction log for CSDP core hole VC-2A (modified from Hulen et al. 1987). Bulk XRD analysis of a sample from a level marked by an asterisk (*) contained 8% anhydrite (Jeff Hulen, University of Utah Research Center, personal communication, 1988); <2-µm size fraction is gypsum.

The Quaternary Valles-Toledo calderas of the Jemez volcanic field have been the subject of intense study because of their high-temperature geothermal potential (Dondanville 1978; Laughlin 1981; Hulen and Nielson 1986; Truesdell and Janik 1986). The bulk of the hydrothermal system and outflow plume within

Valles is controlled by fracture and subordinate stratigraphic permeability along northeast-trending faults of the Jemez fault zone (Dondanville 1978; Hulen and Nielson 1983; Goff et al. 1988). The Neogene thermal history of the Jemez volcanic field has been investigated by several methods (K/Ar and U-series geochronology and paleomagnetic data).

Age determinations and stable isotope studies have been carried out to evaluate the temporal and spatial evolution of the Valles hydrothermal system (Ghazi and Wampler 1987; Goff and Shevenell 1987; Geissman 1988; Sturchio and Binz 1988). K/Ar dates of clays (0.2-2.0 and <0.2 μm) from brecciated and hydrothermally altered rocks of the Madera Limestone from VC-1 (Fig. 1) yielded an age of about 1.0 ± 0.3 m.y. that is presumably associated with the Valles caldera-forming eruption at 1.12 m.y. ago (Ghazi and Wampler 1987). The rest of the clay fractions from the Madera Limestone and the underlying Sandia Formation have K/Ar ages (67.6-2.9 m.y.) older than the volcanic rocks of the area (Ghazi and Wampler 1987). However, U-Th disequilibrium dates and stable isotope analysis of travertine deposits accumulated on Paleozoic and Precambrian rocks at Soda Dam (Fig. 1, inset map) indicate pulses in travertine deposition around ~1.0 to 0.48 m.y., 0.107 to 0.058 m.y., and 0.005 m.y. to present (Goff and Shevenell 1987). Moreover, thermal perturbations constrained from paleomagnetic and rock magnetic data on unoriented core samples of VC-1 revealed that alteration and mineralization in the late Paleozoic sequences are contemporaneous with the development of the Toledo-Valles caldera-forming eruptions (Geissman 1988). In the laboratory, unblocking temperature information indicated that the Paleozoic section was heated to temperatures of approximately 250°-300°C related to Toledo- and Valles-age silicic activity. Radioisotope dilution analyses of U and Th by alpha spectrometry (uranium-series disequilibrium geochronology) on calcite veins from the Madera Limestone in CSDP core hole VC-1 were used to determine the temporal and spatial relationship of the calcite veins to the hydrothermal activity of the area (Sturchio and Binz 1988). The ages obtained by this method range between 0.095 and 1.0 m.y. and indicate different pulses of hydrothermal activity since caldera formation. The oldest U-series disequilibrium age (~1.0 m.y) reported on VC-1 calcite veins is similar to the age of the Soda Dam travertine obtained by the same technique (Goff and Shevenell 1987). The U-series data are also similar to those from the illite age (0.83 ± 0.11 m.y.) (Ghazi and Wampler

1987), and as suggested earlier, they could be related to the beginning stages of hydrothermal activity after the formation of the Valles caldera.

IV. HYDROTHERMAL ALTERATION PRODUCTS

Petrographic and clay mineralogic information supplemented by K/Ar and oxygen isotope data is essential in constraining the thermal and alteration history of a volcanic field. Twenty-nine samples were selected from various levels of the 527.6-m-deep VC-2A core hole at Sulphur Springs (Fig. 2) on the basis of degree of alteration and signs of mineralization in order to investigate the temporal and spatial relationships of the alteration-mineralization episodes. Alteration is pervasive in the core samples, although its intensity varies with depth. Illite and interstratified illite/smectite occur throughout the core hole, but calcite and chlorite appear below about 171 m. Moreover, 16 outcrop samples of altered rhyolites and andesites from the Cochiti mining district were analyzed in the same manner. Clay mineralogy, EDX analyses, and petrographic summary of the individual samples are presented in the following two tables and Appendix A, respectively.

A. Petrography

1. VC-2A Core Hole. Generalized petrographic data of all the samples described here are presented in Appendix A. The stratigraphy, temperature profile, and major mineralogic assemblages observed in VC-2A are given by Hulen et al. (1987) (Fig. 2). The uppermost two samples (VC2A 9-4 and 9-5) were obtained from near-surface caldera-fill sediments and debris flows that consist of a breccia intensely altered to quartz-sericite-pyrite aggregates and volcaniclastic sediments with accretionary lapilli that extend between 7.9-17.4 m. In thin section the rocks contain 10%-15% crystal contents dominated by fractured quartz and microcrystalline silica overgrowth. The feldspars are totally replaced by birefringent ribbon-like sericite. The matrix contains abundant recrystallized microcrystalline silica, sericite, and a few minor accessory minerals of apatite and cavity-filling euhedral pyrite grains. Based on grain contacts, pyrite appears to have formed last after authigenic sericite and quartz formation.

The top part of the Upper Tuffs (24-32.3 m) (Fig. 2) contains less crystal (about 5%) in a matrix constituted by abundant sericite and secondary

microcrystalline silica (cherty). Rock fragments and pumice clasts are also totally altered. Feldspars are moderately transformed to sericite, and the quartz grains are cracked and show wavy extinctions. Alteration is less intense below about 36.6 m. These rocks are part of the Upper Tuffs and are moderately affected, although the matrix like the overlying samples contains altered glass with abundant secondary silica that occasionally appears spherulitic. Collapsed pumice fragments show pectinate structures that are due to the replacement of secondary silica. Resorbed and cracked quartz grains are wrapped with sericite. Unlike the total replacement of feldspars in the near-surface samples, sericite is confined to cleavage traces. Two stages of sericite formation are recognized as indicated by the paragenetic association (contacts) of the secondary minerals. Two phases of sericite developed contemporaneously with microcrystalline quartz, and pyrite crystallized last. The intensity of alteration increases again from about 61 m down, as judged by the complete transformation of feldspars to sericite and the amount of secondary silica overgrowth around the semirounded (resorbed) quartz grains. Crystal contents also decrease to about 1%. Like the feldspars, welded pumice clasts are transformed to sericite.

The base of the Upper Tuff (crystal poor) at about 67 m is marked by a sandstone unit (S_2, Nielson and Hulen 1984) that contains more than 45% crystals by volume mostly represented by subrounded to rounded quartz grains that are rimmed by silica overgrowth and cherty aggregates. The interstices are filled with sericite. Altered feldspars are replaced by secondary silica. Three types of quartz grains were recognized, and they were identified by (1) strained quartz grains with undulatory extinction, (2) clear unstrained grains with secondary silica overgrowth, and (3) clear unstrained grains that imply a complex multisource petrologic history. This sedimentary horizon represents a time gap between the Upper Tuffs and the Tshirege Member of the Bandelier Tuff eruptions (Nielson and Hulen 1984).

The partially altered Tshirege Member of the Bandelier Tuff (80-354 m) below the sandstone is fairly crystal rich (>10%) compared with the overlying ignimbrite flows. The matrices are recrystallized, feldspars are moderately sericitized, and the quartz grains are coarse, anhedral, and strongly strained (sheared grains) with coarse authigenic silica. Two phases of sericite and a few allanite grains were recognized in some of the samples; pyrite formed last in altered feldspars and open cavities.

At about 244 m calcite and chlorite appear as part of the secondary mineral assemblage. These rocks are moderately welded and contain 10%-15% phenocrysts with plagioclase (polysynthetic twinning) partially altered to sericite and replaced by calcite. Quartz is resorbed and contains silica overgrowths around the edges. The matrix is strongly recrystallized and spherulitic, and calcite seems to have developed after sericite but before chlorite and pyrite. At the base of these fairly crystal rich welded tuffs (~330 m), the degree of alteration is moderate, calcite and chlorite disappear, and crystal contents decrease to about 5%, except for a sandstone layer at about 360 m that contains abundant fine-grained crystals. Point counts of the S_3 in VC-2A average 41.6% crystals and 12.6% lithic clasts (Jeff Hulen, UURI, personal communication, 1988). This unit is probably a reworked volcaniclastic deposit, characterized by angular and subrounded quartz grains and partially altered feldspars (alkali and plagioclase feldspars). Minor amounts of sericite, calcite, and pyrite are also noted. This unit corresponds to the S_3 sandstone that separates the Tshirege and Otowi Members of the Bandelier Tuff (Hulen et al. 1988).

The lower Bandelier Tuff (Otowi) core samples unlike the upper Bandelier has lower crystal contents (>5%). The matrix is totally recrystallized (i.e., pumice clasts and glass shards are fully replaced by microcrystalline silica and feldspar). Quartz grains are partly corroded, and fractured feldspars are replaced by sericite and calcite. Pyrite crystals are confined to cavities, altered feldspars, pumice, and chloritized mafics. The intensity of alteration in the Otowi Member is uniform, and the secondary mineral assemblages are dominated by sericite, chlorite, calcite, pyrite, and secondary silica. A few altered andesite lithics are also noted.

At about 480 m the altered pyroclastic units are crystal poor (<1%). The matrix is dominated by sericite and secondary silica aggregates (cherty). Welded pumice fragments and glass shards are replaced by microcrystalline silica. Moreover, altered accretionary lapilli (Hulen et al. 1988) are recognized in these samples. Sericite, silica, calcite, chlorite, and pyrite crystals form the bulk of the secondary minerals in chronological order from oldest to youngest. In some samples from this unit, sericite forms cross-cutting veinlets on/through chlorite clots, suggesting some of it postdates chlorite (Jeff Hulen, UURI, personal communication, 1988). EDX analyses of

clays from VC-2A are similar to analyses for standard illite and to interstratified illite/smectite chemical analysis data (Table II).

2. Cochiti Mining District. The late Miocene volcanic rocks of this area are dominated by porphyritic andesites with minor amounts of dacite (Paliza Canyon Formation of the Keres Group). These rocks were later intruded by Bearhead Rhyolite of the Keres Group. The altered andesites are greenish gray, porphyritic, and sometimes strongly sheared. Most of the phenocrysts are transformed into soft white spots of clayey texture. In thin section the rocks are olive gray, and the matrix is replaced by secondary silica with minor epidote, sericite, chlorite, and calcite. Partially altered hornblende, biotite, and magnetite are also present.

A dacite (VG87-1) directly underlying the Bandelier Tuff is exposed along road cuts (Fig. 1). The rock is porphyritic, and like the andesites, it contains abundant secondary silica-filled fractures and sericite with calcite replacing the moderately altered feldspars (plagioclase). Minor amounts of hornblende and pyrite also form part of the mineral assemblage.

The rhyolite samples (VG87-3, VG87-5, VG87-7, and VG87-11) are whitish and silicified and either lie unconformably beneath the Bandelier Tuff or intrude the Keres Group andesites. They are generally emplaced as dikes cutting across the andesites. These dikes are narrow (4-5 m wide), flow banded, fine grained, strongly sheared, and occasionally studded with sulfides (pyrite). Some of the outcrops are cut by quartz veins, mainly along breccia zones. Petrographic examination indicates that most of the flows are devitrified (less than 5% for VG87-3,-7, and -11 and about 30% for VG87-5), sericitized, and spherulitic. Quartz, alkali feldspars and minor amounts of hornblende, biotite, muscovite (coarse sericite), zircon, calcite, and pyrite constitute the mineral assemblage.

SEM analyses on selected hydrothermally altered core hole and surface samples from the Sulphur Springs and Cochiti mining district, respectively, show the morphology and distribution of the secondary minerals. Magmatic-driven hot hydrothermal fluids have left their mark by altering the various rocks of the Jemez volcanic field to diverse authigenic products deposited by replacing altered rock fragments, minerals, and by filling secondary pore spaces. The morphology and analyses of the alteration products are briefly outlined in Table II and Fig. 3.

TABLE II

ENERGY DISPERSIVE X-RAY (EDX) ANALYSES OF INTERSTRATIFIED ILLITE/SMECTITE AUTHIGENIC CLAYS FROM CORE HOLE VC-2A AND THE COCHITI MINING DISTRICT

	VC-2A					Cochiti Mining District			
	9-5	34-1	55-2A	119-9	336E	V687-1	V687-5	V687-7	V687-11
SiO_2	58.9	80.4	63.0	86.4	58.79	74.31	65.22	58.84	53.85
Al_2O_3	26.2	11.0	22.4	7.92	26.86	15.55	22.89	22.15	29.03
Fe_2O_3	0.82	1.42	0.6	0.01	2.22	2.70	0.19	3.42	2.68
FeO	--	--	--	--	--	--	--	--	--
MgO	--	0.5	0.9	--	0.79	1.19	1.40	0.50	0.34
CaO	0.13	0.33	0.4	--	0.60	0.33	--	--	0.32
Na_2O	--	0.61	--	--	--	1.36	1.53	0.51	--
K_2O	12.3	5.9	12.8	5.63	10.69	4.17	8.85	14.59	13.45
TiO_2	--	--	--	--	--	--	--	--	--
H_2O+	--	--	--	--	--	--	--	--	--
H_2O-	--	--	--	--	--	--	--	--	--

The Cochiti district rocks exhibit abundant authigenic interstratified I/S, quartz, and pyrite. The mixed-layer clays are crystallized as thin flakes in cavities and on the surface of primary quartz and feldspar phenocrysts (Fig. 3). EDX analyses of the authigenic clays are similar to the chemical formulas of diagenetic clay types (Table II). The intensity of alteration in VC-2A is shown by the SEM images of selected core samples from various levels. Stacks of coarse and fine authigenic illite mat with a flaky habit are commonly noticed in these altered rocks. EDX analyses yield the major elements Si, Al, and K, with minor amounts of Fe, Mg, Ca, and Mn (Table II). Authigenic quartz and minor amounts of pyrite are also associated with the illitic clays. The EDX stoichiometric results (Table II) and the XRD patterns (Appendix B) are similar to standard illite and mixed-layer I/S chemical analyses data presented by Weaver and Pollard (1975).

B. Clay Mineralogy

The composition of clay products ($<2\ \mu m$) from the various altered rocks is strongly dictated by the composition of the parent rock (Table III, Appendix B). The illitic-rich fractions are closely associated with rhyolites and

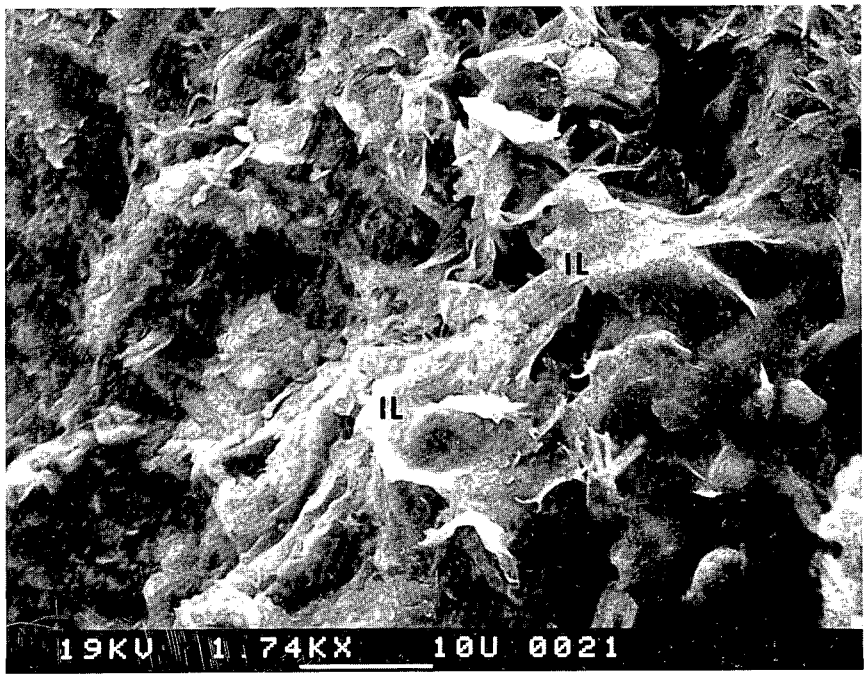

a

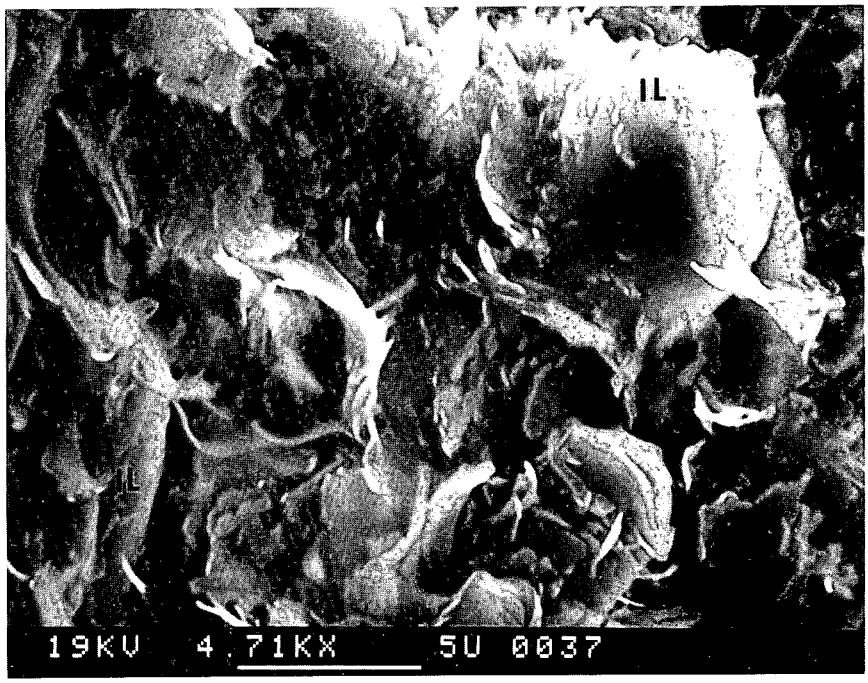

b

Fig. 3. SEM photographs of four altered VC-2A core (a-d) and four samples from the Cochiti mining district (e-h) show alteration and morphology of authigenic clay and quartz minerals. Data from EDX analyses of these and other clays are given in Table II (IL - illite flakes, F - feldspars).

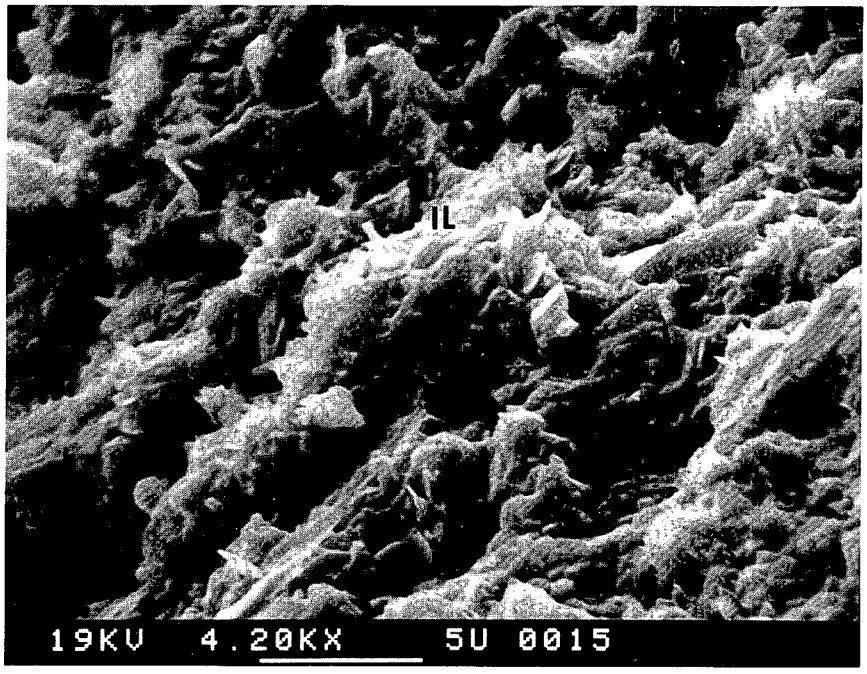

c

VC-2A 111-9

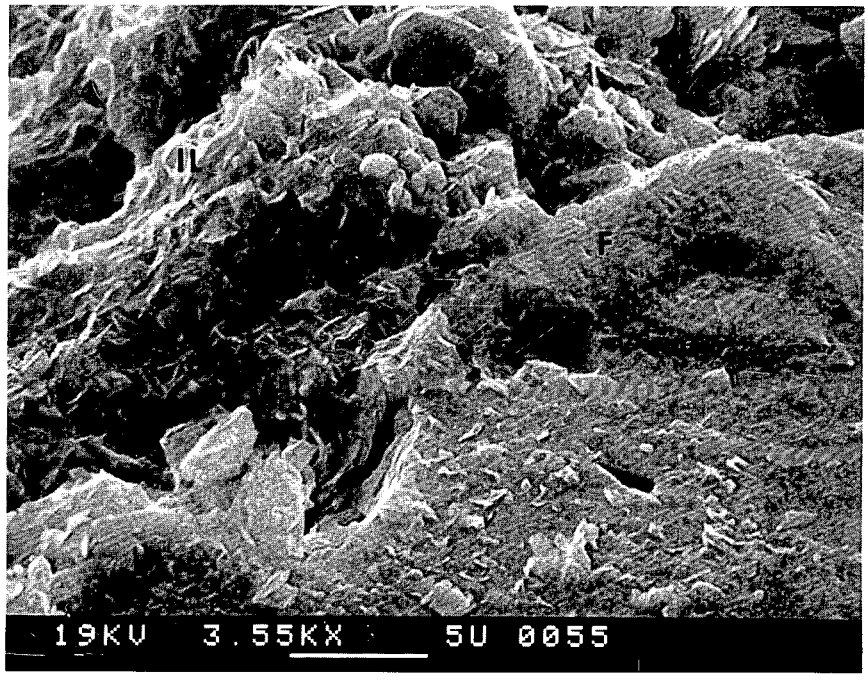

d

VC-2A 333-E

Fig. 3.(cont.)

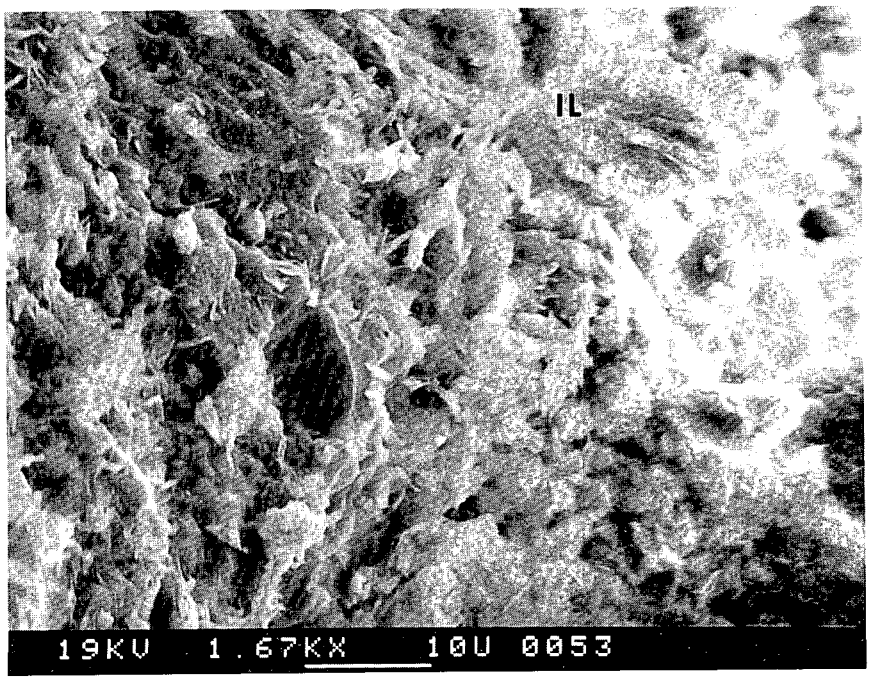

e

VG87-5

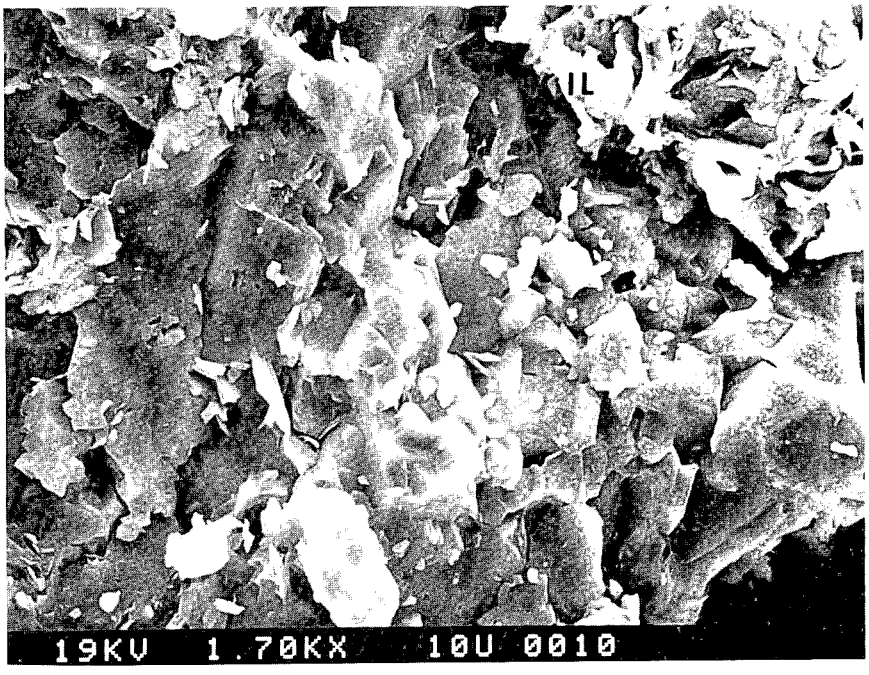

f

VG87-6

Fig. 3. (cont.)

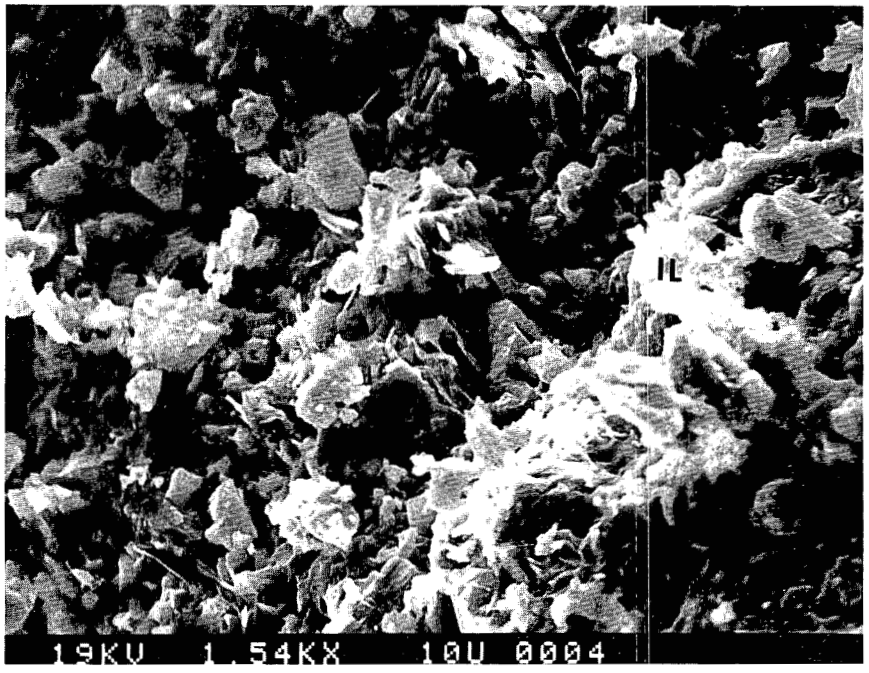

g

VG87-7

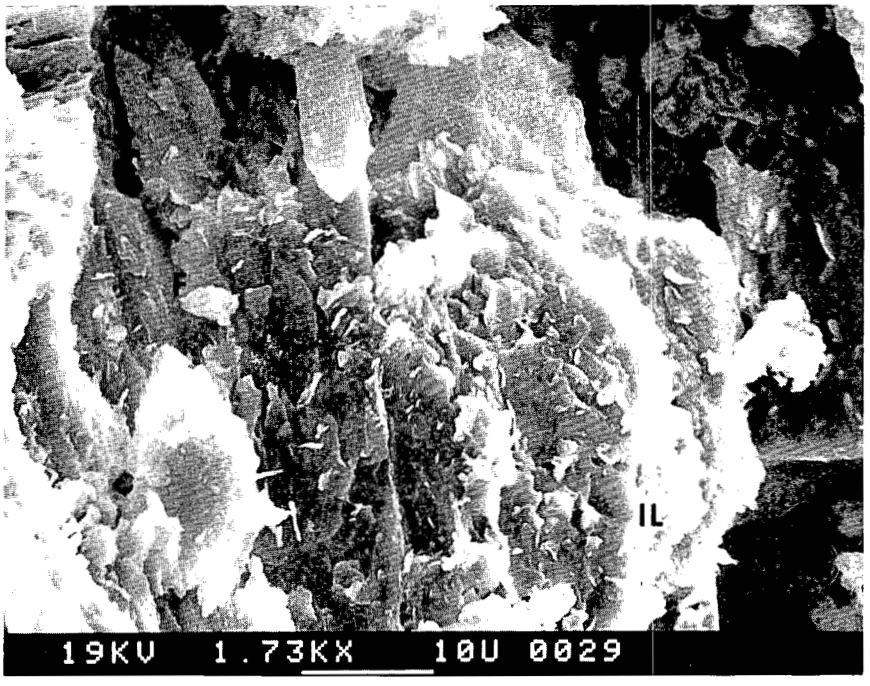

h

VG87-10

Fig. 3.(cont.)

TABLE III

X-RAY DIFFRACTION ANALYSIS OF CLAY FRACTIONS (<2 μm) FROM HYDROTHERMALLY ALTERED ROCKS OF THE JEMEZ VOLCANIC FIELD

Sample No.			Rock Type	Type of Clay or Other Mineral
VC-2A	9-5	(9.91-12.99 m)	Sediment	Illite
	28-9	(30.18-32.16 m)	Upper Tuff[a]	"
	34-1	(38.41-40.40 m)	" "	"
	55-2A	(64.79-67.13 m)	Sediment S_2	"
	104-3	(136.07-138.26 m)	Tshirege	"
	119-9	(158.96-161.25 m)	Member	"
	156-7	(213.11-215.55 m)	"	Illite + Minor Chlorite
	184-4A	(255.79-257.93 m)	"	Illite
	197-3B	(277.16-279.73 m)	"	Illite + Chlorite
	209-12	(293.6-296.34 m)	"	" " "
	230-5	(325.49-327.93 m)	"	" " "
	249-1B	(351.98-354.57 m)	"	" " "
	255-2B	(359.24-362.2 m)	"	" " "
	256-2	(362.2-362.8 m)	Otowi	" " "
	263-3B	(371.49-373.78 m)	Member	" " "
	264-3B	(373.78-376.43 m)	"	Illite
	277-1	(391.71-394.21 m)	"	"
	285-1	(405.79-408.08 m)	"	Gypsum
	298-1B	(426.68-429.12 m)	"	Illite + Chlorite
	323D	(460.98-463.41 m)	Lower Tuff[b]	" " "
	336E	(480.18-482.93 m)	" "	" " "
	366D	(524.70-527.44 m)	" "	" " "
Cochiti Mining District				
	VG87-1		Dacite?	Illite + Smectite
	VG87-2		Andesite	Illite + Smectite + Chlorite
	VG87-3		Rhyolite	" " " " "
	VG87-4		Dacite	Illite
	VG87-5		Rhyolite	"
	VG87-6		Breccia	"
	VG87-7		Rhyolite	Whole rock
	VG87-8		Andesite	Illite + Smectite + Chlorite
	VG87-9		"	Illite + Smectite
	VG87-10		"	" " "
	VG87-12		"	Illite + Smectite + Chlorite
	VG87-13		Basalt	Smectite
	VG87-14		Sandstone	Chlorite + Illite
	VG87-15		Basalt?	Smectite
	VG87-16		"	"

[a] Upper Tuff of Hulen and Nielson (1988).

[b] Lower Tuff of Hulen and Nielson (1988).

dacites, whereas montmorillonites (smectites) and chlorites are dominant in altered mafic rocks (andesites). However, it is also known that with increased temperature and compositional changes smectites undergo transition to interstratified I/S and to pure illite (Roberson and Lahann 1981; Bish 1981; Horton 1985; Whitney and Northrop 1987). X-ray diffraction patterns of the finer clay fractions (<2 μm) were obtained on air-dried random and oriented mounts. Peak positions and intensities for the oriented samples changed

slightly after glycol solvation, showing that most of the illitic clay fractions (<2 μm) from VC-2A altered samples are interstratified with small amounts of smectite (Reynolds 1980). For example, the I/S (>95% illite) separated from the near-surface caldera-fill volcaniclastic sediments (VC-2A 9-5) is characterized in the air-dried condition by strong peaks at 10.26 Å, 5.0 Å, and 3.31 Å; these change to 9.75 Å, 5.05 Å, and 3.33 Å after glycolation, illustrating the interstratified nature of the clay (Fig. 4). The illitic clay is very well crystallized with fairly sharp basal reflections typical of hydrothermal environment with temperatures approaching 200°C as documented in other geothermal systems (Srodon and Eberl 1984). Homogenization temperature data (193°-215°C) for primary fluid inclusions in quartz intergrown with similar sericite at depths as shallow as 39 m from the surface (Hulen et al. 1987) support the above conclusion. It suggests that the shallow I/S and associated quartz could have developed under liquid-dominated conditions; however, the 200°C temperature required for very illitic I/S formation is not attainable in the present hydrothermal system until a depth of about 400 m is reached (Goff et al. 1987). It does not seem likely that the shallow I/S was developed either in the present vapor cap or in the associated condensate zone; instead, the clay formed in a liquid-dominated condition near 200°C under normal hydrostatic conditions provided by a thick (>200-m) chaotic landslide debris from the adjacent eastern valley wall (Jeff Hulen, UURI, and Grant Heiken, LANL, personal communication, 1988) probably about 0.10 m.y. ago. The debris flow (breccia) deposit east of the Sulphur Springs active hydrothermal zone is more than 250 m thick (Goff and Gardner 1980). The breccia that filled the valley of the Sulphur Springs hydrothermal zone was probably removed quickly by erosion because of its unconsolidated nature and the gradient of the valley. As a result the argillic alteration zone was exposed. Outside the caldera in San Diego Canyon at the Soda Dam site, more than 400 m of Bandelier Tuff was eroded away in less than 100,000 years (Goff and Shevenell 1987).

The remaining I/S clays from various sections of the core hole also contain minor smectite as depicted by the collapse of the peaks after glycol solvation. Traces of chlorite are observed in the deepest sample (VC-2A 366-1). The clay size (<2-μm) fraction (VC-2A 285-1) from about 406 m is entirely gypsum (Appendix B). Bulk XRD from 402.5-m depth indicates 53% quartz, 8% anhydrite, 2% pyrite, 1% leucoxene, and 36% illite (Jeff Hulen, UURI, personal communication, 1988).

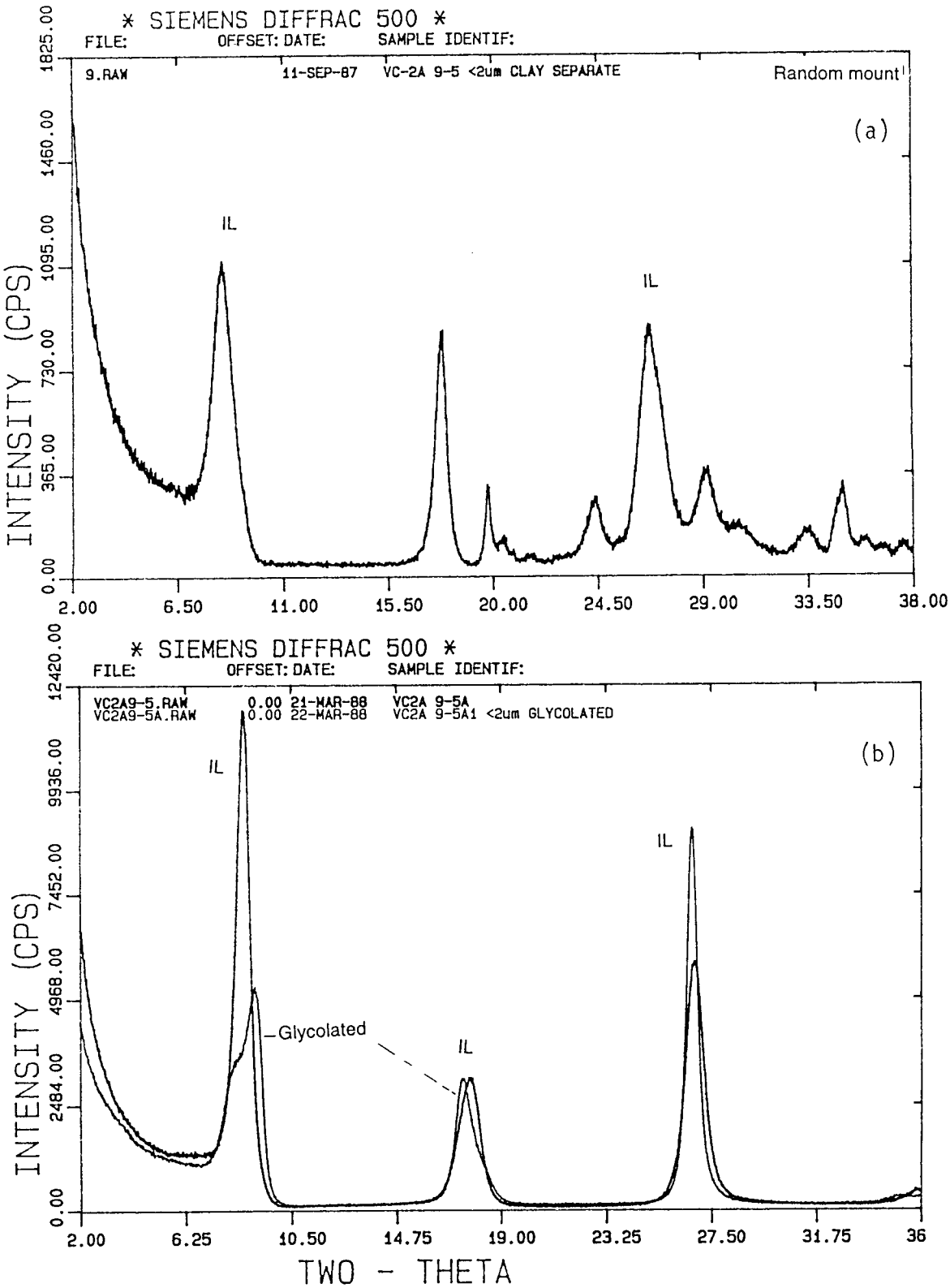

Fig. 4. Diffractograms of random (a) and oriented mount (b) of illitic clay VC-2A 9-5 indicating the amount of collapse after overnight glycolation at 60°C.

At Sulphur Springs gypsum occurs on the surface without other sulphate minerals in the extreme south of the main fumarole area (Charles et al. 1986). However, gypsum in hydrothermal deposits is stabilized below 57°C (Holland 1967) and could not have existed at the 406-m depth in a 200°C environment. It is suggested that the gypsum crystals (<2 μm) may have formed on the surface after the core was removed from the borehole (Robert Charles, LANL, personal communication, 1988) or during the processing of core samples for clay-size mineral separation. Mineralogical studies of Red Sea geothermal brines (44°-56°C) and sediments indicate that the most abundant form of sulfate is an admixture of anhydrite and some gypsum (Kaplan et al. 1969). According to these authors the gypsum formed by inversion from anhydrite during storage at low temperature and as authigenic euhedral crystals and twinned plates surrounding anhydrite prisms. Sediment samples washed by distilled water to remove brines may also cause anhydrite to revert to gypsum (Hardie 1967).

As briefly summarized in the introduction, the Cochiti mining district contains a wide variety of volcanic rocks (felsic and mafic) emplaced from at least 11.7 to 6.2 m.y. The hydrothermal alteration products of these rocks (<2 μm) are characterized by smectite, chlorite, interstratified I/S, and illite. Clay fractions from the altered late Miocene Bearhead Rhyolite are illitic with minor interstratified smectite. They exhibit the same amount of collapse as the VC-2A core hole illitic clays. Most of the andesites on the other hand contain interstratified I/S clays and chlorites. Generally chemical treatment followed by dialysis for about four days results in sharper diffractogram patterns than those in the untreated but mineralogically identical clays (Fig. 5).

The temperature ranges and nature of the fossil hydrothermal systems that were responsible for the alteration processes at Sulphur Springs (core hole VC-2A) and the Cochiti mining district are highlighted from published fluid inclusion studies (Wronkiewicz. et al. 1984; Hulen et al. 1987). Different salinities and temperature ranges were recognized at both locations. Wronkiewicz et al. (1984) recognized three types of primary fluid inclusions from quartz and calcite vein material in the Cochiti mining district. Homogenization temperatures for these primary fluids range between 193°-377°C, and the inclusions contain hydrothermal fluids displaying highly variable salinity equivalent of 0-5 wt% NaCl. Inclusions in quartz and fluorite from the VC-2A core hole are of low salinity (0.2-0.5 wt% NaCl) and are two phase

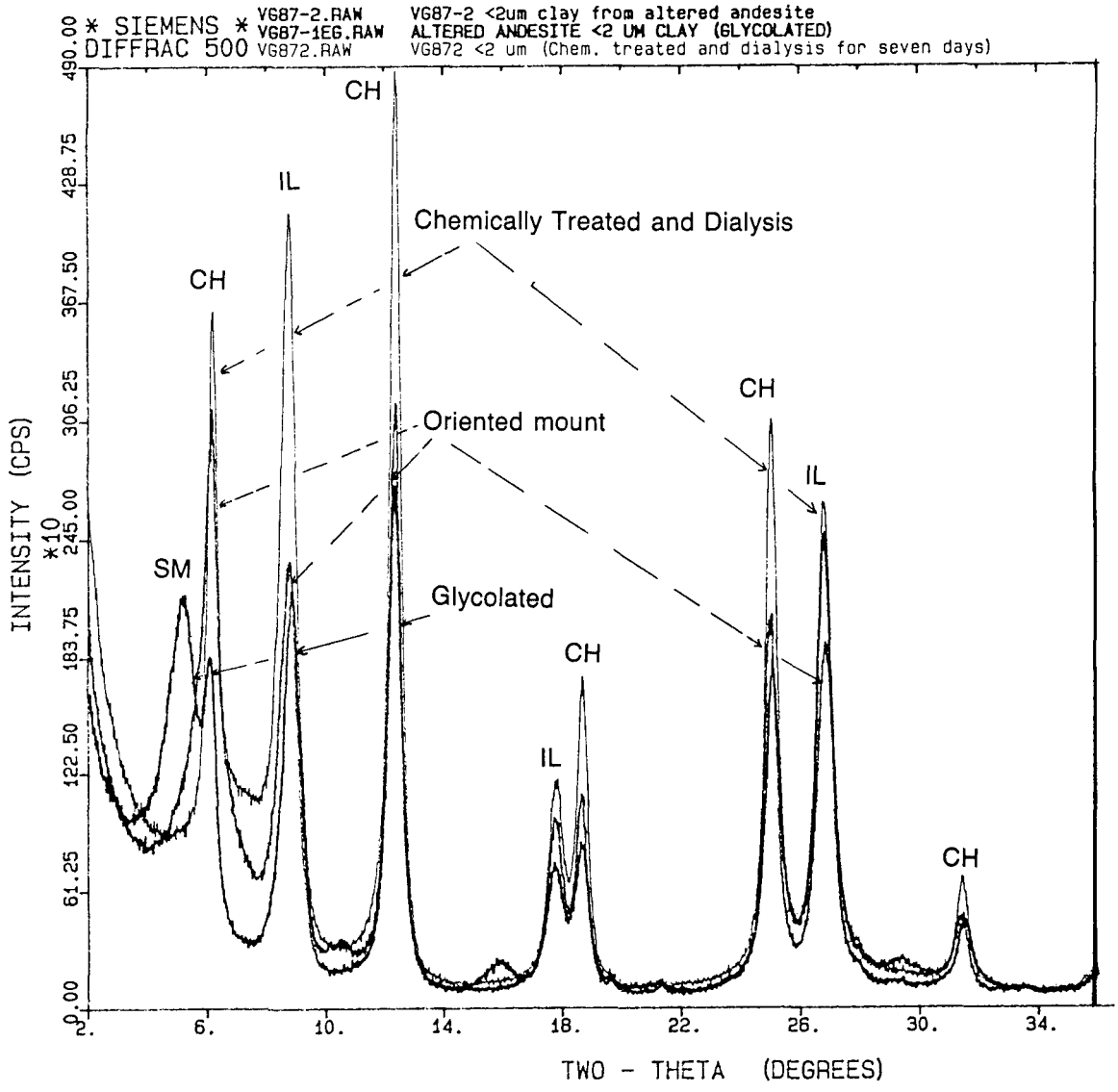

Fig. 5. Comparison of diffractogram patterns of chemically untreated and treated and glycolated clay fractions (<2 μm).

and water dominated at room temperature; they homogenize at temperatures between 195° and 215°C (Hulen et al. 1987). The paleotemperature gradients defined by these homogenization temperatures suggest a cooling trend in the hydrothermal system, so these fluid inclusions may have been trapped during the waning phases of the volcanic eruptions in the respective areas. Furthermore, these data indicate that two totally different hydrothermal pulses were responsible for the alteration-mineralization episodes at both localities. The Sulphur Springs inclusion fluids are very similar in salinity to deep fluids present in the hydrothermal system today (Goff et al. 1987).

Fluid inclusion information on hydrothermal fluids from the Paleozoic sequence (Abo Formation and Madera Limestone) of the VC-1 core hole located halfway between the Cochiti district and core hole VC-2A (Sulphur Springs) (Fig. 1) represents low- and high-salinity compositional groups (Hulen and Nielson 1988; Sasada 1988). Low (<1 wt% NaCl equivalent) and high (up to 5 wt% NaCl equivalent and higher) salinity inclusions homogenize to the liquid phase at temperatures ranging from 229.5° to 283.9°C and 189.4° to 245°C, respectively. The salinity and homogenization temperature data obtained in the Cochiti district and VC-2A core hole could correlate to either of the low or high compositional or thermal ranges documented in VC-1. The variation in salinities and homogenization temperatures in the three locations probably indicates that the magmatic-driven, meteoric, water-dominated hydrothermal fluids were different during different tectonomagmatic periods.

Understanding the tectonomagmatic setting of the three locations mentioned above is important to substantiate the salinity-homogenization temperature variations outlined in the previous paragraphs. As highlighted in the introduction, the Jemez volcanic field formed at the intersection of the NE-SW-trending Jemez Lineament and the Rio Grande rift (Aldrich 1986). Pervasive hydrothermal alteration in some parts of the Jemez volcanic field is apparent in the Cochiti mining district and in the Valles caldera complex. These areas were traversed by the late Miocene Canada de Cochiti fault systems and Quaternary caldera ring fractures, respectively. VC-2A was drilled between the western ring fracture of the caldera and the resurgent dome, whereas VC-1 is located along the precaldera Jemez fault zone adjacent to the southwest ring fracture of Valles caldera. The Valles caldera hydrothermal plume is structurally dominated by lateral flow through this fault zone (Goff et al. 1988). The low-salinity fluid inclusions that were trapped at shallow levels in the VC-1 hydrothermal breccias are younger than the high-salinity low-temperature inclusions and have been assigned to syn- or post-Valles/Toledo caldera formations (Hulen and Nielson 1988). The homogenization temperature difference between VC-1 and VC-2A inclusions can be explained as mentioned earlier by the fact that VC-1 was drilled along an older active fault zone, which has acted as the main channel to the hydrothermal plume of the Valles caldera. The older high-salinity low-temperature inclusions in VC-1 could belong to hydrothermal fluids associated with the Toledo caldera formation (<1.45 m.y. ago) or the Bearhead Rhyolite intrusion of the Cochiti mining

district about 16 km southeast of VC-1. Many (or all) of those inclusions in Precambrian clasts could have been trapped during Precambrian hydrothermal events (Jeff Hulen, UURI, personal communication, 1988). The high salinities (0-5 wt% NaCl) and the homogenization temperatures (193°-377°C) from the Cochiti district could be correlated spatially and temporally to the high-salinity (0-5 wt% NaCl equivalent) and low-homogenization-temperature (189.4°-245°C) fluids from VC-1. The younger hydrothermal fluid (<1 wt% NaCl equivalent and homogenization temperature 229 -283.9°C) from VC-1 was related as suggested by Hulen et al. (1987) to that observed in VC-2A (0.2-0.5 wt% NaCl equivalent and homogenization temperature of 193°-215°C).

Some of the ages (7 • 0.2 m.y. and 1.0 • 0.3 m.y.) obtained on clays from VC-1 (Ghazi and Wampler 1987) are similar to those obtained from VC-2A (0.83-0.66 m.y.) and the Cochiti district (8.07-5.60 m.y.), thereby supporting the hypothesis that the low and high salinities and temperatures obtained from the VC-1 fluid inclusions may have originated from two hydrothermal phases associated with the late Miocene Keres and Quaternary Tewa Group silicic eruptions.

The chemical composition and temperature of the geothermal fluid are evidently important factors controlling hydrothermal alteration. These high-temperature thermal environments enhance illite diagenesis. In the Salton Sea illite laths are transformed to platy illite in hotter zones (>200°C) (Glasmann 1987). Moreover, Whitney and Northrop (1987) have experimentally documented that illite/smectite formation proceeds from random interstratification to an ordered illite/smectite by solid-state transformation and dissolution/precipitation mechanism in a temperature range of 250°-450°C consistent with the fluid inclusion homogenization temperature ranges recognized in the Jemez volcanic field.

C. K/Ar Data

A total of 13 clay separates (<2 μm) and a devitrified whole rock rhyolite dike were dated by the K/Ar method, and the results are presented in Table I. Six of the illite clays were selected from various subsurface units of VC-2A, and the remaining seven were surface samples collected from the Cochiti mining district. The potassium contents (% K_2O) of the illite and interstratified illite/smectite clays vary from 7.34%-10.04% K_2O for felsic rocks and 1.4%-5.75% K_2O for the mafic flows (Table I). The illite from the near-surface volcaniclastic sediments (VC-2A 9-5) was found to be of recent age (0.0 • 0.10

m.y.). Because VC-2A was cored into an active hydrothermal system having acid-sulfate hot springs and surface temperatures near the boiling point (Goff et al. 1985; Charles et al. 1986), it is likely that this sample reflects the age of present surface alteration. Moreover, the maximum age (0.10 m.y.) obtained on the near-surface illite correlates to the last phase of volcanic eruptions (0.13 m.y.) along the southwest ring fracture of the Valles caldera (Smith and Bailey 1968; Marvin and Dodson 1979; Gardner et al. 1986; Self et al. 1988). The other five samples selected from various levels of VC-2A core hole range in age from 0.83-0.66 m.y., with an anomalous age of 1.1 m.y. from the middle section. The older age (1.1 m.y.) is questionable because the mass spectrometer (MS-10) filament was unstable and failed during the data acquisition. The age data suggest that the alteration phase and clay diagenesis took place about 0.3 m.y. after the formation of Valles caldera (1.12 m.y. ago; Doell et al. 1968). The age range suggests two possibilities about the timing of the hydrothermal alteration processes at Sulphur Springs. In the first case alteration processes started soon after caldera collapse (~1.12 m.y.), and clay products were subjected to high-temperature (>200°C) hydrothermal fluids until 0.83 m.y. when the system started to cool off. The other possibility is that the hydrothermal fluids responsible for the alteration processes were associated with the formation of the ring fracture rhyolites of the Valles caldera. Those ring fracture rhyolite domes closer to Sulphur Springs range in age between 0.88 and 0.54 m.y. (Doell et al. 1968). Faults and fracture systems reactivated or formed during the Valles caldera collapse and kept active during resurgence may have aided in channeling hydrothermal fluids responsible for the widespread phyllic-propylitic alterations recognized in and around the Valles caldera. This and the K/Ar data are consistent with the suggestion that resurgence was largely complete 100,000 years after the caldera formation or about 1.0 m.y. ago (Smith and Bailey 1968). Moreover, the shallow molybdenum mineralization in the intensely quartz-sericitized tuff of VC-2A was deposited toward the end of the hydrothermal event (0.66 m.y. ago). There is no evidence in VC-2A of a separate alteration event related to the formation of the Toledo caldera, even though that event must have been associated with a magmatic heat source similar to that of the Valles (Heiken et al. 1986). The clay K/Ar ages (0.83-0.66 m.y.) from VC-2A probably indicate a strong hydrothermal pulse at 0.83 m.y. ago and may have reset the ages of sericites formed previously during the Toledo

caldera-forming eruption at about 1.45 m.y. and during or after the Valles caldera collapse.

Surficial samples were collected randomly from a wide area of altered outcrops within and surrounding the Cochiti mining district (Fig. 1). Two concordant age groups were obtained on six clay fractions and a rhyolite sample (8.07 and 6.1-5.6 m.y.). The older age comes from an altered rhyolite flow, whereas the younger ones are from the Bearhead Rhyolite and a porphyritic andesite. Two I/S clay fractions from altered andesites (VG87-10 and VG87-12), collected from Keres Group rocks close to the southeast topographic margin of the Valles caldera (Fig. 1), are 6.45 and 6.51 m.y. old, respectively. An illite separate from a rhyolite flow (VG87-5) about 10 m east of the Albermarle quartz vein gave an age of 8.07 m.y. This rhyolite is older than the time range of the Bearhead Rhyolite eruptions (7.54-5.8 m.y.) and may belong to an older group of silicic flows (Canovas Canyon Rhyolite?; Fig. 1, inset stratigraphic column). The illite (VG87-6) from the Albermarle vein, a strongly brecciated and fractured zone, is 5.90 m.y. old. An altered and devitrified rhyolite dike (VG87-7), an illite fraction from a rhyolite flow (VG87-1), and a porphyritic andesite (VG87-2) close to these rhyolite intrusions range in age between 6.1 and 5.6 m.y. The Albermarle mineralized veins generally occupy a fault zone between Keres Group andesites, a quartz-monzodiorite stock (11.7 m.y., Stein 1983), and flows of the Bearhead Rhyolite (7.54-5.8 m.y.). It has been suggested that the mineralization was associated with the rhyolite intrusions (Wronkiewicz et al. 1984). A gradational age is observed between the main vein zone (5.9 m.y.) and that of the adjacent altered rhyolite (8.07 m.y.); however, the other altered silicic rocks are distributed a kilometer or more east of the main vein and their K/Ar ages are much younger (6.1-5.6 m.y.) implying different ages of eruption and alteration phases. The Bearhead Rhyolite flows are bracketed between 7.4 and 5.8 m.y. (Gardner and Goff 1984) and are similar to the clay ages (6.1-5.6 m.y.) mentioned above. This temporal and spatial relationship indicates that the alteration-mineralization process associated with the Cochiti veins took place more or less contemporaneously with the various units of the Bearhead Rhyolite extrusions, although the present data strongly indicate that the main alteration-mineralization episode along the Albermarle vein system and adjacent zones occurred about 5.9 m.y. ago.

D. Oxygen Isotope Data

All clay samples dated by the K/Ar method were also investigated for their oxygen-isotopic characteristics. The $\delta^{18}O$ values, although few in number, are used to compare and contrast the illite and interstratified illite/smectite clays from the various locations with published mineral, whole rock, and meteoric water isotope data from the area (Lambert and Epstein 1980; Vuataz and Goff 1986; Musgrave et al., in preparation). Such information can be used to delineate the origin of hydrothermal fluids responsible for the alteration-mineralization occurrences in volcanic regions (Taylor 1974; Criss and Taylor 1986).

The illites from the four main stratigraphic units of VC-2A gave similar isotopic results (Fig. 6, Table I) and get generally lighter with depth (+1.65 to -0.20°/oo), reflecting a possible approach toward isotopic equilibrium (Eslinger and Savin 1973a). However, unlike the trend shown by samples from the deeper levels, an illite separate (VC2A 9-5) from the near-surface breccia is lighter (+0.42°/oo). This value indicates probably a high-temperature (195°-215°C, Hulen et al. 1987) water-rock interaction consistent with the intense surface alteration of the active Sulphur Springs hydrothermal zone compared with the underlying shallow horizons that are partially altered as documented from petrographic examination (slightly altered feldspars). Several intervals deeper in the core hole are as altered as the near-surface rocks. A similar variation is indicated by $\delta^{18}O$ values of three quartz vein samples collected from altered cores. Fragments of quartz from vein (VC-2A 34-35) from the shallow levels (~40 m) are heavier (+2.95°/oo) than the clay fractions but slightly lighter than those reported by Musgrave et al. (in preparation) from three levels at about 59 m (4.0°/oo), 118 m (3.1°/oo), and 343 m (6.5°/oo). Such differences are attributed to resistance to isotopic exchange during hydrothermal interaction, to differences in isotope character and temperature of hydrothermal fluids with time, or to continuous hot meteoric water/rock interaction (Eslinger and Savin 1973a). However, the lighter $\delta^{18}O$ value (+2.95°/oo on quartz and +0.42°/oo on illite) from the near-surface samples of the active Sulphur Springs hydrothermal source zone is isotopically equilibrated and probably represents the effect of a younger hydrothermal phase unlike the rest of the core hole samples. This assumption is further supported by the fact that the near-surface alteration product is ~90% illitic and 0 ± 0.10 m.y. old. This implies that the fluids may have exceeded 200°C to form

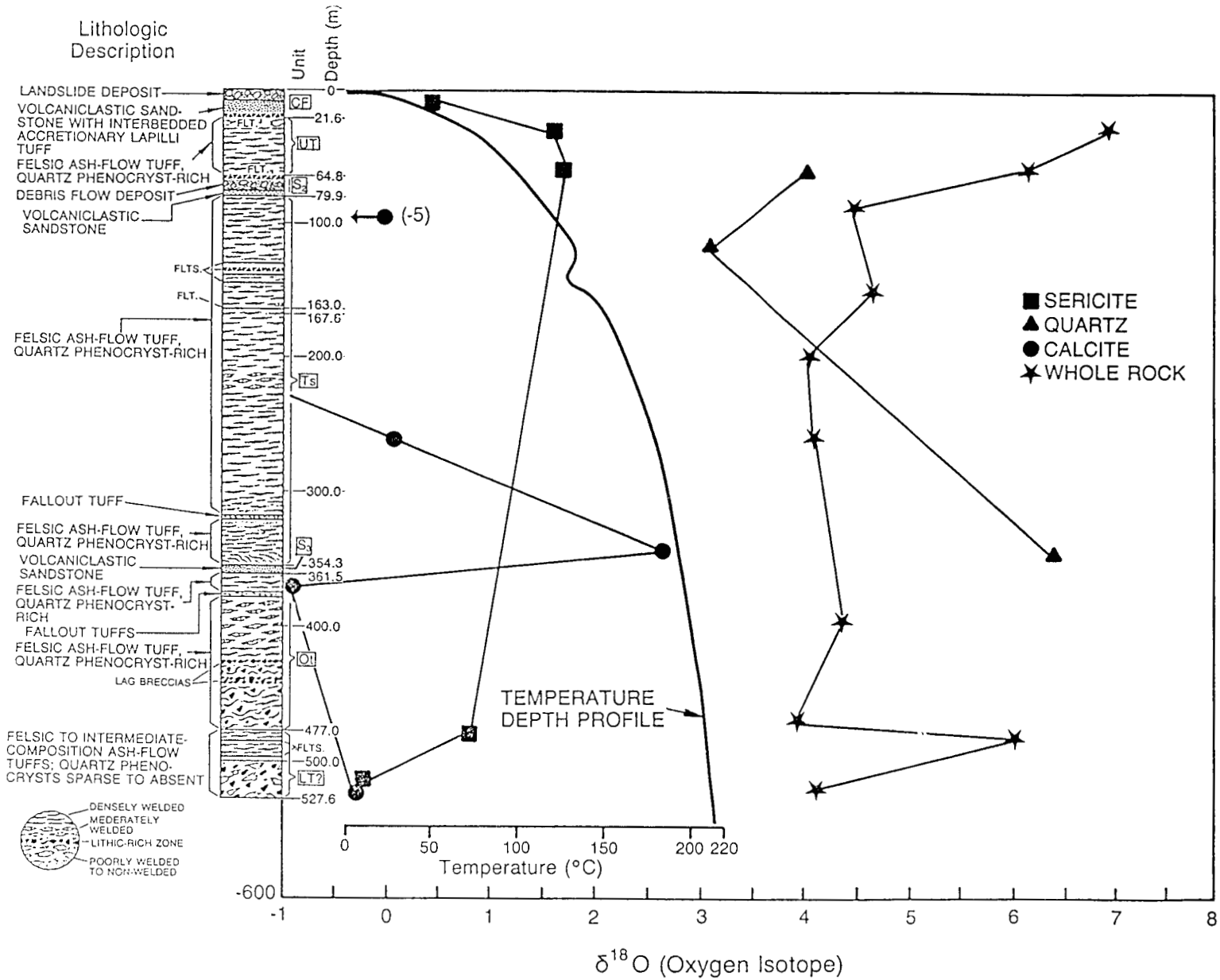

Fig. 6. Oxygen isotope ratios of hydrothermally altered whole rock samples, clays (sericite), minerals (quartz and calcite), and whole rocks from CSDP core hole VC-2A plotted as a function of depth (isotope data of whole rocks and minerals from Musgrave et al., in preparation), geologic section (CF = Caldera Fill; UT = Upper Tuffs; S_2 = S_2 Sandstone; Ts = Tshirege Member; S_3 = S_3 Sandstone; Ot = Otowi Member; LT = Lower Tuffs) and temperature depth profile after Hulen et al (1987).

the fairly pure illite as experimentally demonstrated by Eberl and Hower (1976), Roberson and Lahann (1981), Whitney and Northrop (1987), although these authors suggest that time, fluid, and solid compositions influence the course and rate of reaction in illite formation.

The illite from the Albermarle breccia zone (VG87-6) is much lighter (-2.15°/oo) than the adjacent surface samples and the VC-2A clay separates. Oxygen stable isotope data from the Cochiti area appear to be distributed zonally and to get heavier away from the vein zone, which is consistent with the argillic and propylitic zones around the vein system. The illite/smectite isotope data vary from -2.15°/oo at the vein zone to +0.49°/oo close to the vein (<10 m away), +2.98°/oo about 300-400 m outward and +5 to +7.97°/oo kilometers away, suggesting a decrease in temperature and water/rock interaction away from the vein. In general, among the altered volcanic rocks, the andesite clays are heavier than those obtained from the silicic units (Table I).

Whole rock and mineral (quartz and calcite) oxygen-, deuterium-, and carbon-isotope data (Musgrave et al., in preparation) on VC-2A samples exhibit general patterns similar to those of clay fractions (Fig. 6). The $\delta^{18}O$ values of altered whole rocks (+7 to +4.1°/oo) and $\delta^{13}C$ of calcite veins (-4.1 to -5.5°/oo) get lighter with depth, whereas δD values show the opposite trend (-148 to -85°/oo). Oxygen-isotope data of altered whole rocks are heavier by +4 to +6°/oo than are clay fractions due to incomplete alteration of the bulk rock, although rocks from the Valles caldera are regarded as having been moderately exchanged isotopically with a meteoric water-dominated hydrothermal fluid (Fig. 7) (Lambert and Epstein 1980).

The $\delta^{18}O$ of present-day meteoric waters in the Valles caldera average about -12°/oo, while hydrothermal fluids (220°-300°C) average about -9°/oo (Truesdell and Janik 1986; Shevenell et al. 1987). When the $\delta^{18}O$ of welded and devitrified Bandelier Tuff (+7.3 to +7.4°/oo) and its hydrothermally altered equivalent (+1.8 to +2.4°/oo) (Lambert and Epstein 1980) are considered, the illite fractions of the altered Bandelier Tuff from VC-2A (-0.20 to +1.65°/oo) are lighter but similar to the whole-rock-altered Bandelier Tuff in Baca No. 7, 700-930 m depth. At deeper levels (969-1539 m depth) in Baca No. 4, the Bandelier Tuff is even lighter than VC-2A samples, implying a more profound hydrothermal alteration at higher temperatures where the water-rock interaction generally leads to significant reduction of the $^{18}O/^{16}O$ of the rock with

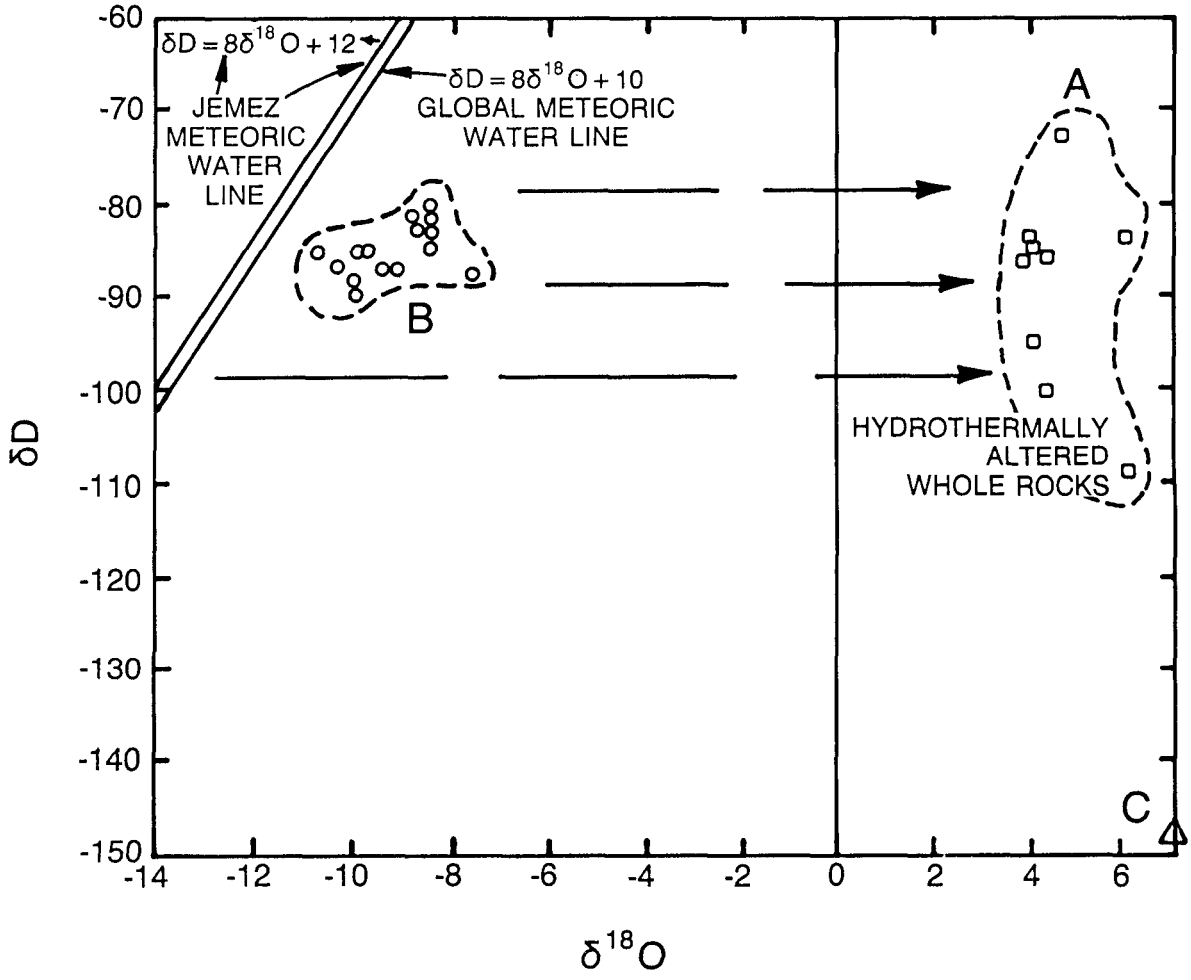

Fig. 7. Plot of δD versus $\delta^{18}O$ for various hydrothermally altered CSDP core hole VC-2A samples indicating (A) the influence of thermally driven meteoric water alteration (data from Musgrave et al., in preparation). Isotopes of present 220° to 300°C hydrothermal fluids (B) are from Truesdell and Janik (1986). One near-surface (29-m-deep) sample (C) is different from the rest of the altered rocks. Jemez Mountains meteoric line from Vuataz and Goff (1986).

corresponding enrichment of the water (Lambert and Epstein 1980; Criss and Taylor 1986). The oxygen-isotope variations of the clay fractions from Cochiti (late Miocene) and Sulphur Springs (Quaternary) are attributed mainly to temperature differences of 50°-100°C at the time of alteration rather than to isotopically different formation waters. Temperatures during alteration as deduced from fluid inclusions were higher in the Cochiti area (240°-315°C) than in VC-2A (195°-215°C) (Wronkiewicz et al. 1984; Hulen et al. 1987). Moreover, the general decrease with depth of $\delta^{18}O$ of whole rocks and clays samples (Figs.

6 and 7) indicates an approach toward isotopic equilibrium with increased temperature (Eslinger and Savin 1973a) and possibly time or water/rock ratio.

V. DISCUSSION

Evidence of fossil hydrothermal activity in the form of argillized aureoles and widespread alteration zones, pervasive silicification and oxidation, surficial acid-sulfate alteration, and active fumaroles and hot springs is well documented in the Valles caldera (Doell et al. 1968; Dondanville 1971, 1978; Goff and Gardner 1980; Stein 1983; Wronkiewicz et al. 1984; Hulen and Nielson 1986; Goff and Shevenell 1987). K/Ar ages and oxygen-isotopic data have been used to help constrain the conditions and timing of the different clay mineralogies that resulted from two major alteration events in the Jemez volcanic field.

As mentioned in the introduction, illitic material from a variety of geologic settings such as fossil hydrothermal systems and diagenetic processes can be dated by the K/Ar method (Aronson and Lee 1986; Eberl et al. 1987; Glasmann 1987). The ages of seven illitic and interstratified illite/smectite fractions from the Cochiti district and surrounding areas are late Miocene (8.07-5.6 m.y.) in age, whereas six other clay samples from the VC-2A core hole at Sulphur Springs are Quaternary in age (0.83-0 m.y.) with most ages bracketed around 0.75 m.y. The age ranges represent at least four phases of hydrothermal alteration (clay formation): 8.07 m.y., n = 1; 6.5-5.6 m.y., n = 6; 0.83-0.66 m.y., n = 4; and 0 ± 0.10 m.y., n = 1. The oldest event correlates with waning stages of the Paliza Canyon Formation andesitic volcanism (≥13 to ≤8.5 m.y.), whereas a somewhat younger event is consanguineous with intrusions and gold- and silver-bearing quartz veins associated with the Bearhead Rhyolite (7.54 to 5.8 m.y.). Most of the the K/Ar dates in the hydrothermally altered, caldera-fill rocks of core hole VC-2A developed about 0.3 m.y. after the formation of the Valles caldera (1.12 • 0.03 m.y.). A single age of 0 • 0.10 m.y. was obtained from a near-surface (upper 13 m of the hole) postcaldera acid-altered landslide debris. This probably represents the date of the current acid-sulphate hot spring activity through which VC-2A was cored. It is likely that this hydrothermal system is possibly related to the youngest silicic activity along the southwest ring fracture of the caldera dated at 0.13 m.y. (Gardner et al. 1986). Such a relationship would be consistent with recent data, obtained

using U-series geochronology (Goff and Shevenell 1987; Sturchio and Binz 1988), that suggest several hydrothermal periods, some of which are in the time range of 0.10 m.y. and less. Moreover, the difference in oxygen-isotope between the upper 13-m landslide debris (+0.42°/oo) and the rest of the deeper samples that get lighter with depth (+1.62 to -0.20°/oo) possibly indicates the effect of two types of hydrothermal fluids at Sulphur Springs similar to what prevails today: a deep-neutral-chloride fluid ≥200°C and a shallow acid sulphate fluid ≤120°C.

The tectonomagmatic activity in the Jemez volcanic field started about 16.5 • 1.4 m.y. ago (Gardner and Goff 1984; Gardner et al. 1986). This episode was followed by the Keres Group (13-6 m.y.) and Polvadera Group (Lobato Basalt, Tschicoma Formation, and El Ruchuelos Rhyolite; 14.05-2 m.y.) eruptions (Fig. 1, inset stratigraphic column). These flows and domes are composed of diverse magmatic types ranging from olivine tholeiite basalt to high silica rhyolite that are volumetrically dominated by andesite vented along dilational conduits of the Canada de Cochiti fault zone in the southeastern Jemez volcanic field. The K/Ar data on clay separates from the hydrothermally altered Paliza Canyon Formation andesites are similar to the age range of the unaltered rocks (13.2-7.4 m.y.). For example, illite and interstratified illite/smectite separates from two andesites and a rhyolite flow yielded dates of 8.07-6.45 m.y. However, the three samples were collected from widely separated sites (Fig. 1) and had undergone different degrees of alteration. The 8.07-m.y.-old rhyolite flow (VG87-5) is intruded by a 15-m-wide quartz vein system and is strongly brecciated, devitrified, thermally altered and contains abundant pyrite crystals. Fluid inclusion and oxygen-isotope data indicate that the rock was affected by a high-temperature hydrothermal fluid. Homogenization temperatures of primary inclusions in quartz and calcite veins from the Cochiti district suggest a primary hydrothermal temperature of 240° to 315°C (Wronkiewicz et al. 1984). Moreover, the rhyolite is depleted ($\delta^{18}O$ = +0.49°/oo), indicating a high-temperature fluid-rock interaction. However, the age and isotope data of an illite fraction from the vein zone (VG87-6) are younger (5.9 m.y.) and lighter (-2.15 °/oo) than the age (8.07 m.y.) and isotope value (+0.49°/oo) of the illite separates from the altered rhyolite sample (VG87-5) about 10 m away from the vein zone. It is suggested here that the clay ages represent two hydrothermal events, and the older clays were not

reset probably due to impermeability created by the high illite content in the older thermally altered rhyolite.

Unlike the rhyolite, the andesite samples (VG87-2 and VG87-10) were collected along shear zones a few kilometers to the northeast (Fig. 1). They are less altered by hydrothermal fluids, and their oxygen-isotope values are slightly depleted (+7.11 to +7.97°/oo), which is consistent with their peripheral location with respect to the vein-intruded fault zones. In like manner, illitic clays separated from altered Bearhead Rhyolite flows and dikes gave concordant ages (6.1-5.6 m.y.) that closely match the dates of the fresh rocks. The pervasive alteration responsible for the formation of propylitic and localized argillic zones is consistent with data related to illite diagenesis recognized in geothermal areas and experimental work as mentioned above. For example, in the Salton Sea, it has been reported (Glasmann 1987) that illite laths are formed from destablized smectites in a thermal gradient of 150°-200°C/km, whereas in the deeper zones (temperature >200°C) the illite laths are transformed to platy illite. These two alteration age groups demonstrate that rocks of the Cochiti mining district, which is considered to represent the exhumed interior of Keres Group volcanoes (Gardner et al. 1986), were affected by two hydrothermal events. This observation is consistent with an earlier study that recognized two hydrothermal phases induced by hydrothermal convection associated with the Paliza Canyon Formation and a second phase that postdated the Bearhead Rhyolite flows (Stein 1983; Wronkiewicz et al. 1984; Gardner et al. 1986). However, the present K/Ar data constrain precisely the temporal and spatial alteration processes in the area. The similarity between the ages of the clay and the unaltered units suggests that the alteration events were the result of meteoric-water-dominated late-stage residual hydrothermal fluids from either the latest dacitic eruptions of the Paliza Canyon Formation (10.1-7.4 m.y.) or the earliest flows of the Bearhead Rhyolite (7.54-5.8 m.y.).

Unlike the Cochiti district, which is characterized by late Miocene hydrothermal alteration activity, the VC-2A core hole samples from the Sulphur Springs area represent Quaternary events. The hydrothermal alteration-mineralization episodes formed after caldera collapse and were associated with post-caldera hydrothermal activity (Hulen et al. 1987). Most of the hydrothermally altered, caldera-fill rocks of core hole VC-2A developed between 0.83 and 0.66 m.y. ago, and another episode occurred 0.1 m.y. ago. These ages demonstrate a

progressive I/S formation from deeper to shallower levels. Additional thermal resetting was probably inhibited by the growth of clays and diminishing permeability in the altered rocks. Faults and fracture systems created and reactivated during collapse, resurgence of Valles caldera, and ring fracture postcaldera rhyolite intrusions may have aided in channeling hydrothermal fluids responsible for the widespread phyllic-propylitic alterations recognized in and around the caldera. The depletion of oxygen isotope values with depth is consistent with increased temperature. Whole rock and mineral (quartz and calcite) oxygen-, deuterium-, and carbon-isotope data (Musgrave et al., in preparation) on VC-2A samples exhibit similar general patterns as the clay fractions (Fig. 6). The $\delta^{18}O$ values of altered whole rocks (+7 to +4.1°/oo) and $\delta^{13}C$ of calcite veins (-4.1 to -5.5°/oo) get lighter with depth, whereas δD values show the opposite trend (-148 to -85°/oo). Oxygen-isotope data of altered whole rocks are heavier by +4 to +6°/oo than the clay fractions probably due to incomplete alteration of the bulk rocks (Fig. 6). Rocks from the Valles caldera are regarded as having been moderately exchanged isotopically with a meteoric water-dominated hydrothermal fluid (Lambert and Epstein 1980).

Data from VC-2A are consistent with K/Ar and uranium-series geochronology and paleomagnetic results from other locations in the Jemez Mountains (VC-1 and Soda Dam) (Ghazi and Wampler 1987; Goff and Shevenell 1987; Geissman 1988; Sturchio and Binz 1988), indicating that the Valles caldera hydrothermal system began development 1 m.y. ago. The growth of I/S at VC-2A spans an apparent time interval of 0.83 to 0.66 m.y. The near-surface breccia zone is leached and totally transformed to clays (>95% illite), compared with the underlying tuff that contains less affected feldspars and minor amounts of secondary silica. In the middle and bottom of the core hole, alteration is intense again. This would imply that the young (<0.10 m.y.) hydrothermal system at Sulphur Springs was confined to very shallow levels. The variation in the intensity of alteration can be attributed to the impermeability of welded tuffs to thermal fluids, the destruction of porosity by secondary mineral growth in pore spaces, and the localized hydrothermal entry points associated with fractured zones. The samples from greater depths are presently at temperatures near or at 200°C, a temperature that could have affected (lowered) the ages of these clays. The I/S at 40 m (0.66 m.y.) occurs in a zone of intense phyllic alteration

associated with the sub-ore-grade molybdenite, but this zone is now in a vapor cap of the Sulphur Springs hydrothermal system having a present temperature range of about 95°to 150°C.

Trainer (1984) has indicated that the vapor cap to the present Valles hydrothermal system developed well after initial formation of a liquid-dominated system. Based on cessation of travertine formation at Soda Dam (0.48 m.y., Goff and Shevenell 1987) and breaching of the southwestern caldera wall (0.50 to 0.43 m.y., Doell et al. 1968), Goff and Shevenell (1987) suggested that vapor cap formed sometime after 0.5 m.y. due to draining of caldera lakes, loss of hydraulic head, and lowering of water table. The dates from VC-2A indicate that the vapor cap formed no earlier than 0.66 m.y. ago. Moreover, the eruption of the El Cajete Pumice and the Banco Bonito Obsidian (0.13 m.y, Marvin and Dobson 1979) was regarded to have been responsible for the resumption of travertine deposition at Soda Dam about 0.11 m.y. ago (Goff and Shevenell 1987). This latest episode is contemporaneous with a single age of 0 ± 0.10 m.y on illitic clay from a near-surface postcaldera acid-altered landslide debris that probably represents the date of the current acid-sulphate hot spring activity through which VC-2A was cored. The temporal relationships of the travertine and illite formation indicate that the hydrothermal activities were related to the tectonomagmatic pulses of the active caldera environment.

In summary, alteration was pervasive (i.e., phyllic to advanced argillic) in the two areas of the Jemez volcanic field characterized by interstratified I/S clays. The K/Ar data indicate at least two fossil and one active hydrothermal episodes in the two localities. These hydrothermal fluids were contemporaneous with the waning phases of the tectonomagmatic activities in the late Miocene and early Pleistocene periods.

ACKNOWLEDGMENTS

I thank Grant Heiken and Fraser Goff for introducing me to the Jemez volcanic field and for making this study successful. I also thank James Aronson and Sam Savin, Geological Sciences, Case Western Reserve University, for allowing me access to their K/Ar and Stable Isotope Laboratories. Special thanks go to Linda Abel (of the same institution) for helping me obtain all the oxygen isotope data. I am grateful to Fraser Goff, Larry Maassen, and John Musgrave for helping me collect samples from the Cochiti mining district. Help from Dave Bish, Steve Chipera, and Roland Hagan in the use and interpretation

of XRD patterns and SEM images is gratefully acknowledged. Drafting of the figures by Anthony Garcia and typing of the manuscript by Barbara Hahn are greatly appreciated. The manuscript benefited greatly from the reviews of an earlier version by Dave Bish, Fraser Goff, Grant Heiken, and Jeff Hulen (University of Utah Research Institute). This project was funded by the U.S. Department of Energy, Office of Basic Energy Sciences, and by a Director-funded postdoctoral fellowship from Los Alamos National Laboratory.

REFERENCES

Aldrich, M.J., Jr., "Tectonics of the Jemez Lineament in the Jemez Mountains and Rio Grande Rift", J. Geophys. Res., 91, 1753-1762 (1986).

Aronson, J.L., and M. Lee, "K/Ar Systematics of Bentonite and Shale in a Contact Metamorphic Zone, Cerrillos, New Mexico," Clays Clay Miner., 34, 483-487 (1986).

Bailey, R.A., R.L. Smith, and C.S. Ross, "Stratigraphic Nomenclature of Volcanic Rocks in the Jemez Mountains, New Mexico," U.S. Geol. Surv. Bull., 1274-P, 29 pp. (1969).

Bish, D.L., "Detailed Mineralogical Characterization of the Bullfrog and Tram Members in USW-G1, with Emphasis on Clay Mineralogy," Los Alamos National Laboratory report LA-9021-MS (October 1981).

Charles, R.W., R.J. Vidale Bulen, and F. Goff, "An Interpretation of the Alteration Assemblages at Sulphur Springs, Valles Caldera, New Mexico," J. Geophys. Res., 91, B2, 1887-1897 (1986).

Clayton, R.N., and T.K. Mayeda, "Oxygen Isotope Exchange Between Quartz and Water," J. Geophys. Res., 77, 3057-3067 (1963).

Criss, R.E., and H.P. Taylor, "Meteoric-Hydrothermal Systems," in Valley, J.W., H.P. Taylor, and J.R. O'Neil (eds.), "Stable Isotopes in High-Temperature Geological Processes," Mineral. Soc. Am., 16, 373-424 (1986).

Doell, R.R., G.B. Dalrymple, R.L. Smith, and R.A. Bailey, "Paleomagnetism, Potassium-Argon Ages, and Geology of Rhyolites and Associated Rocks of the Valles Caldera," Mem. Geol. Soc. Am., 116, 211-248 (1968).

Dondanville, R.F., "The Hydrothermal Geology of the Valles Caldera, Jemez Mountains, New Mexico," Union Oil Co., Internal Rept., Univ. Utah Res. Inst., Earth Sci. Lab., Open-File Rept., NM/Baca 21, 36 pp. (1971).

Dondanville, R.F., "Geologic Characteristics of the Valles Caldera Geothermal System, New Mexico," Geoth. Res. Counc. Trans., 2, 157-160 (1978).

Eberl, D.D., and J. Hower, "Kinetics of Illite Formation," Geol. Soc. Am. Bull., 87, 1326-1330 (1976).

Eberl, D.D., J. Srodon, M. Lee, P.H. Nadeau, H.R. Northrop, "Sericite from the Silverton Caldera, Colorado: Correlation Among Structure, Composition, Origin, and Particle Thickness", Am. Mineral., 72, 914-934 (1987).

Eslinger, E.V., and S.M. Savin, "Mineralogy and Oxygen-Isotope Geothermometry of the Hydrothermally Altered Rocks of the Ohaki-Broadlands, New Zealand, Geothermal Area," Am. J. Sci., 273, 240-267 (1973a).

Eslinger, E.V., and S.M. Savin, "Oxygen-Isotope Geothermometry of the Burial Metamorphism Rocks of the Precambrian Belt Supergroup, Glacier National Park, Montana," Geol. Soc. Am. Bull., 84, 2549-2560 (1973b).

Gardner, J.N., and F. Goff, "Potassium-Argon Dates from the Jemez Volcanic Field: Implication for Tectonic Activity in the North-Central Rio Grande Rift," Field Conf. Guidebook N. M. Geol. Soc., 35, 75-81 (1984).

Gardner, J.N., F. Goff, S. Garcia, and R.C. Hagan, "Stratigraphic Relations and Lithologic Variations in the Jemez Volcanic Field, New Mexico," J. Geophys. Res., 91, No. B2, 1763-1778 (1986).

Geissman, J.W., "Paleomagnetism and Rock Magnetism of Quaternary Volcanic Rocks and Late Paleozoic Strata, VC-1 Core Hole, Valles Caldera, New Mexico, with Emphasis on Remagnetization of Late Paleozoic Strata," J. Geophys. Res., 93, B6, 6001-6026 (1988).

Ghazi, A.M., and J.M. Wampler, "Potassium-Argon Dates of Clays from Brecciated and Hydrothermally Altered Rocks from VC-1, Valles Caldera, New Mexico" (abs.), EOS, 68, 44, p. 1515 (1987).

Glasmann, J.R., "Smectite Diagenesis in Bentonites of the Shale Wall Member of the Seabee Formation, North Slope, Alaska" (abs.), AAPG Res. Conf., Radiogenic Isotopes and Evolution of Sedimentary Basins, New Orleans, Louisiana (1985).

Glasmann, J. R., "Argon Diffusion in Illite During Diagenesis: How Good is the K/Ar Clock?" (abs.), Clay Minerals Society 24th Annual Meeting, Socorro, New Mexico, p. 60 (1987).

Goff, F., and J.N. Gardner, "Geologic Map of the Sulphur Springs Area, Valles Caldera Geothermal System, New Mexico," Los Alamos Scientific Laboratory report LA-8634-MAP (1980).

Goff, F., and C.O. Grigsby, "Valles Caldera Geothermal Systems, New Mexico, USA," J. Hydrol., 56, 119-136 (1982).

Goff, F., and L. Shevenell, "Travertine Deposits of Soda Dam, New Mexico, and Their Implications for the Age and Evolution of the Valles Caldera Hydrothermal System," Geol. Soc. Am. Bull., 99, 292-302, (1987).

Goff, F., J.N. Gardner, R. Vidale, and R. Charles, "Geochemistry and Isotopes of Fluids from Sulphur Springs, Valles Caldera, New Mexico," J. Volcanol. Geotherm. Res., 23, 273-297 (1985).

Goff, F., J. Rowley, J.N. Gardner, W. Hawkins, S. Goff, R. Charles, D. Wachs, L. Maassen, and G. Heiken, "Initial Results from VC-1 First Continental Scientific Drilling Program Corehole in Valles Caldera, New Mexico," J. Geophys. Res., 91, 1742-1752 (1986).

Goff, F., D.L. Nielson, J.N. Gardner, J.B. Hulen, P. Lysne, L. Shevenell, and J.C. Rowley, "Scientific drilling at Sulphur Springs, Valles Caldera, New Mexico, Core Hole VC-2A," EOS, 68, 661-662 (1987).

Goff, F., L. Shevenell, J.N. Gardner, F.-D. Vuataz, and C. O. Grigsby, "The Hydrothermal Outflow Plume of Valles Caldera, New Mexico, and A Comparison with Other Outflow Plumes," J. Geophys. Res., 93, No. B6, 6041-6058 (1988).

Hardie, L.A., "The Gypsum-Anhydrite Equilibrium at One Atmosphere Pressure," Am. Mineral., 52, 171 (1967).

Heiken, G., F. Goff, J. Stix, S. Tamanyu, M. Shafiqullah, S. Garcia, and R. Hagan, "Intracaldera Volcanic Activity, Toledo Caldera and Embayment, Jemez Mountains, New Mexico," J. Geophys. Res., 91, 1799-1815 (1986.)

Holland, H.D., "Gangue Minerals in Hydrothermal Deposits," in Barnes, H.L. (ed.), Geochemistry of Hydrothermal Ore Deposits (Holt, Rinehart, and Winston, Inc., New York, 1967) pp. 382-436.

Horton, D.G., "Mixed-Layer Illite/Smectite as a Paleotemperature Indicator in the Amethyst Vein System, Creede District, Colorado, USA," Contrib. Mineral. and Petrol., 91, 171-179 (1985).

Hulen, J.B., and D.L. Nielson, "Stratigraphy of the Bandelier Tuff and Characterization of High-Level Clay Alteration in Borehole B-20, Redondo Creek Area, Valles Caldera, New Mexico," Geoth. Res. Counc. Trans., 7, 163-168 (1983).

Hulen, J.B., and D.L. Nielson, "Hydrothermal Alteration in the Baca Geothermal System, Rodondo Dome, Valles Caldera, New Mexico," J. Geophys. Res., 91, 1867-1886 (1986).

Hulen, J.B., and D.L. Nielson, "Hydrothermal Brecciation in the Jemez Fault Zone, Valles Caldera, New Mexico--Results from CSDP Corehole VC-1," J. Geophys. Res., 93, 6077-6090 (1988).

Hulen, J.B., D.L. Nielson, F. Goff, J.N. Gardner, R. Charles, "Molybdenum Mineralization in an Active Geothermal System, Valles Caldera, New Mexico," Geology, 15, 748-752 (1987).

Hulen, J.B., J.N. Gardner, J.D. Nielson, and F. Goff, "Stratigraphy, Structure, Hydrothermal Alteration and Ore Mineralization Encountered in CSDP Core Hole VC-2A, Valles Caldera, New Mexico: A Detailed Overview," Univ. of Utah Res. Inst., Earth Sci. Lab. Rept. ESL-88001-TR, 44 pp. (1988).

Izett, G., J. Obradovich, C. Naeser, and G. Cebula, "K/Ar and Fission Track Zircon Ages of Cerro Toledo Rhyolite Tephra Units in the Jemez Mountains, New Mexico," U.S. Geol. Surv. Prof. Pap., 1199, 37-41 (1980).

Jackson, M.L., "Soil Chemical Analysis: Advanced Course, Univ. of Wisconsin, College of Agriculture, Dept. of Soils, Madison, Wisconsin," Edition 2 (1978).

Kaplan, I.R., R.E. Sweeney, and A. Nissenbaum, "Sulfur Isotope Studies on Red Sea Geothermal Brines and Sediments," in Degens, E.T., and D.A. Ross (eds.), Hot Brines and Recent Heavy Metal Deposits in the Red Sea: A Geochemical and Geophysical Account (Springer-Verlag, New York, 1969) pp. 474-498.

Lambert, S.J., and S. Epstein, "Stable Isotope Investigation of an Active Geothermal System in Valles Caldera, Jemez Mountains, New Mexico," J. Volcanol. Geoth. Res., 8, 111-129 (1980).

Laughlin, A.W., "The Geothermal System of the Jemez Mountains, New Mexico, and Its Exploration," in Geothermal Systems: Principles and Case Histories, Rybach, L., and L.J.P. Muffler (eds.) (John Wiley and Sons, Inc., New York, 1981), pp. 295-320.

Marvin, R.F., and S.W. Dobson, "Radiometric Ages: Compilation B, U.S. Geol. Surv.," Isochron/West, 26, 3-32 (1979).

Musgrave, J., F. Goff, L. Shevenell, P.E. Trujillo, D. Counce, G. Luedemann, S. Garcia, B. Dennis, J.B. Hulen, C. Janik, and F.A. Tomei, "Selected Data from Continental Scientific Drilling Core Holes VC-1 and VC-2A, Valles Caldera, New Mexico," in preparation.

Nielson, D. L. and J. B. Hulen, "Internal Geology and Evolution of the Redondo Dome, Valles Caldera, New Mexico," J. Geophys. Res., 89, 8695-8711 (1984).

Reynolds, R. C., "Interstratified Clay Minerals in Crystal Structures of Clay Minerals and Their X-Ray Identification," Min. Soc. London Mon., 5, 249-304 (1980).

Roberson, H.E., and R.W. Lahann, "Smectite to Illite Conversion Rates: Effects of Solution Chemistry," Clays Clay Miner., 29, 129-135 (1981).

Sasada, M., "Microthermometry of Fluid Inclusions from the VC-1 Corehole in Valles Caldera, New Mexico," J. Geophys. Res. (in press).

Self, S., F. Goff, J.N. Gardner, J.V. Wright, and W. Kite, "Explosive Rhyolitic Volcanism in the Jemez Mountains, Vent Location, Caldera Development, and Relation to Regional Structure," J. Geophys. Res., 91, 1779-1798 (1986).

Self, S., D.E. Kircher, and J.A. Wolff, "The El Cajete Series, Valles Caldera, New Mexico," J. Geophys. Res., 93, B6, 6113-6128 (1988).

Shevenell, L., F. Goff, F. Vuataz, P.E. Trujillo, D. Counce, C. Janik, and B. Evans, "Hydrogeochemical Data for Thermal and Nonthermal Waters and Gases of the Valles Caldera, Southern Jemez Mountains Region, New Mexico," Los Alamos National Laboratory report LA-10923-OBES (1987), 100 pp.

Sillitoe, R.H., "Epochs of Intrusion-Related Copper Mineralization in the Andes," J. S. Am. Earth Sci., 1, 89-107 (1988).

Smith, R.L., "Ash-Flow Magmatism," Spec. Pap. Geol. Soc. Am., 180, 5-27 (1979).

Smith, R.L., and R.A. Bailey, Resurgent Cauldrons," Mem. Geol. Soc. Am., 116, 613-662 (1968).

Smith, R.L., R.A. Bailey, and C.S. Ross, "Geologic Map of the Jemez Mountains, New Mexico," U.S. Geol. Surv. Misc. Invest. Map I-571 (1970).

Srodon, J., and D.D. Eberl, "Illite in Mica," in Bailey, S.W. (ed.), Min. Soc. America, "Review in Mineralogy," 13, 498-544 (1984).

Steiger, R.H., and E. Jager, "Subcommission on Geochronology: Convention on the Use of Decay Constants in Geo- and Cosmochronology," Earth Planet Sci. Lett., 36, 359-362 (1977).

Stein, H.L., "Geology of the Cochiti Mining District, Jemez Mountains, New Mexico," M.S. thesis, Univ. of New Mexico, Albuquerque, NM, 122 pp. (1983).

Sturchio, N.C., and C.M. Binz, "Uranium-Series Age Determination of Calcite Veins, VC-1 Drill Core, Valles Caldera, New Mexico," J. Geophys. Res., 93, 6097-6102 (1988).

Taylor, H. P., "The Application of Oxygen and Hydrogen Isotope Studies to Problems of Hydrothermal Alteration and Ore Deposition," Econ. Geol., 69, 843-883 (1974).

Taylor, H.P., "Oxygen and Hydrogen Isotope Relationships in Hydrothermal Mineral Deposits," in Barnes, H.L. (ed.), Geochemistry of Hydrothermal Ore Deposits" (Wiley and Sons, Inc., New York, 1976), 236-277.

Trainer, F. W., "Thermal Mineral Springs in Canon de San Diego as a Window into Valles Caldera, New Mexico," in Rio Grande Rift: Northern New Mexico, Baldridge, S. W., P.W. Dickerson, R.E. Riecker, and J. Zidek (eds.), New Mexico Geological Society Thirty-Fifth Annual Field Conference, pp. 249-256 (1984).

Truesdell, A.H., and C.J. Janik, "Reservoir Processes and Fluid Origin in the Baca Geothermal System, Valles Caldera, New Mexico," J. Geophys. Res., 91, 1817-1833 (1986).

Vuataz, F., and F. Goff, "Isotope Geochemistry of Thermal and Nonthermal Waters in the Valles Caldera, New Mexico," J. Geophys. Res., 91, 1835-1853 (1986).

Weaver, C.E., and L.D. Pollard, The Chemistry of Clay Minerals (Elsevier, Amsterdam, 1975).

Whitney, G., and H.R. Northrop, "Experimental Investigation of the Smectite to Illite Reaction: Dual Reaction Mechanisms and Oxygen-Isotope Systematics," Am. Mineral., 73, 77-90 (1987).

Wronkiewicz, D.J., D.I. Norman, G.A. Parkison, and K.M. Emanuel, "Geology of the Cochiti Mining District, Sandoval County, New Mexico," N.M. Geol. Soc. Guidebook, 35, 219-222 (1984).

APPENDIX A

SELECTED PETROGRAPHIC DESCRIPTIONS

I. VC2A

9-4 (7.62-9.91 m)	Altered breccia and volcaniclastic sediments with abundant rock fragments. Feldspars are mostly altered to sericite, whereas quartz grains are anhedral and fractured and contain abundant trains of inclusions. Secondary silica overgrowth observed around primary quartz grains, without optical discontinuity. Matrix is recrystallized and pumice and glass shards(?) are also recrystallized and show pectinate structures. Pyrite crystals are common in cavities, and minor apatite grains were noted.
9-5 (9.91-12.99 m)	Volcaniclastic sediment: It contains abundant rock fragments. The matrix is constituted by recrystallized silica and sericite, possibly derived from the alteration of rock fragments and feldspars. Rock contains 10%-15% of crystal contents, mostly dominated by crushed quartz grains, with wavy extinctions and conchoidal fractures. Secondary silica overgrowth, represented by cherty aggregates, is common. Feldspars are mostly transformed to sericite. Euhedral pyrite grains are associated with the sericite. Pyrite grains formed after the formation of sericite.
24-9 (24.09-25.79 m)	Altered Upper Tuff. The rock contains less than 5% crystal. The matrix is constituted by abundant sericite and secondary cherty silica. Primary quartz grains are cracked and show wavy extinctions. Rock fragments are mostly represented by altered pumice fragments. Coarse muscovite and pyrite crystals were also noted. Grain contacts indicate that the order of formation is represented by sericite, secondary silica aggregates, and pyrite.
28-9 (30.18-32.16 m)	Altered and welded Upper Tuff. The rock is altered and strongly recrystallized. It is generally crystal poor, except for few fractured (cracked) quartz grains with abundant inclusions and feldspars totally altered to sericite. The collapsed pumice and other rock fragments are also transformed to sericite. Abundant secondary silica (cherty) and euhedral pyrite grains are also common.
34-1 (38.41-40.40 m)	Moderately altered Upper Tuff. This rock is less thermally altered, compared with the overlying samples described above. The matrix of the rock is characterized by recrystallized glass with abundant secondary silica. Collapsed pumice fragments show

	pectinate structures caused by the recrystallization of silica. Resorbed quartz grains are wrapped with sericite. Sericite in feldspars is confined to cleavage traces. Sericite preceded secondary silica and pyrite crystallization respectively.
43-5 (46.95-49.33)	Partially altered Upper Tuff. Moderately altered and recrystallized. The rock is similar to the previous sample (34-1). Welded shards and pumice clasts are recrystallized to silica with cherty aggregates representing several veinlets. Radial chalcedony replacing pumice clasts is also common (spherulitic). Feldspars are partly altered to sericite, whereas quartz grains are cracked. Vein filling preceded with sericite and was followed by secondary cherty silica growth. Two stages of sericite formation are recognized. The sequence of formation is represented by sericite, secondary silica, sericite, and pyrite. Euhedral pyrite grains are mostly confined to cavities.
54-3 (62.96-64.79 m)	Altered Upper Tuff. The rock is altered and contains abundant recrystallized secondary silica (cherty). Feldspars are altered to sericite. Resorbed quartz grains have silica overgrowth around them. Minor amounts of pyrite are also noted. Total crystal content is less than 2%.
55-2A (64.79-67.13 m)	Volcaniclastic sediments (S_2). Alteration followed by widespread recrystallization dominated by secondary silica, sometimes aggregating in cavities. Crystal poor (1%) with the feldspars totally sericitized. A dark brown clayey staff dominates the matrix. Pyrite and epidote form accessory secondary minerals.
63-5A (74.24-77.13 m)	Volcaniclastic sediment (S_2). Rock contains abundant subrounded to rounded quartz grains. These grains are rimmed by silica overgrowth and cherty aggregates. Microcrystalline silica also replaced altered feldspars. The interstices between the mineral grains are filled by sericites. Some feldspars show "microcline-type" twinning, possibly derived from the basement rocks. Three types of quartz grains are noted: (1) strained quartz with undulatory extinction, (2) clear unstrained grains, and (3) clear unstrained grains with secondary overgrowth. Crystal contents of the rock are almost 50%.
71-2B (88.72-91.16 m)	Partially altered Tshirege Tuff. Rock is crystal rich (>10%) with partially recrystallized matrix. Feldspars are moderately sericitized and quartz grains are coarse, anhedral, and strongly strained (sheared cracks) with secondary silica growth. Pyrite crystals are confined to altered feldspars or cavities. Two

	phases of sericite formed before and after the cherty silica crystallization. Pyrite is the last mineral to form.
84-2 (108.54-110.82 m)	Partially altered Tshirege Tuff. Rock is crystal rich (>10%) with matrix altered and recrystallized. Quartz grains are anhedral and coarse and contain silica overgrowth along their edges. Feldspars are moderately sericitized. Pyrites are confined to cavities. Relicts of altered shards and collapsed pumice are replaced by secondary silica aggregates (cherty).
104-3 (136.07-138.26 m)	Altered Tshirege Tuff. Rock has lesser amount of crystal contents, compared with previous sample (84-2). Quartz grains show a glomeroporphyritic texture, whereas feldspars are scattered and moderately altered to sericite. Secondary silica and sericite are concentrated along cracks as veinlets. Rock contains abundant minute grains of pyrite.
119-9 (158.99-161.25 m)	Moderately altered Tshirege Tuff. Sparsely crystal-rich rock (~5%) with feldspars partially sericitized and cracked subangular quartz grains. Matrix dominated by secondary silica aggregates and sericite. Pyrite is also widely distributed in the matrix. Sericite formation was followed by secondary silica and pyrite.
156-7 (213.11-215.55 m)	Moderately altered Tshirege Tuff. Crystal-rich rock (15%-20%) with strongly recrystallized (devitrified) matrix containing microcrystalline silica. Devitrified glass, shard-wrapped quartz, and feldspar grains. Recrystallized pumice clasts are noted. Minor pyrite and allanite grains constitute the secondary minerals.
184-4A (255.79-257.93 m)	Altered Tshirege Tuff. The rock is moderately welded and contains few recrystallized pumice clasts. It contains 10%-15% crystals with plagioclase, moderately altered to sericite and calcite. Quartz grains are subrounded (resorbed?) and contain secondary silica overgrowth. Spherulitic textures, represented by silica aggregates, are also noted. From grain contacts calcite seems to have formed after sericite.
197-3B (277.16-279.73 m)	Moderately altered and welded Tshirege Tuff. Rock is similar to the previous example (184-4A). It contains recrystallized pumice clasts, partially altered feldspar, and resorbed quartz grains. Calcite is the dominant secondary mineral followed by sericite, chlorite, pyrite, and microcrystalline silica. Calcite is confined to the altered feldspars. The order of formation among the secondary minerals is

	represented by sericite, calcite, chlorite, and pyrite.
209-12 (293.6-296.34 m)	Altered Tshirege Tuff. Rock is similar to the previous example (197-3B). Matrix is strongly dominated by secondary silica. Altered feldspars are replaced by calcite, whereas quartz grains are moderately resorbed and cracked and contain abundant inclusions. Rock is constituted by 10%-15% crystals with secondary minerals of sericite, secondary silica, calcite, chlorite, and pyrite in chronological order. Feldspars show polysynthetic twinning (plagioclase composition). Some spherulitic textures also observed.
230-5 (325.49-327.93 m)	Moderately altered welded Tuff. Matrix is devitrified and contains recrystallized collapsed pumice clasts and other rock fragments. Rock contains 10%-15% crystals dominated by feldspar replaced by calcite. Quartz grains are moderately resorbed and cracked. Secondary minerals are represented by sericite, secondary silica, calcite, chlorite, and pyrite in chronological order.
249-1B (351.98-354.57 m)	Altered and welded Tshirege Tuff. Rock is crystal rich (~15%) with matrix and collapsed pumice fragments strongly recrystallized (devitrified) to secondary silica. Feldspars are moderately altered but without significant sericite or calcite replacement. Quartz grains are partially resorbed and strained with numerous cracks. Few euhedral pyrite grains observed.
255-2B 359.24-362.20 m)	Sandstone? (S_3). Rock is crystal rich (~35%) with angular to subrounded quartz grains. Feldspars are of minor content and are partly altered. Some mineral grains are strained and show variable twinning patterns, probably implying their xenocrystic origin. Calcite and sericite replaced feldspars and occur in cavities too. Rock fragments are replaced by secondary silica. Minor pyrite and epidote are noted.
256-2 (362.2-362.8 m)	Altered and welded Otowi Tuff. Rock characterized by strongly devitrified (recrystallized) matrix, pumice clasts, and glass shards. Crystal contents are about 5% with coarse, fractured, and partly resorbed quartz grains. Feldspars are replaced by sericite and calcite. Secondary silica overgrowth noted around primary quartz grains. Pyrite crystals are confined to cavities and altered feldspars following the formation of sericite and calcite.
263-3B (371.49-373.78 m)	Altered Otowi Tuff. Matrix and pumice fragments are strongly recrystallized. Rock contains coarse and cracked quartz grains, whereas the feldspars are totally replaced with calcite and sericite. A dark

	brownish-gray clayey staff is associated with the altered matrix. Pyrite and chlorite also form part of the secondary mineral aggregates.
264-2B (373.78-376.43 m)	Altered welded Tuff. Matrix represented by welded glass and collapsed pumice clasts with sericite and calcite disseminations. Quartz grains contain silica overgrowth, whereas the feldspars are replaced by sericite and calcite. Minor pyrite grains are scattered throughout the rock associated with secondary silica. Sericite, secondary silica, calcite, and pyrite formed in chronological order.
277-1 (391.71-394.21 m)	Altered Otowi Tuff. Matrix is replaced by secondary silica, calcite, and sericite. Phenocrysts are represented by corroded edges, occasionally with secondary silica overgrowth. Feldspar grains totally transformed and replaced by calcite and sericite. Abundant euhedral pyrite grains are associated with the secondary minerals.
285-1 (405.79-408.08 m)	Altered and welded Otowi Tuff. Rock contains less than 5% crystals. The phenocrysts (mostly quartz) are meshed in a sericite matrix. Welded pumice fragments are replaced by sericite and secondary silica. Coarse and glomeroporphyritic muscovite is associated with altered feldspars. Rock characterized by a layered sequence of a strongly recrystallized and poorly altered matrix. A few scattered pyrite grains are also noted.
298-16 (426.68-429.12 m)	Altered Otowi Tuff. Fairly crystal-poor rock (<2%). Phenocrysts represented by coarse quartz grains and moderately altered feldspars (plagioclase). Sericite and calcite are the replacement minerals. Welded shards are also replaced by secondary silica aggregates (cherty) and sericite.
323D (460.98-463.41 m)	Altered Otowi Tuff. Fairly crystal-poor rock (<5%). Matrix is replaced by secondary silica and sericite. Feldspars (plagioclase) are moderately altered and filled with calcite and sericite. Quartz grains are corroded and contain cherty aggregates of secondary silica. A few altered andesitic lithics are also noted.
336E (480.18-482.93 m)	Altered pre-Bandelier tuff. It is a crystal-poor rock (<1%), and the matrix is dominated by sericite and secondary silica aggregates (cherty). Welded pumice fragments and shards are replaced and show linear aggregates of sericite and silica. Totally altered rock fragments and accretionary lapilli (>4 mm) are commonly noted. Sericite, silica, calcite, chlorite, and abundant pyrite crystals form the bulk of the secondary minerals in a chronological order.

366D (524.70-527.44 m) Altered pre-Bandelier tuff. Rock is characterized by devitrified matrix with secondary silica and sericite. A few phenocrysts of partially altered feldspars and corroded quartz are associated with chloritized andesitic rock fragments. Calcite replacement confined to altered feldspars.

II. FIELD AND PETROGRAPHIC DESCRIPTIONS OF SURFICIAL, ALTERED SAMPLES FROM COCHITI DISTRICT (See Fig. 1 for sample location.)

VG87-1 Dacite? Rock exposed along a roadcut (Forest Route 268) underlying the Bandelier Tuff. It is totally altered, friable, and limonite coated. It is porphyritic with altered (ghost) phenocrysts. In thin section, the phenocrysts are moderately altered and are represented by sericitized plagioclase, hornblende, pyrite, and abundant silica overgrowth (cherty). Coarse recrystallized silica are confined to "healed" cracks.

VG87-2 Porphyritic andesite. Sample collected from an adit south of the dacite outcrop (Route 268). It is greenish gray and contains coarse plagioclase phenocrysts, epidote, and chlorites. In thin section the rock is olive brown with plagioclase pseudomorphs transformed to granular and radial crystals of secondary silica. The rock is spherulitic and contains few rock fragments.

VG87-3 Rhyolite? Soft and whitish in color. Phenocrysts are altered and the rock underlies the Bandelier pyroclastic sequence. Petrographic examination indicates moderately altered alkali feldspar partially replaced with calcite. Matrix is recrystallized and contains abundant microlites wrapping around the phenocrysts. Cavities are filled with cherty secondary silica with pectinate structures. Epidote, pyrite, and rock fragments are also noted.

VG87-4 Dacite. Collected along the road to the Albermarle Mine, south of the main entrance to the Bland Mine. The rock is soft, white, and limonite coated. Feldspar phenocrysts are moderately altered. Plagioclase with albite twinning dominate the crystal contents. The matrix contains abundant secondary silica and sericite. Calcite is associated with the altered feldspars.

VG87-5 Rhyolite. Flow banded and fine grained, partially silicified (microveinlets). It is yellowish gray and contains abundant tiny crystals of pyrite. The rock is platy and crops out east of the Albermarle quartz vein (~10 m). In thin section, the rock is strongly recrystallized showing a granular texture with interlocking quartz grains. Perlitic cracks filled with secondary silica and sericite are also common. Tiny silica-filled veinlets cut the matrix in random directions.

VG87-6 Fault (vein) breccia. Sample collected along the roof of an adit along the main Albermarle quartz vein. The rock is

strongly brecciated, pyritized, and silicified. It shatters into pieces when hammered. In thin section it is dominated by recrystallized cherty silica and sericite. The rock is strongly sheared. Aggregates of epidote, euhedral pyrite crystals, and needlelike grains of rutile(?) were noted. Abundant silica veinlets cut the matrix.

VG87-7 Rhyolite dike. Very fine grained, white, dotted with brown spots (hematite). Collected about 1/2 km east of the Albermarle vein. The dike cuts a coarse andesitic flow. The rock is sparsely porphyritic with a strongly recrystallized and sericitized matrix. Quartz, alkali feldspar, minor hornblende, and zircon are the essential phenocrysts; however, muscovite from recrystallized sericite and calcite are also noted. The rock exhibits a spherulitic texture.

VG87-8 Andesite. It is greenish gray and coarse porphyritic with altered phenocrysts. Collected about 1 km south of the Bland Mining entrance (Route 268). In thin section the coarse plagioclase phenocrysts are replaced with calcite. Hornblende, biotite, magnetite, minor apatite, chlorite, and abundant silica overgrowth are the main mineral assemblages.

VG87-9 Andesite. Porphyritic, strongly sheared, and altered. Section is exposed along a road cut. The sheared zones are colorful ranging from violet to yellowish brown implying a different degree of alteration. The rock is extremely friable and was not studied petrographically. Collected along Route 280 about 0.5 km east of the Route 268 intersection.

VG87-10 Andesite. Collected about 100-150 m west of VG87-9, along the same road cut. The rock is not sheared like the previous sample, but it is totally altered with most of the phenocrysts changing from a clear to a milky color. The thin section indicates a porphyritic texture with a matrix replaced with secondary silica, sericite, chlorites, and calcite. The plagioclase phenocrysts are replaced with calcite. Partly altered biotite and magnetite are also noted.

VG87-11 Rhyolite. This rock is a fine-grained dike that cuts an altered andesite flow. It is banded, silicified, and platy in outcrop with limonite coating. The sample was collected about 50 m from Highway 4 on Route 286. The matrix in thin section is dominated by recrystallized silica and sericite. Minor opaque mineral (pyrite?) aggregates are noted in the matrix.

VG87-12 Andesite. Porphyritic and olive gray in color. The rock is strongly sheared and most of the intense alteration occurred along these zones. Sample collected a few meters north of VG87-11. Microlites, chlorite, and secondary silica dominate the matrix. The plagioclase phenocrysts are

sericitized and partially replaced with calcite. A few magnetite crystals were also noted.

VG87-13 Basalt. Sample collected from a shear zone along a landslide basalt block adjacent to New Mexico State Highway 4. It is fine grained and dark gray in color. The sample from the shear zone is soft. Soily and yellowish brown in color. No thin section was prepared.

VG87-14 Paleozoic sandstone. Collected about 8 km from Highway 126 along Forest Route 376 in the San Antonio Canyon. It is fine grained and well sorted and contains abundant chlorite.

VG87-15 and -16 Altered andesites. Collected about 2 km from Highway 126 on Route 376 south of VG87-14. The rock is completely altered and powdery in outcrop (no thin section).

APPENDIX B

DIFFRACTOGRAMS OF THE LESS THAN 2-μm FRACTION OF HYDROTHERMALLY ALTERED CORE HOLE VC-2A AND COCHITI MINING DISTRICT VOLCANIC SAMPLES
(In most cases the random and oriented mounts of identical samples are plotted together.)

(Samples are described in Appendix A.)

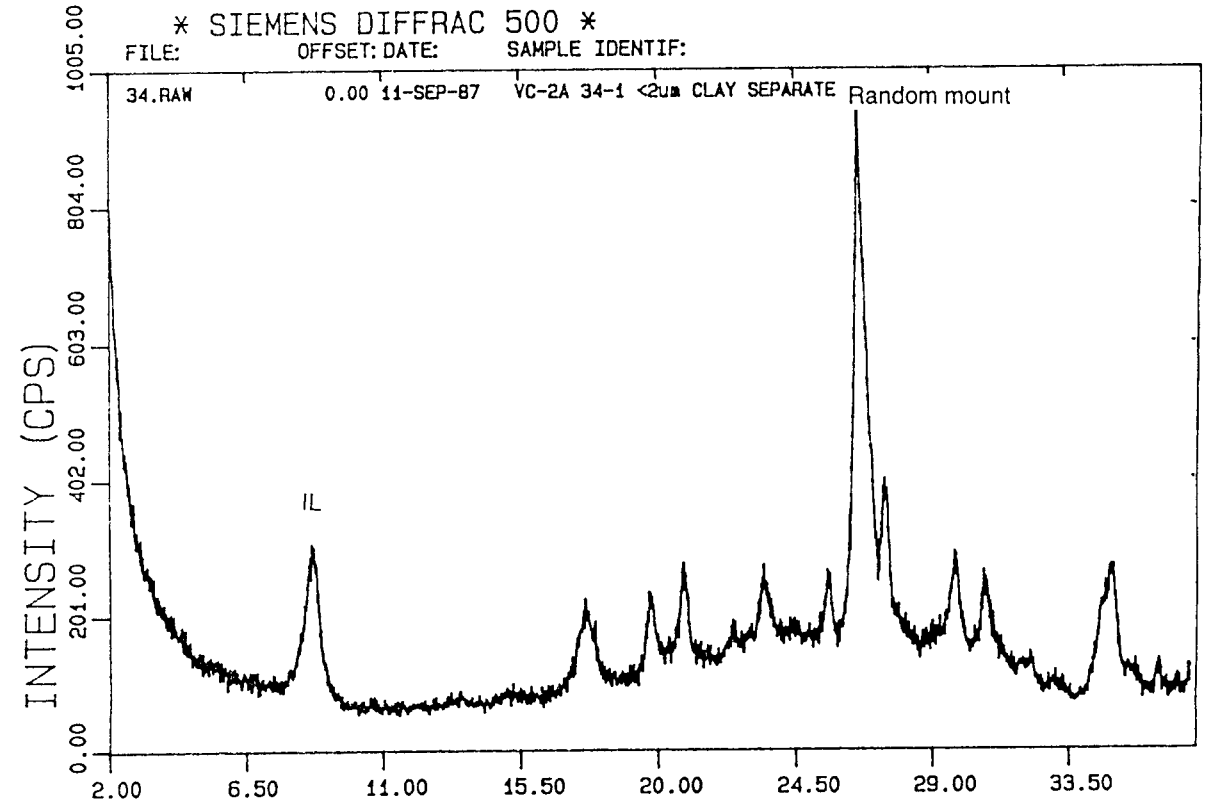
* SIEMENS DIFFRAC 500 *
FILE:
OFFSET: DATE:
SAMPLE IDENTIF:
34.RAW
0.00 11-SEP-87
VC-2A 34-1 <2um CLAY SEPARATE
Random mount
IL
INTENSITY (CPS)
1005.00
804.00
603.00
402.00
201.00
0.00
2.00
6.50
11.00
15.50
20.00
24.50
29.00
33.50

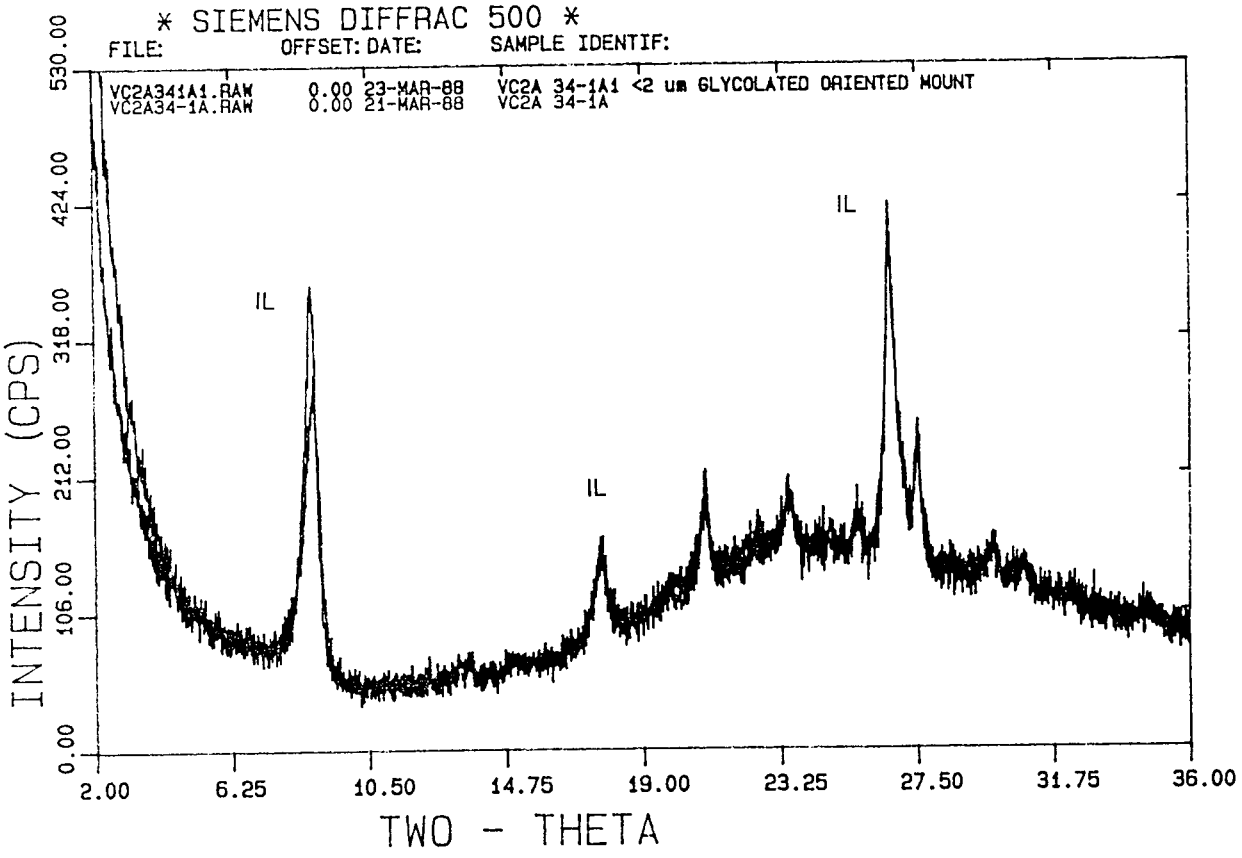
* SIEMENS DIFFRAC 500 *
FILE:
OFFSET: DATE:
SAMPLE IDENTIF:
VC2A341A1.RAW
0.00 23-MAR-88
VC2A 34-1A1 <2 um GLYCOLATED ORIENTED MOUNT
VC2A34-1A.RAW
0.00 21-MAR-88
VC2A 34-1A
IL
IL
IL
INTENSITY (CPS)
530.00
424.00
318.00
212.00
106.00
0.00
2.00
6.25
10.50
14.75
19.00
23.25
27.50
31.75
36.00
TWO - THETA

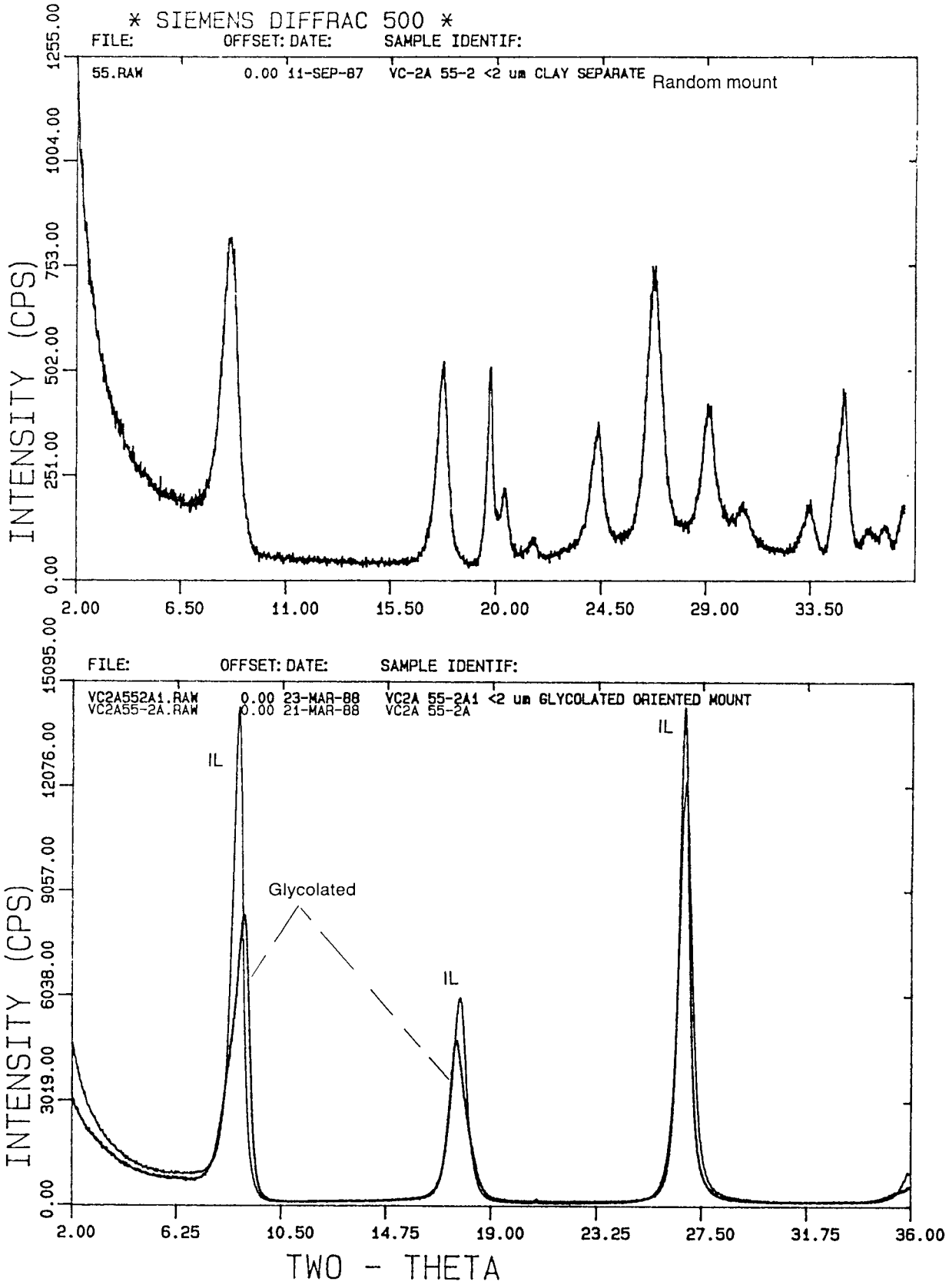
* SIEMENS DIFFRAC 500 *
FILE: OFFSET: DATE: SAMPLE IDENTIF:
55.RAW 0.00 11-SEP-87 VC-2A 55-2 <2 um CLAY SEPARATE
Random mount
INTENSITY (CPS)
1255.00
1004.00
753.00
502.00
251.00
0.00
2.00
6.50
11.00
15.50
20.00
24.50
29.00
33.50
FILE: OFFSET: DATE: SAMPLE IDENTIF:
VC2A552A1.RAW 0.00 23-MAR-88 VC2A 55-2A1 <2 um GLYCOLATED ORIENTED MOUNT
VC2A55-2A.RAW 0.00 21-MAR-88 VC2A 55-2A
IL
IL
IL
Glycolated
INTENSITY (CPS)
15095.00
12076.00
9057.00
6038.00
3019.00
0.00
2.00
6.25
10.50
14.75
19.00
23.25
27.50
31.75
36.00
TWO - THETA

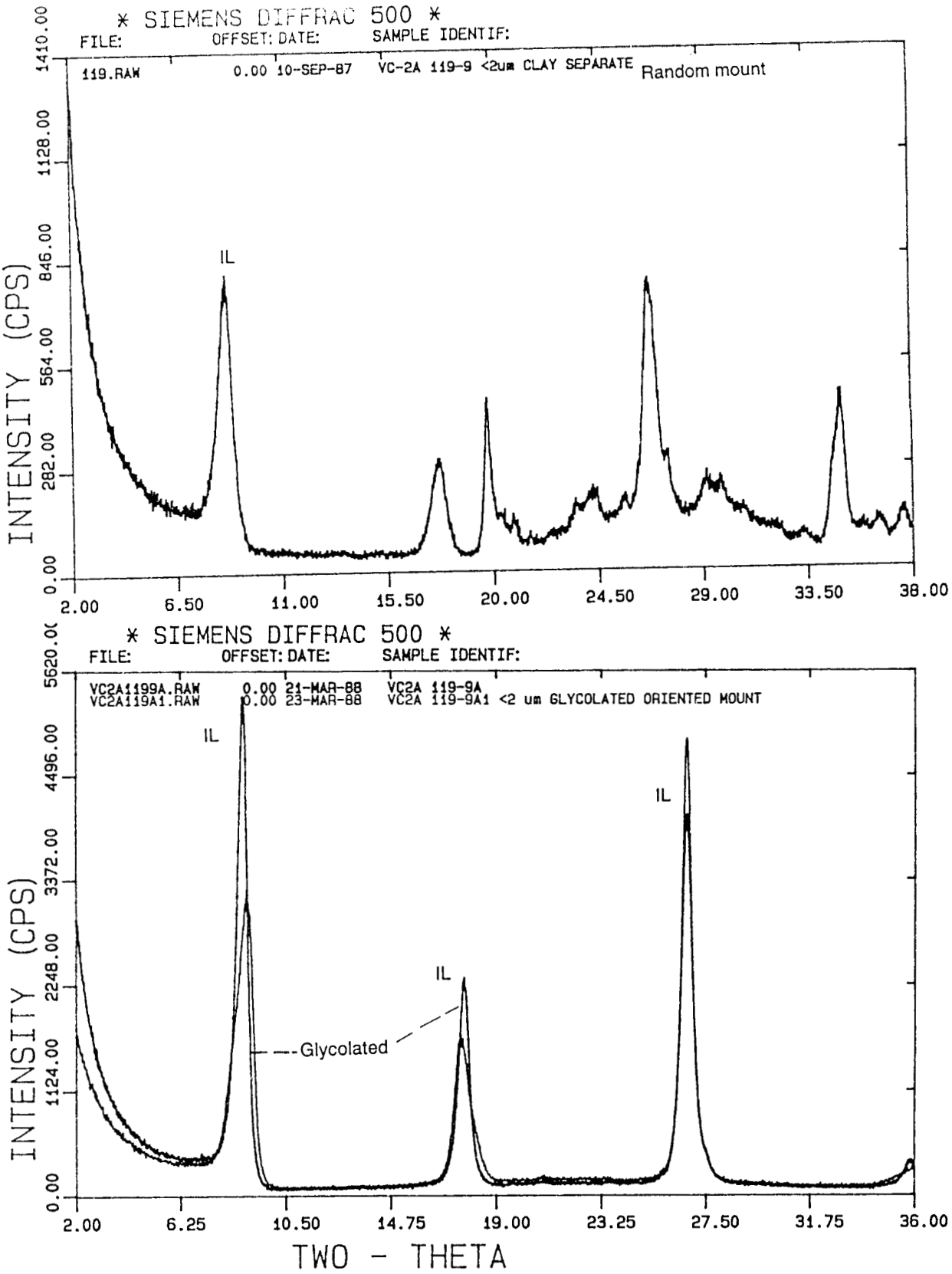
* SIEMENS DIFFRAC 500 *
FILE: OFFSET: DATE: SAMPLE IDENTIF:
119.RAW 0.00 10-SEP-87 VC-2A 119-9 <2um CLAY SEPARATE
Random mount
IL
INTENSITY (CPS)
1410.00
1128.00
846.00
564.00
282.00
0.00
2.00
6.50
11.00
15.50
20.00
24.50
29.00
33.50
38.00
* SIEMENS DIFFRAC 500 *
FILE: OFFSET: DATE: SAMPLE IDENTIF:
VC2A1199A.RAW 0.00 21-MAR-88 VC2A 119-9A
VC2A119A1.RAW 0.00 23-MAR-88 VC2A 119-9A1 <2 um GLYCOLATED ORIENTED MOUNT
IL
IL
IL
Glycolated
INTENSITY (CPS)
5620.00
4496.00
3372.00
2248.00
1124.00
0.00
2.00
6.25
10.50
14.75
19.00
23.25
27.50
31.75
36.00
TWO - THETA

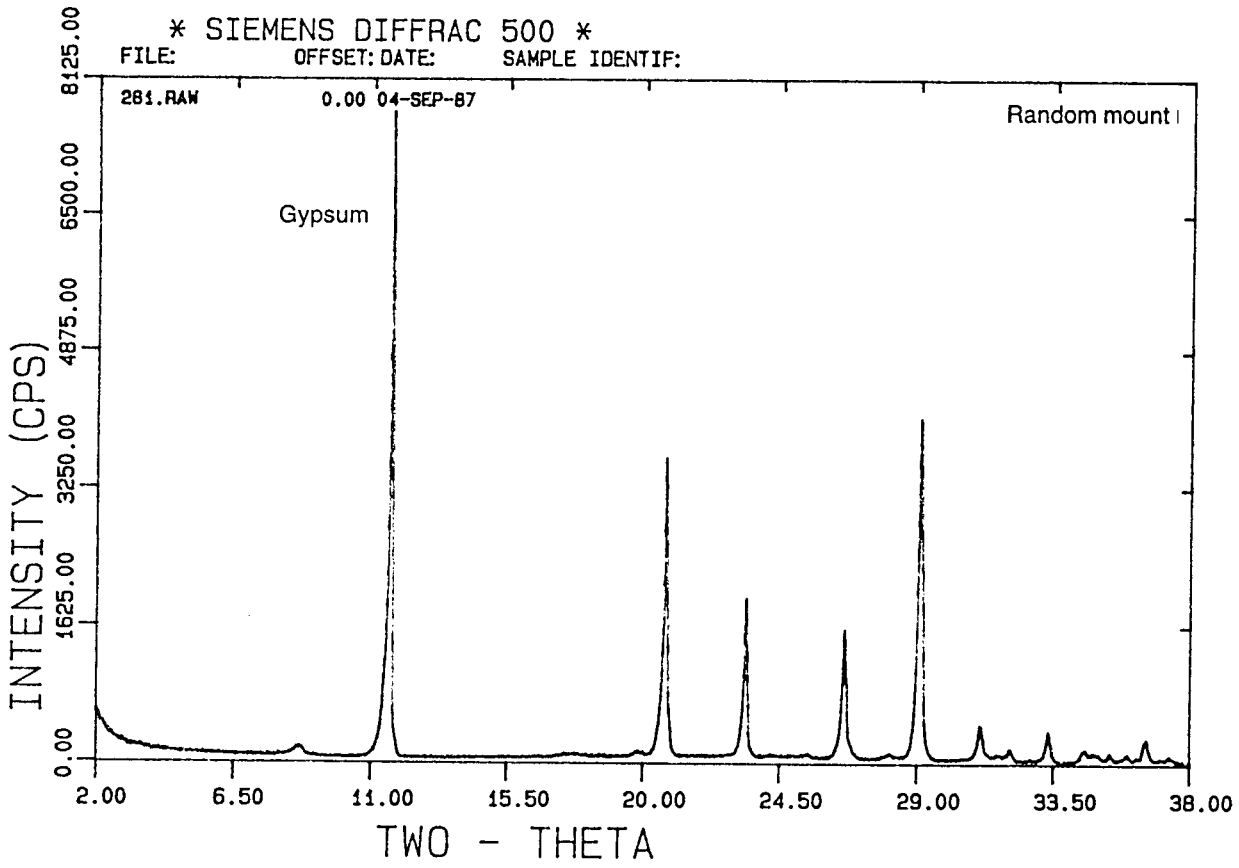
* SIEMENS DIFFRAC 500 *
FILE:
OFFSET:
DATE:
SAMPLE IDENTIF:
281.RAW
0.00
04-SEP-87
Random mount
Gypsum
INTENSITY (CPS)
8125.00
6500.00
4875.00
3250.00
1625.00
0.00
2.00
6.50
11.00
15.50
20.00
24.50
29.00
33.50
38.00
TWO - THETA

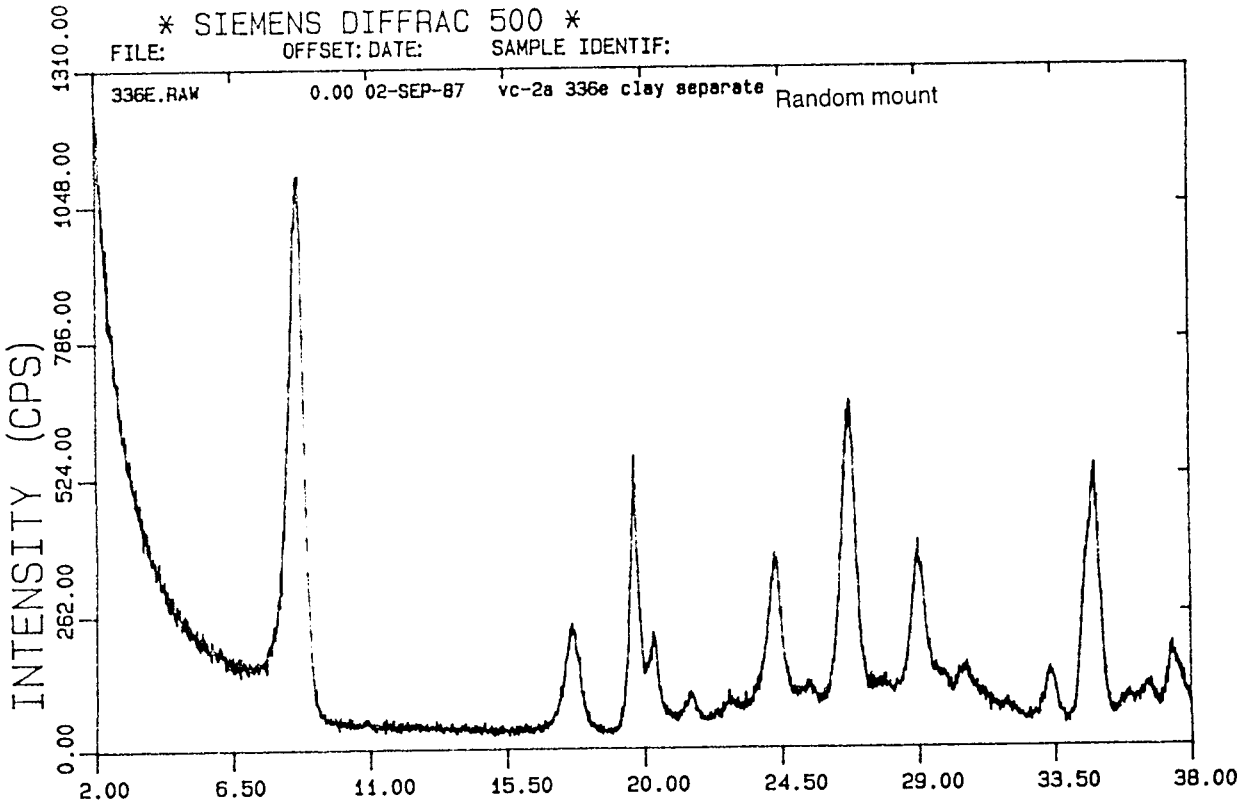
* SIEMENS DIFFRAC 500 *
FILE:
OFFSET: DATE:
SAMPLE IDENTIF:
336E.RAW
0.00 02-SEP-87
vc-2a 336e clay separate
Random mount
INTENSITY (CPS)
1310.00
1048.00
786.00
524.00
262.00
0.00
2.00
6.50
11.00
15.50
20.00
24.50
29.00
33.50
38.00

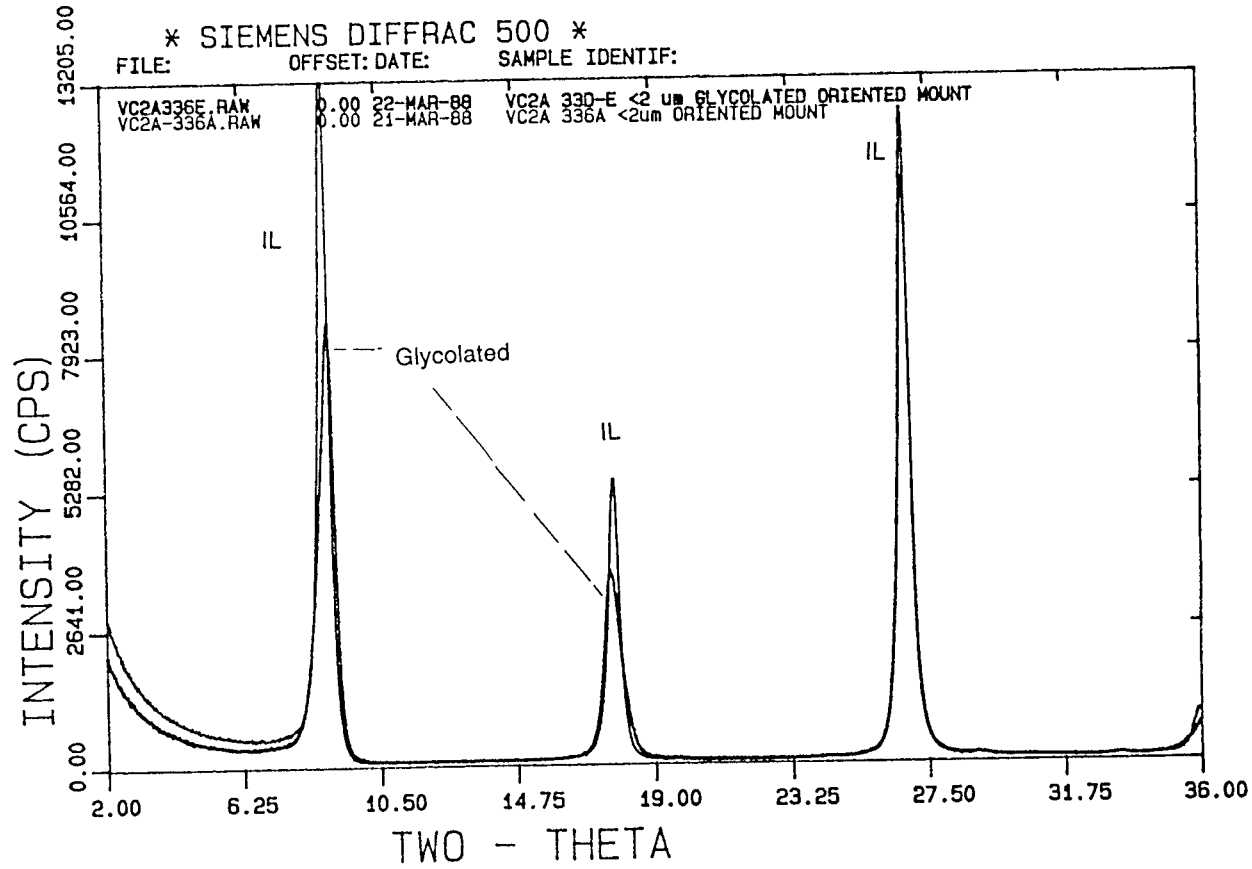
* SIEMENS DIFFRAC 500 *
FILE:
OFFSET: DATE:
SAMPLE IDENTIF:
VC2A336E.RAW
0.00 22-MAR-88
VC2A 330-E <2 um GLYCOLATED ORIENTED MOUNT
VC2A-336A.RAW
0.00 21-MAR-88
VC2A 336A <2um ORIENTED MOUNT
IL
IL
IL
Glycolated
INTENSITY (CPS)
13205.00
10564.00
7923.00
5282.00
2641.00
0.00
2.00
6.25
10.50
14.75
19.00
23.25
27.50
31.75
36.00
TWO - THETA

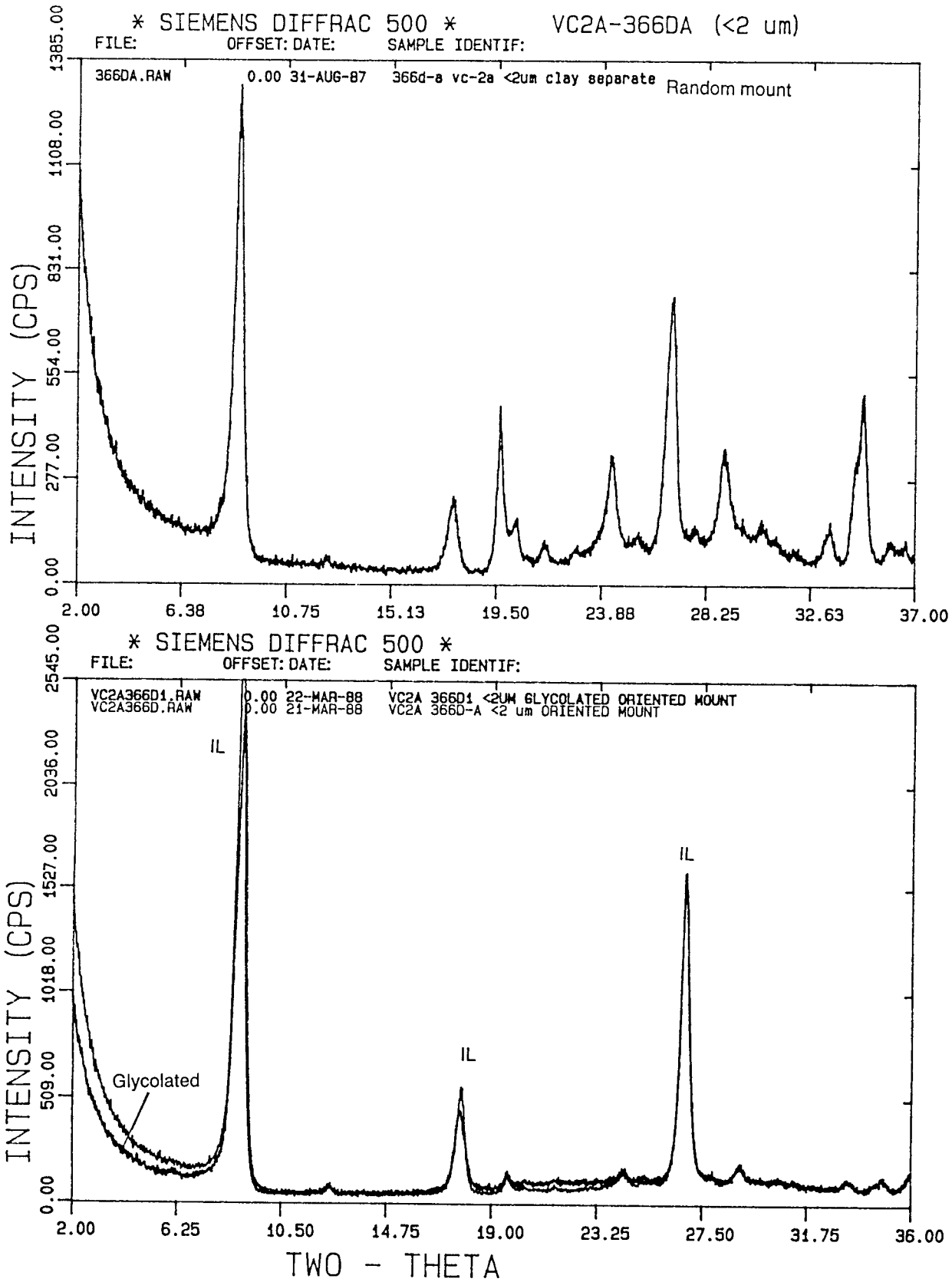
* SIEMENS DIFFRAC 500 *
VC2A-366DA (<2 um)
FILE:
OFFSET: DATE:
SAMPLE IDENTIF:
366DA.RAW
0.00 31-AUG-87
366d-a vc-2a <2um clay separate
Random mount
INTENSITY (CPS)
1385.00
1108.00
831.00
554.00
277.00
0.00
2.00
6.38
10.75
15.13
19.50
23.88
28.25
32.63
37.00
* SIEMENS DIFFRAC 500 *
FILE:
OFFSET: DATE:
SAMPLE IDENTIF:
VC2A366D1.RAW
0.00 22-MAR-88
VC2A 366D1 <2UM GLYCOLATED ORIENTED MOUNT
VC2A366D.RAW
0.00 21-MAR-88
VC2A 366D-A <2 um ORIENTED MOUNT
IL
IL
IL
Glycolated
INTENSITY (CPS)
2545.00
2036.00
1527.00
1018.00
509.00
0.00
2.00
6.25
10.50
14.75
19.00
23.25
27.50
31.75
36.00
TWO - THETA

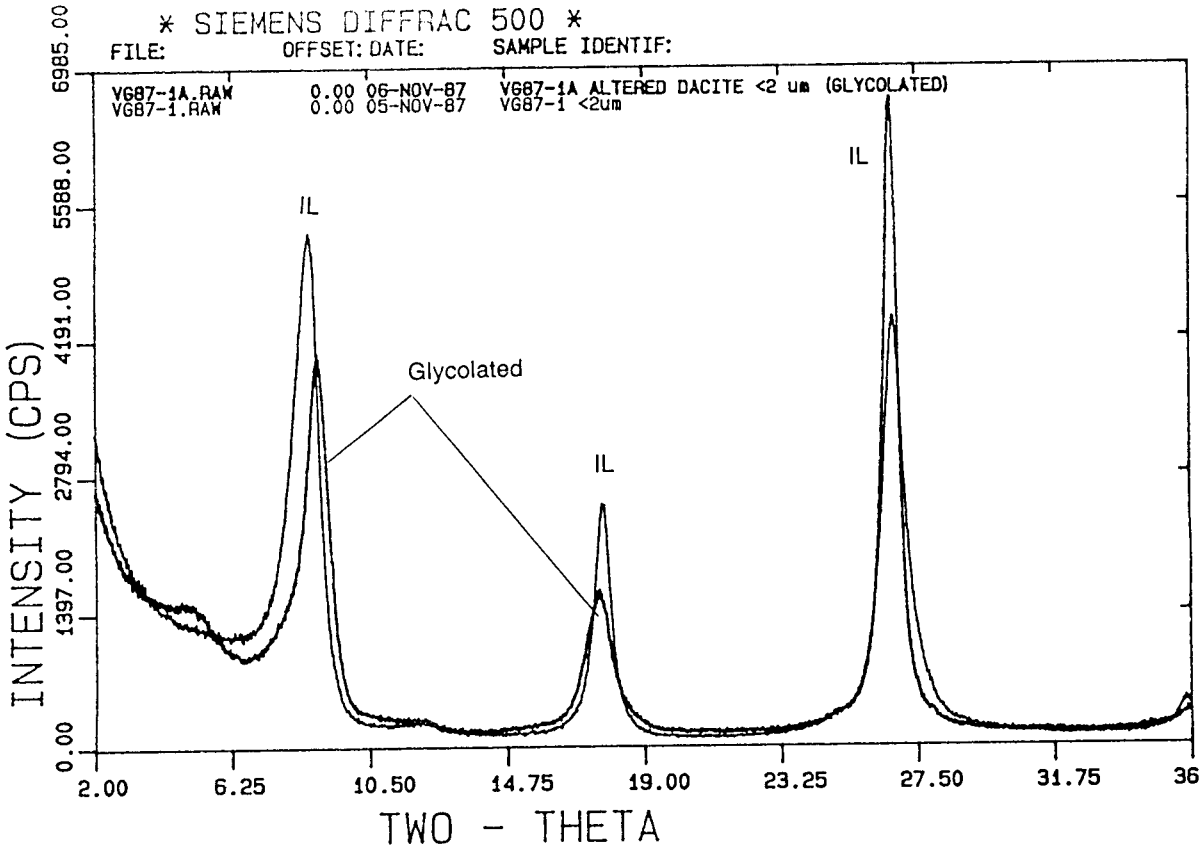
* SIEMENS DIFFRAC 500 *
FILE: OFFSET: DATE: SAMPLE IDENTIF:
VG87-1A.RAW 0.00 06-NOV-87 VG87-1A ALTERED DACITE <2 um (GLYCOLATED)
VG87-1.RAW 0.00 05-NOV-87 VG87-1 <2um
IL
IL
IL
Glycolated
INTENSITY (CPS)
6985.00
5588.00
4191.00
2794.00
1397.00
0.00
2.00
6.25
10.50
14.75
19.00
23.25
27.50
31.75
36
TWO - THETA

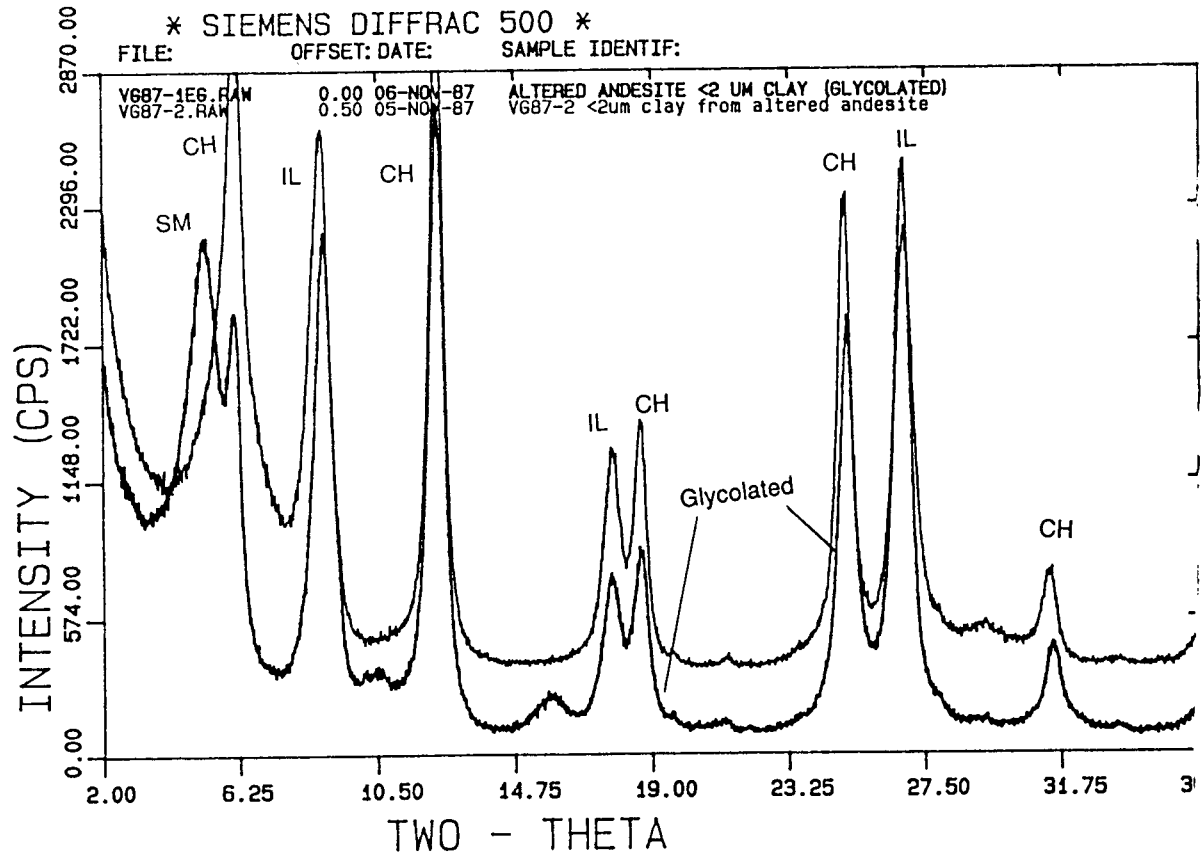
* SIEMENS DIFFRAC 500 *
FILE: OFFSET: DATE: SAMPLE IDENTIF:
VG87-1E6.RAW 0.00 06-NOV-87 ALTERED ANDESITE <2 UM CLAY (GLYCOLATED)
VG87-2.RAW 0.50 05-NOV-87 VG87-2 <2um clay from altered andesite
CH
SM
IL
CH
IL
CH
CH
IL
Glycolated
CH
INTENSITY (CPS)
2870.00
2296.00
1722.00
1148.00
574.00
0.00
2.00
6.25
10.50
14.75
19.00
23.25
27.50
31.75
TWO - THETA

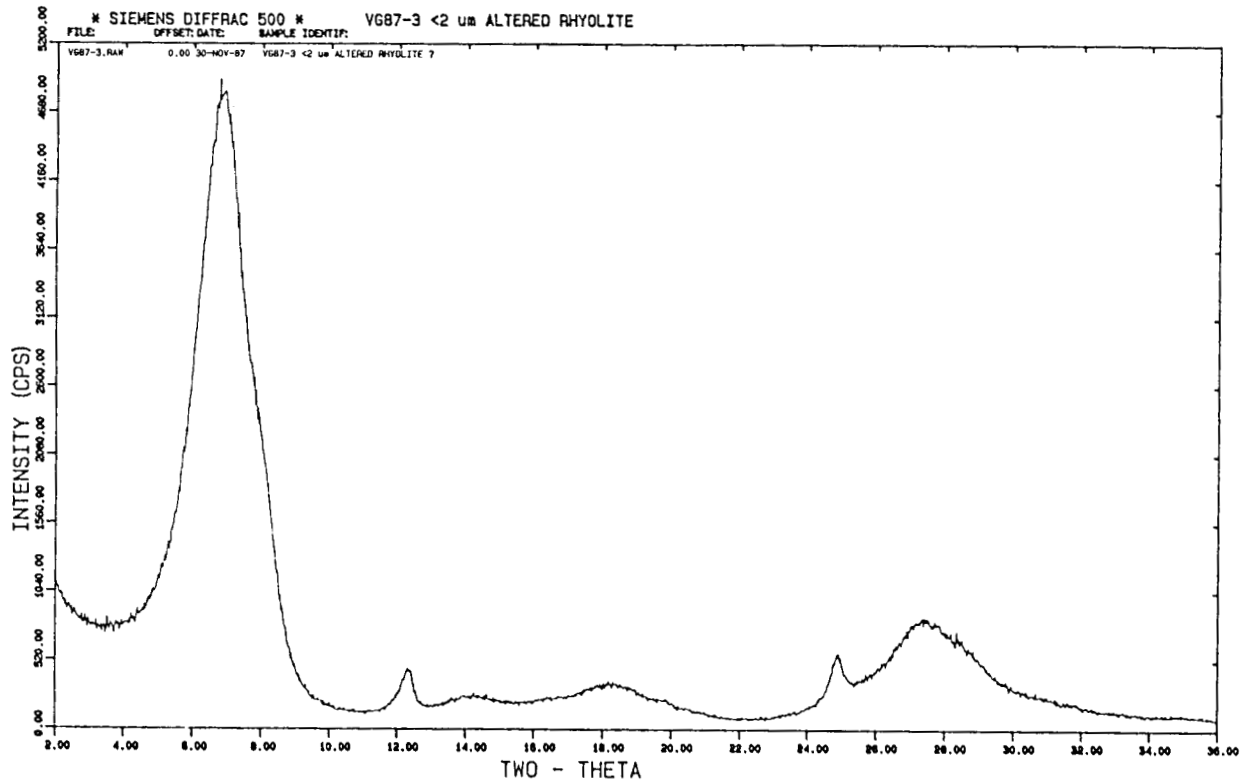
* SIEMENS DIFFRAC 500 *
VG87-3 <2 um ALTERED RHYOLITE
FILE: OFFSET: DATE: SAMPLE IDENTIF:
VG87-3.RAW 0.00 30-NOV-87 VG87-3 <2 um ALTERED RHYOLITE 7
INTENSITY (CPS)
TWO - THETA

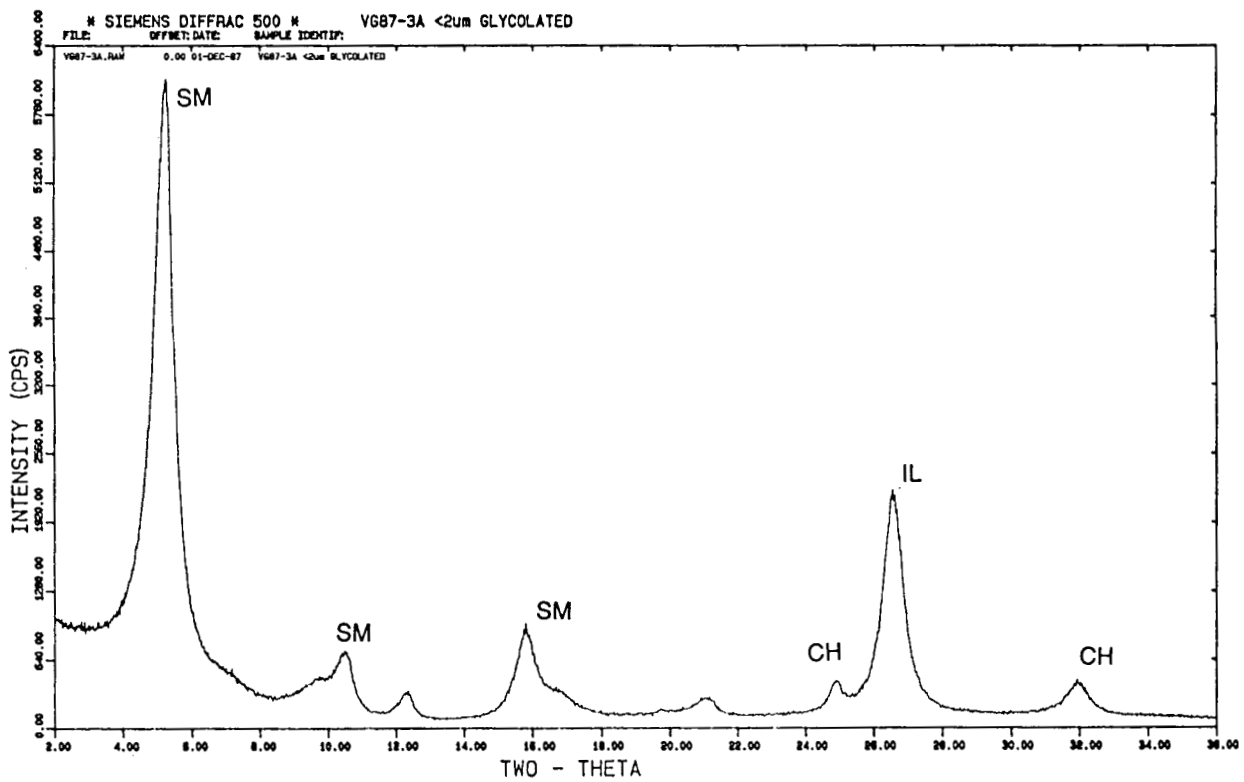
* SIEMENS DIFFRAC 500 *
VG87-3A <2um GLYCOLATED
FILE: OFFSET: DATE: SAMPLE IDENTIF:
VG87-3A.RAW 0.00 01-DEC-87 VG87-3A <2um GLYCOLATED
SM
SM
SM
CH
IL
CH
INTENSITY (CPS)
TWO - THETA

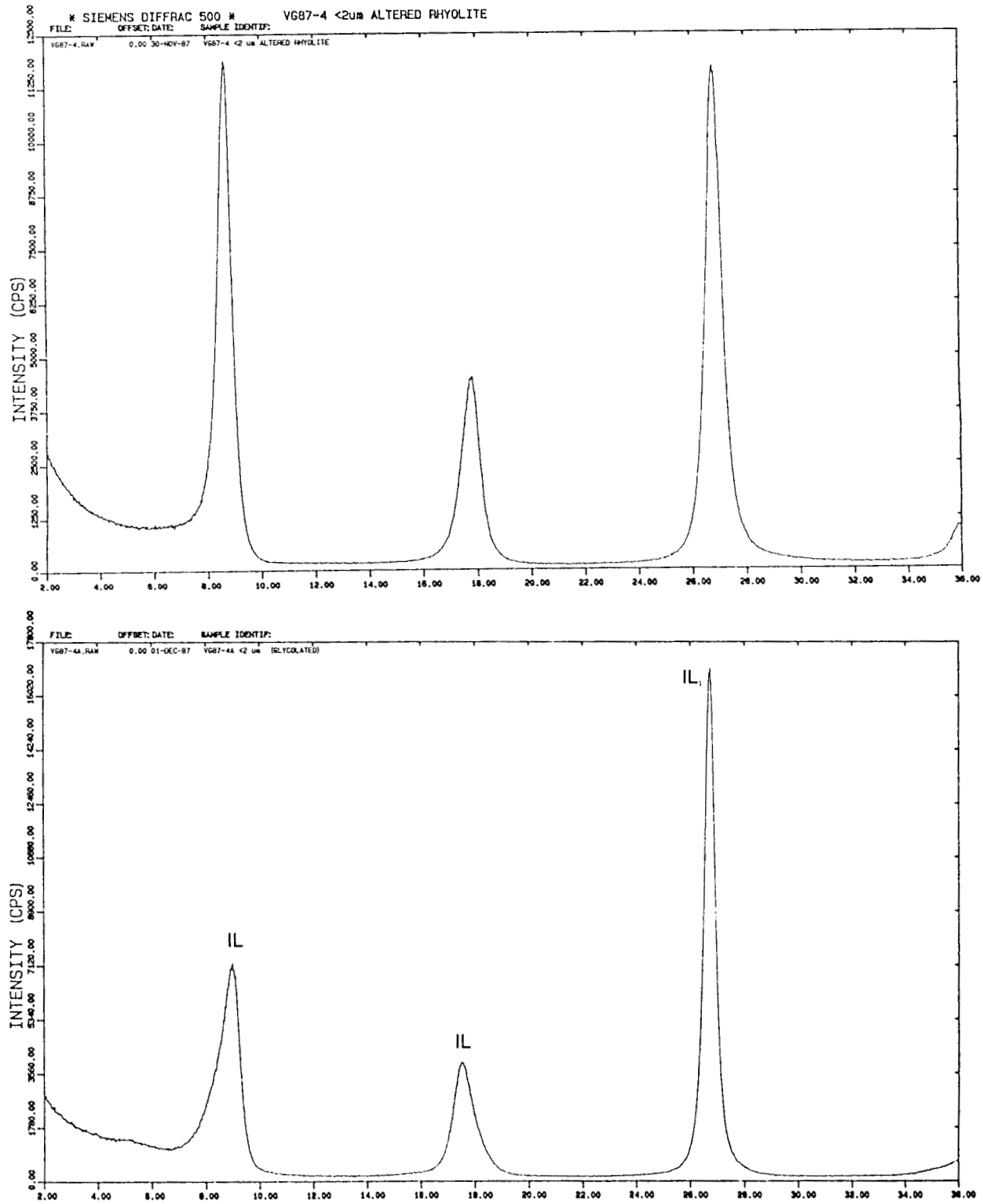
* SIEMENS DIFFRAC 500 *
VG87-4 <2um ALTERED RHYOLITE
FILE:
OFFSET: DATE:
SAMPLE IDENTIF:
VG87-4.RAW
0.00 30-NOV-87
VG87-4 <2 um ALTERED RHYOLITE
INTENSITY (CPS)
FILE:
OFFSET: DATE:
SAMPLE IDENTIF:
VG87-4A.RAW
0.00 01-DEC-87
VG87-4A <2 um (GLYCOLATED)
IL
IL
IL

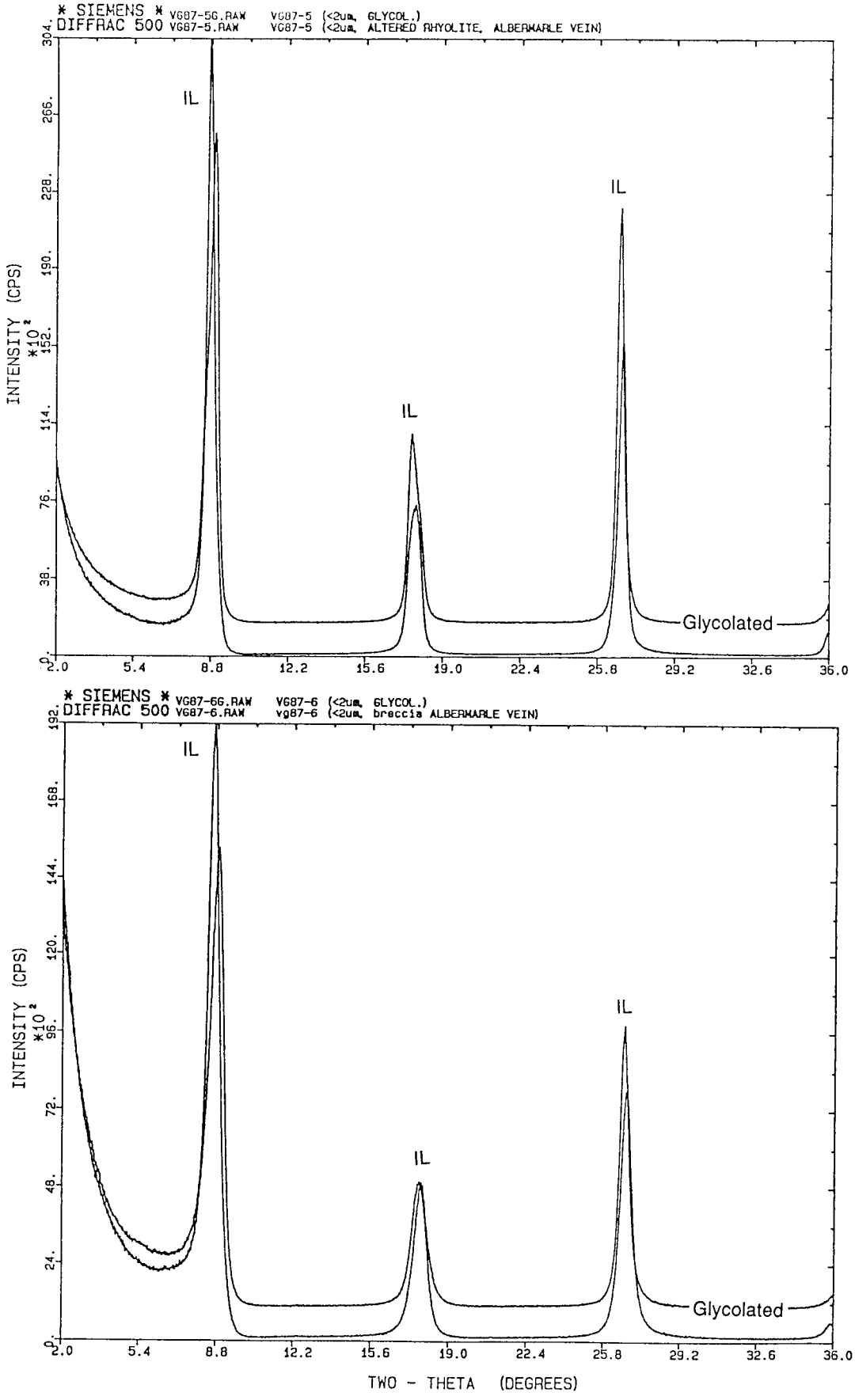
* SIEMENS * VG87-5G.RAW VG87-5 (<2um, GLYCOL.)
DIFFRAC 500 VG87-5.RAW VG87-5 (<2um, ALTERED RHYOLITE, ALBERMARLE VEIN)
IL
IL
IL
Glycolated
INTENSITY (CPS) *10²
304.
266.
228.
190.
152.
114.
76.
38.
0.
2.0
5.4
8.8
12.2
15.6
19.0
22.4
25.8
29.2
32.6
36.0
* SIEMENS * VG87-6G.RAW VG87-6 (<2um, GLYCOL.)
DIFFRAC 500 VG87-6.RAW vg87-6 (<2um, breccia ALBERMARLE VEIN)
IL
IL
IL
Glycolated
INTENSITY (CPS) *10²
192.
168.
144.
120.
96.
72.
48.
24.
0.
2.0
5.4
8.8
12.2
15.6
19.0
22.4
25.8
29.2
32.6
36.0
TWO - THETA (DEGREES)

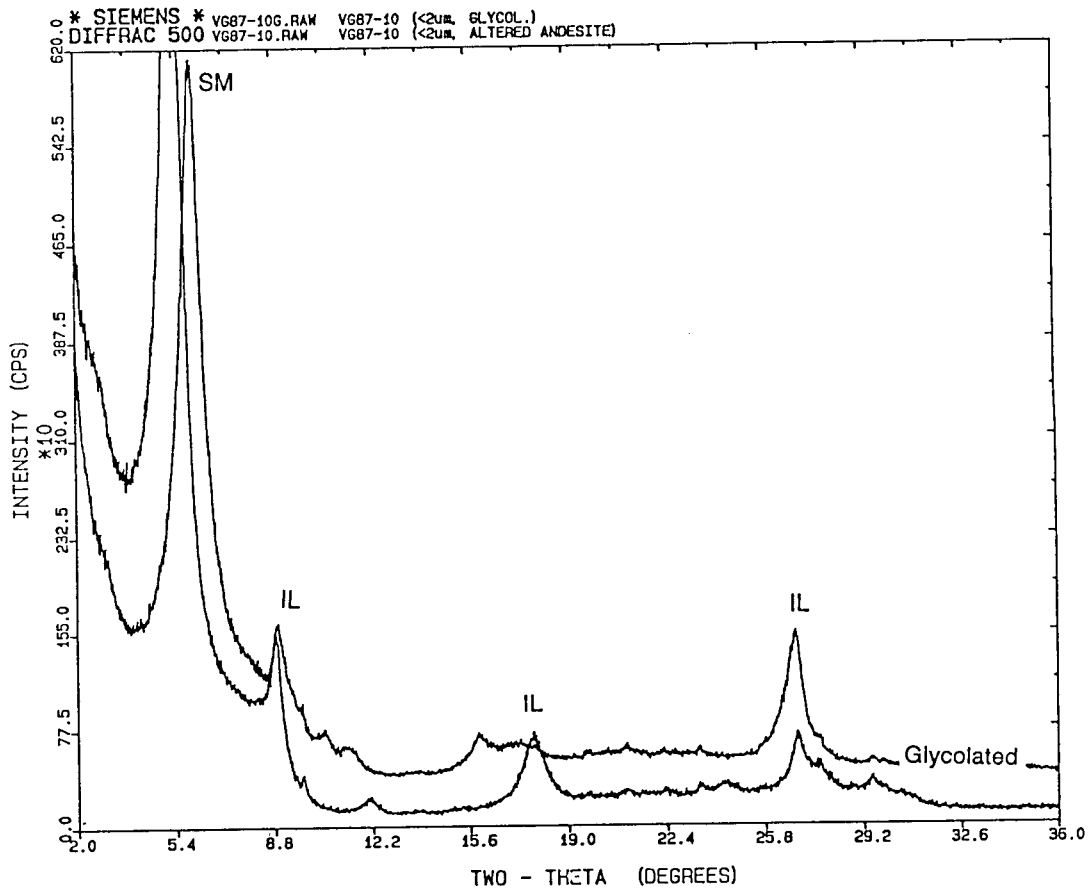
* SIEMENS * VG87-10G.RAW VG87-10 (<2um, GLYCOL.)
DIFFRAC 500 VG87-10.RAW VG87-10 (<2um, ALTERED ANDESITE)
SM
IL
IL
IL
Glycolated
INTENSITY (CPS)
*10
620.0
542.5
465.0
387.5
310.0
232.5
155.0
77.5
0.0
2.0
5.4
8.8
12.2
15.6
19.0
22.4
25.8
29.2
32.6
36.0
TWO - THETA (DEGREES)

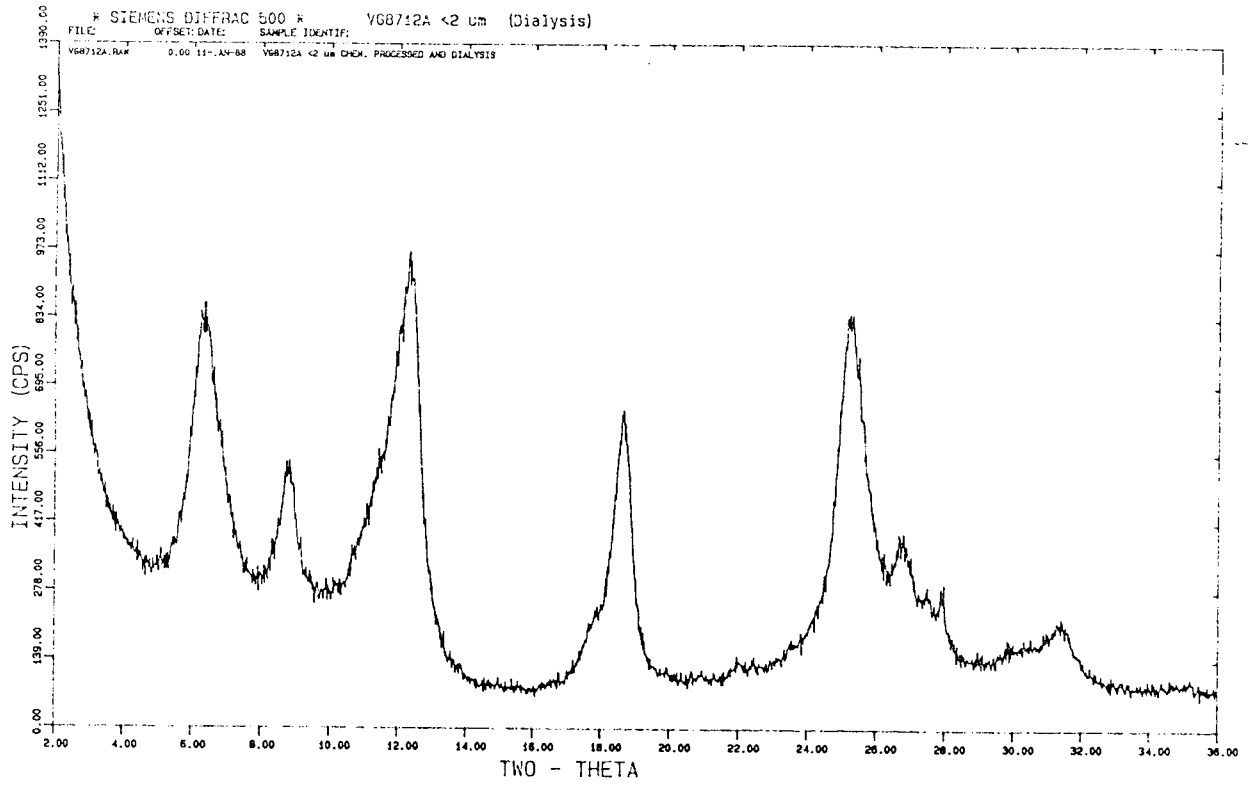
* SIEMENS DIFFRAC 500 *
VG8712A <2 um (Dialysis)
FILE: OFFSET: DATE: SAMPLE IDENTIF:
VG8712A.RAW 0.00 11-.AN-88 VG8712A <2 um CHEM. PROCESSED AND DIALYSIS
INTENSITY (CPS)
TWO - THETA

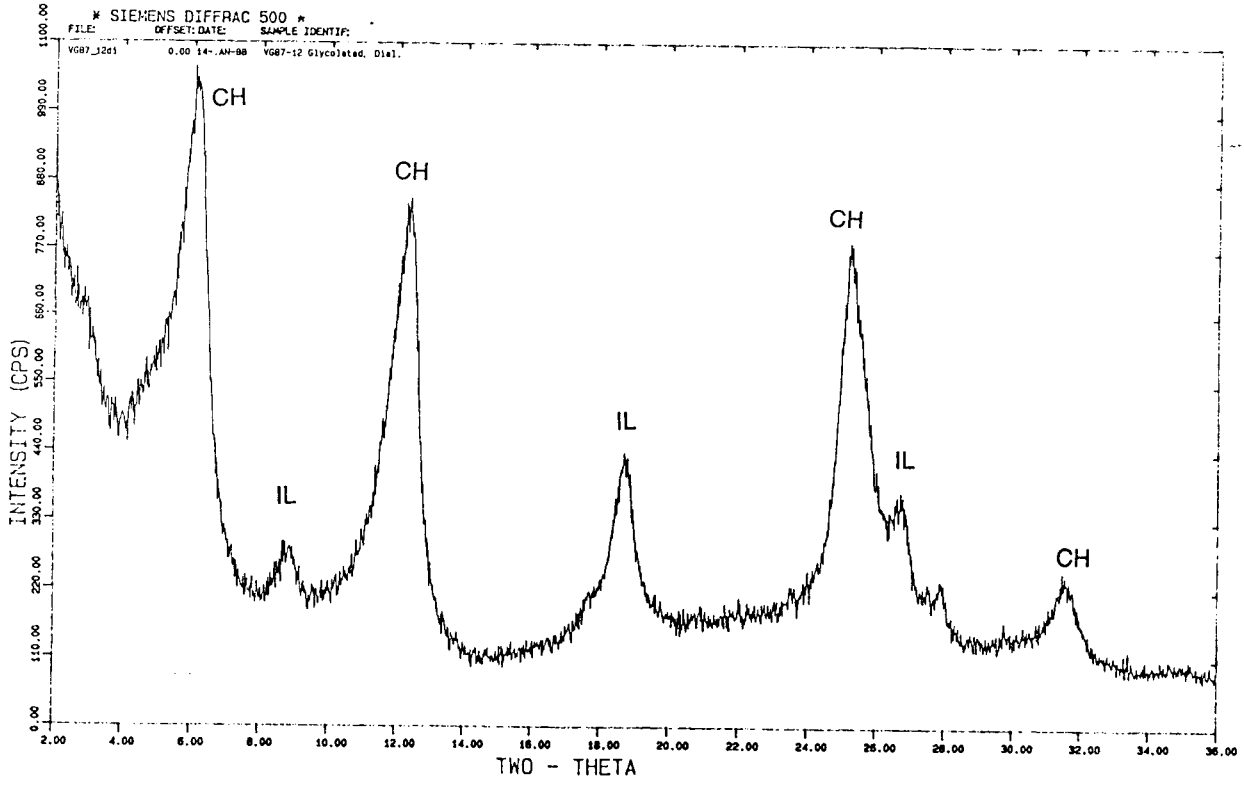
* SIEMENS DIFFRAC 500 *
FILE: OFFSET: DATE: SAMPLE IDENTIF:
VG87_12d1 0.00 14-.AN-88 VG87-12 Glycolated, Dial.
CH
CH
CH
IL
IL
IL
CH
INTENSITY (CPS)
TWO - THETA

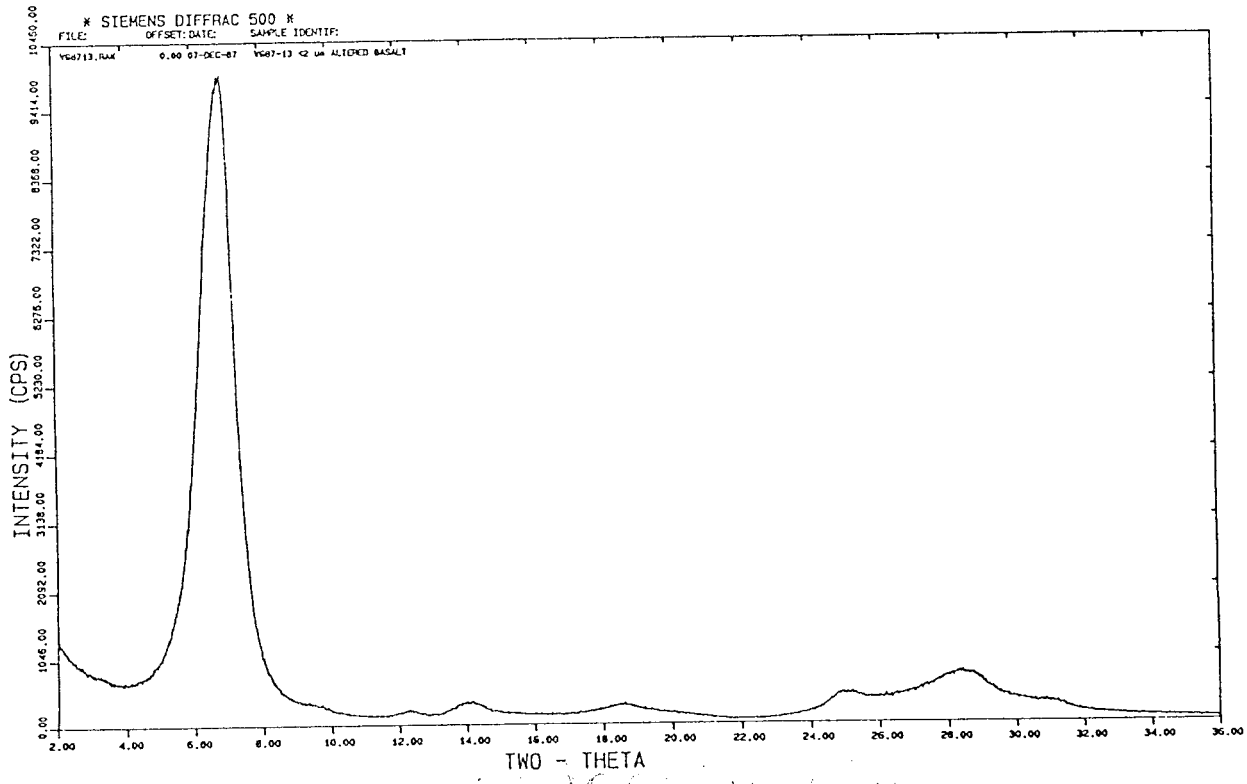

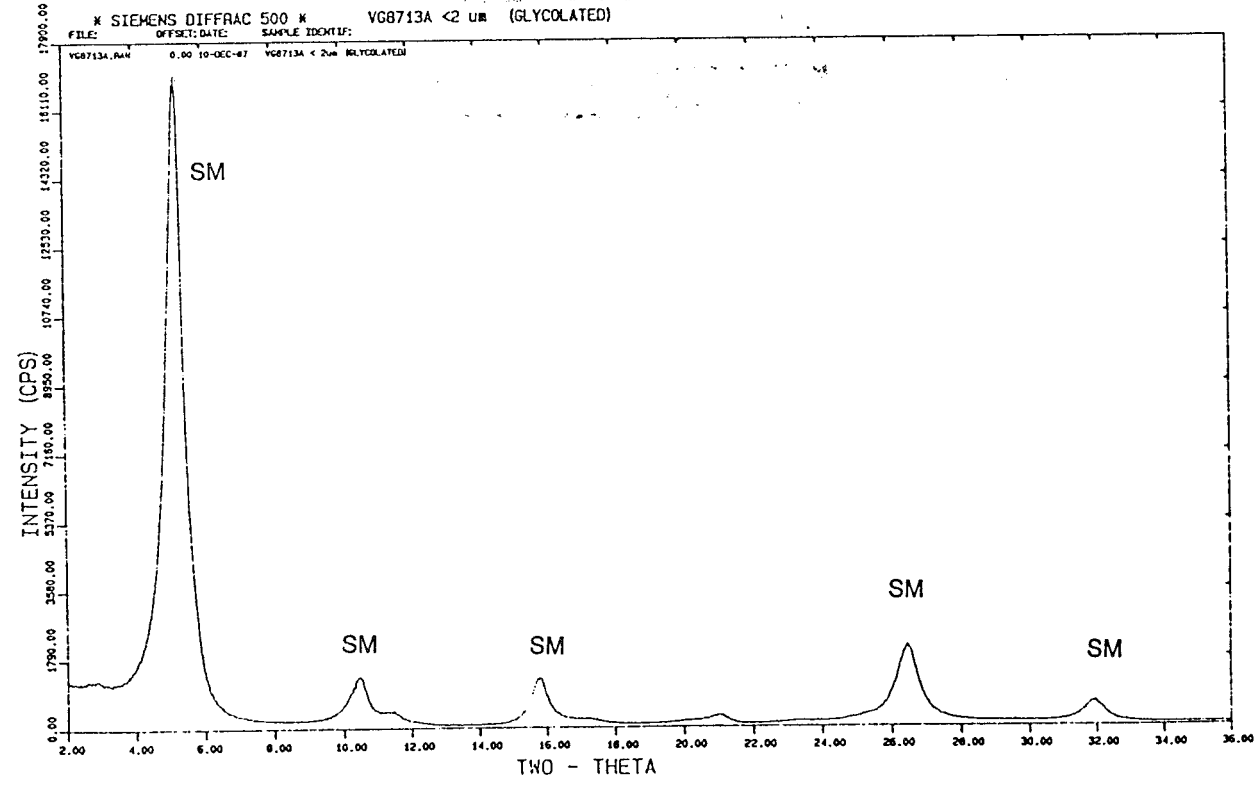

☆ U.S. GOVERNMENT PRINTING OFFICE: 1989—673-104/80068